

**SCUOLA DI SCIENZE**

**Dipartimento di Chimica Industriale “Toso Montanari”**

Corso di Laurea Magistrale in

**Chimica Industriale**

Classe LM-71 - Scienze e Tecnologie della Chimica Industriale

**Electrochemical oxidation of Kraft lignin for  
the production of value-added chemicals on Ni  
and Co electrocatalysts**

Tesi di laurea sperimentale

**CANDIDATO**

Monica Nota

**RELATORE**

**Chiar.ma Prof.ssa** Patricia Benito Martin

**CORRELATORE**

**Chiar.ma Prof.ssa** Teresa Andreu

**Dott.** Giancosimo Sanghez De Luna

*Sessione II*



## **Kay words**

Kraft lignin

Electro-deposition

Nichel foam

Nichel hydroxide

Cobalt hydroxide

Vanillin



## ABSTRACT

Vanillin is an important aromatic aldehyde, from an industrial point of view, because it is widely used by food, cosmetics and pharmaceutical industries. Currently, vanillin is obtained through catalytic oxidation of lignin. An alternative process is the electro-catalytic oxidation of lignin, which is gaining considerable interest, because able to work at mild conditions. The aim of this work is to synthesize electro-catalysts that favour the depolymerization of Kraft lignin allowing to obtain vanillin selectively. Open cell Ni bare foams with and without electro-deposited Ni-Co and Co hydroxides have been used as electrocatalysts. The formation of metal oxohydroxides on the foam surface and the OER contribute to the electro-oxidation of lignin. The vanillin yield depends on both the type of catalyst and the reaction conditions chosen, in particular, the applied potential and the reaction time. The highest yield of vanillin was obtained by applying a 0.6 V vs SCE potential with a reaction time of one hour and using Ni bare as catalyst. Regardless of the type of catalyst used, increasing the reaction time the vanillin yield decreases, probably due to re-condensation reactions involving vanillin itself. Finally, the presence of Ni-Co and Co hydroxides on Ni foam surface does not improve its catalytic activity. The Co/Ni foam exhibits a high accumulated charge and high conversion, which is probably due to the side reactions that offset the vanillin accumulation. The Ni-Co/Ni foams, on the other hand, present both an intermediate vanillin yield, between the other two foams and also a low charge passed. These are an encouraging result for future developments.

## AIM OF THE WORK

Currently, one of the most important scientific and environmental issues is to reduce global dependence on fossil sources. Among the possible routes, the use of lignocellulosic biomass allows to obtain molecules with a considerable commercial importance.

Lignin is a component of biomass that gaining interest as source for sustainable and renewables aromatics source, currently produced by petrochemical processes. Vanillin is one of the most important aromatic aldehydes on an industrial level, and it can be obtained through lignin oxidation. This molecule is widely exploited by the confectionery, cosmetic and pharmaceutical industry.

An alternative to the conventional catalytic oxidation process is the electro-catalytic pathway, this is a branch of catalysis that in recent years has been gaining considerable interest, both because it allows the use of temperature and ambient pressure and of green solvents such as water. In addition, the ability to carry out the entire process with electricity produced from renewable sources, makes it completely sustainable.

In this context the aim of this thesis work has been to look for known materials to be active in oxidation processes and Kraft lignin degradation with the aim of synthesizing electrocatalysts that are selective in the catalytic electro-oxidation of Kraft lignin to vanillin.

Ni foams with Ni/Co hydroxides or Co-hydroxides electro-deposited as active phases and the counterpart Ni bare foam, were selected as catalysts. The electrochemical analysis of catalytic systems was carried out by cyclic voltammetry, to evaluate and compare their behaviour with the variation of the scanned potential in basic solutions (1 M NaOH) in absence and presence of Kraft lignin (10 g/L). This has allowed a qualitative estimation of the catalytic activity in both the oxidation of lignin and the oxygen evolution reaction and has allowed to estimate the potential values to carry out the chronoamperometry tests. At the end of the cyclic voltammetry analyses the most promising catalysts were subjected to a chronoamperometry test, studying the effect of the applied potential and reaction time and analysing the products obtained.



# Summary

<b>1</b>	<b>Introduction.....</b>	<b>1</b>
1.1	Biorefineries.....	2
1.2	Biomass.....	5
1.2.1	<i>Lignocellulosic biomass composition.....</i>	<i>6</i>
1.2.2	<i>Lignocellulosic biomass treatments and lignin extraction .....</i>	<i>11</i>
1.3	Lignin properties and applications.....	13
1.4	Lignin depolymerization products.....	15
1.5	Degradation processes of lignin .....	20
1.5.1	<i>Thermochemical methods for lignin treatment.....</i>	<i>21</i>
1.5.2	<i>Depolymerization by hydrolysis.....</i>	<i>23</i>
1.5.3	<i>Depolymerization by hydrogenolysis.....</i>	<i>24</i>
1.5.4	<i>Biological depolymerization .....</i>	<i>25</i>
1.5.5	<i>Oxidative lignin depolymerization.....</i>	<i>27</i>
1.6	Lignin depolymerization catalysts.....	29
1.7	Electrocatalysis.....	31
1.7.1	<i>Evaluation of the performance of the electrocatalyst.....</i>	<i>33</i>
1.7.2	<i>Electrocatalytic kinetics.....</i>	<i>36</i>
1.8	Theoretical notes on electrocatalytic oxidation.....	37
1.8.1	<i>Experimental approaches for the electro-oxidation of organic substance.....</i>	<i>41</i>
1.8.2	<i>Electrolysis of water and evolution of oxygen and hydrogen.....</i>	<i>43</i>
1.9	Electrocatalytic oxidation of lignin.....	45
1.9.1	<i>Electro-deposition methods.....</i>	<i>50</i>
1.9.2	<i>Choice of Ni-Co catalyst for lignin electro-oxidation.....</i>	<i>54</i>
1.10	Parameters affecting electro-catalytic oxidation of lignin.....	58
1.10.1	<i>Influence of the nature of the metal.....</i>	<i>58</i>
1.10.2	<i>Effect of current density and potential applied.....</i>	<i>60</i>
1.10.2	<i>Influence of the electrolysis temperature.....</i>	<i>60</i>
1.10.4	<i>Effect of the nature and concentration of the organic reagent.....</i>	<i>63</i>
1.10.5	<i>Influence of the pH.....</i>	<i>63</i>



<b>2. Experimental part.....</b>	<b>65</b>
2.1 Material and reagents used.....	65
2.2 Electrocatalyst preparation.....	66
2.3 Electro-deposition of the active phase.....	66
2.3.1 <i>Electrochemical cell used for electro-deposition</i> .....	66
2.3.2 <i>Preparation of solutions</i> .....	68
2.3.3 <i>Substrate pretreatment</i> .....	68
2.3.4 <i>Electro-deposition</i> .....	68
2.4 Characterisation of catalysts.....	69
2.4.1 <i>SEM-EDS analysis</i> .....	69
2.4.2 <i>Raman spectroscopy</i> .....	71
2.4.3 <i>X-Ray diffraction spectroscopy</i> .....	73
2.5 Electrochemical study of electro-catalysts.....	74
2.5.1 <i>Cyclovoltammetry</i> .....	76
2.5.2 <i>Chronoamperometry</i> .....	77
2.5.3 <i>Catalytic cycle</i> .....	77
2.6 Analysis of the reaction products.....	78
2.6.1 <i>Nuclear magnetic resonance spectroscopy analysis</i> .....	79
2.6.2 <i>Gas chromatography with mass spectroscopy (GC-MS)</i> .....	81
2.6.3 <i>Attenuated total reflectance analysis</i> .....	82
<b>3. Results and discussion.....</b>	<b>84</b>
3.1 Catalysts characterization.....	84
3.2 Cyclic-voltammetry in NaOH 1M.....	87
3.3 Cycle-voltammetry in Lignin 10g/L.....	90
3.4 Electrochemical oxidation of Kraft lignin.....	91
3.4.1 <i>Characterization of side-products</i> .....	94
3.4.2 <i>Characterization of the lignin after reaction</i> .....	96
3.5 Cyclic-voltammetry in NaOH 1M post-reaction.....	97
3.6 Cyclic-voltammetry in Lignin 10g/L post reaction.....	98
3.7 Characterization of the post-reaction catalysts.....	99
<b>4. Conclusions.....</b>	<b>101</b>
<b>5. References.....</b>	<b>102</b>



# 1. Introduction

Fossil resources like petroleum, coal, and natural gas are the most used raw materials to obtain energy, fuels, and chemical substances [1].

The transition from a fossil fuels based economy to a renewable one is not only motivated by their scarcity and future supply risk, but also because fossil fuels are the responsible for the rising values of Greenhouse gas (GHG) emissions, in particular CO<sub>2</sub>, as it is considered one of the leading causes of global warming [2].

According to article 194, paragraph one, of the Treaty on the functioning of the European Union (TFUE), the promotion of the utilization of renewables, instead of fossil sources, represents one of the objectives of the union's energy policy [3].

Moreover, the utilization of renewable energy sources would be essential to respect the union's commitments in the Paris agreement of 2015. The most binding goal of the European Union is to reduce emissions by at least 40% compared to 1990 levels by 2030 [4].

In 2018, compared to the year before, the CO<sub>2</sub> emission increased by 1.7%, equating to an additional 33.1 tons of CO<sub>2</sub>. This is the highest annual growth rate since 2013; these data were reported by the annual report of the international energy agency (IEA) [5].

That is why it is needed to implement the utilization of renewables for energy, fuels, and chemical substances.

An energy source is defined renewable only if it regenerates in less time than the speed at which it is consumed. Some examples are wind, hydroelectric, solar, geothermal energy, and of course, that obtainable from biomass. Fossil sources, therefore, being consumed a higher speed than that necessary for their formation, cannot be considered as such [1].

In order to reduce our reliance on the oil industry, new avenues for biomass conversion must be investigated, and it is a big challenge for catalysis [6].

Inedible vegetable biomass is the one that is currently being used to avoid ethical problems. Raw materials like cellulose and lignocellulose are the reference now since they are abundant in nature as they do not compete with the food market.

# 1.1 Biorefinery

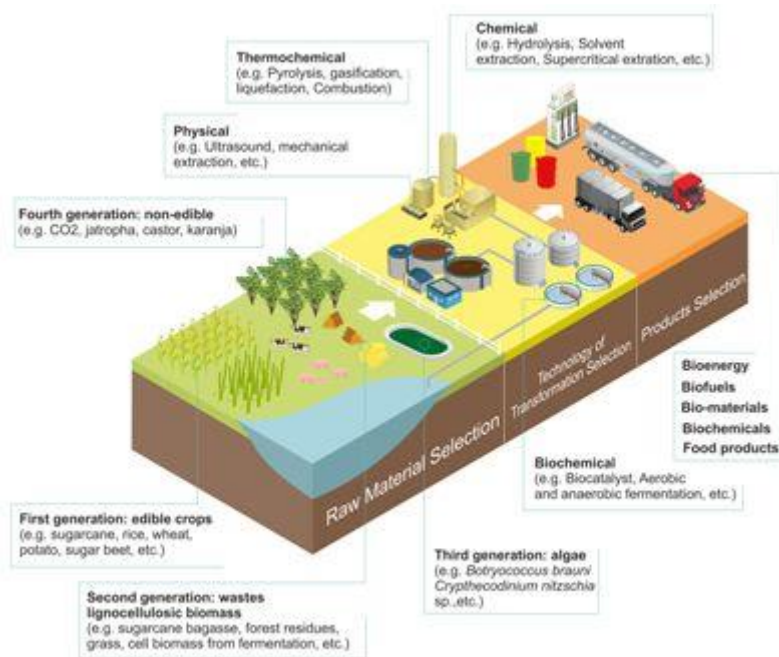


Figure 1.1 Biomass treatment cycle in the biorefinery

Among the various definitions of biorefinery (Figure 1.1), the most exhaustive is the one given by the IEA Bioenergy Task 42: “Biorefining is the sustainable processing of biomass into a spectrum of marketable products and energy” [7].

In general, the biorefinery concept includes a wide range of technologies able to separate biomass (wood, grasses, corn, etc.) into their building blocks (carbohydrates, proteins, triglycerides, etc.), which can be converted into value-added products, like biofuels and chemicals.

Moreover, biomass resources are readily available in many countries. Their use should contribute to reducing national dependence on imported fossil fuels.

The products of biorefinery systems can be divided into two broad categories: material products and energy products. The products of a biorefinery must be able to replace fossil fuel-based products coming from oil refinery, both chemicals and energy products.

Concerning the chemicals, the goal of the biorefinery would be to produce the same chemical species but starting from biomass instead of fossil fuels. An alternative would be to make molecules with a different structure, but an equivalent function.

In order to introduce the biorefinery concept, a conversion of the global economy/industry into a sustainable biobased society having bioenergy, biofuels, and biobased products as main pillars and biorefineries as the basis is needed.

Therefore, the replacement of oil with biomass will require some change in today's production of goods and services; for this purpose, biological and chemical sciences will play an essential role in the generation of future industries, and new synergies of biological, physical, chemical and technical sciences must be developed.

Most biofuels and biochemicals obtained until now have been produced at a laboratory scale and not with a biorefinery concept. One of the main problems is that the most promising results are obtained with materials in competition with the food industry [8].

Concerning the conversion plant, an efficient biomass use should be maximized to adopt the "Zero waste" philosophy; in this way, consumption of non-renewable energy should be minimized.

In this context, the bio-industries should reach a complete utilization of all biomass components: the residue from one bio-industry (e.g., lignin from a lignocellulosic ethanol production plant) becomes an input for other industries, giving rise to integrated bio-industrial systems [1].

Biomass composition is not homogeneous because the biomass feedstock might be made of grains, wood, grass, biological waste and so on. The elemental composition is a mixture of C, H, and O (plus other minor components such as N, S, and other mineral compounds). The inhomogeneities of the biomass feedstocks are both an advantage and a disadvantage. The advantage is that these materials can make a wide range of products; the disadvantage is that a broad range of processing technologies is needed and that most of these technologies are still at a pre-commercial stage. If compared to petroleum, biomass generally has too little hydrogen, too much oxygen, and a lower fraction of carbon [9].

The main aim of the technological process in biorefinery is depolymerizing and deoxygenating the biomass components. Several technological processes must be applied; these can be divided into four main groups: thermochemical, biochemical, mechanical/physical and chemical processes [10].

Unlike petroleum, biomass suffers a seasonal change, since the harvesting is not possible all year. A switch from petroleum-refinery to bio-refinery requires a change in the capacity of

chemical industries. The generation of materials and chemicals in a seasonal time-frame will be needed [11].

Although, in principle, all oil refinery platform chemicals can also be derived from biomass, but with lower yields and higher costs, the future biorefineries are expected to be based on a limited number of platforms, from which all the other commodity and bulk chemicals can be derived. In particular, the carbohydrate fraction of biomass feedstock (i.e., cellulose and hemicellulose in lignocellulosic biomass) is expected to play the most significant role as a renewable carbon source for biochemical products. Biomass polysaccharides can be effectively hydrolysed to monosaccharides which can then be converted, via fermentation or chemical synthesis, to an array of bio Platform Molecules (bPM – building block chemicals with potential use in the production of numerous value-added chemicals), analogous to the petrol-platform molecules of the current oil refinery [2]. In 2004, a list of the most promising bPMs was compiled by the US Department of Energy [12] (Figure 1.2).

Bio-PM	Structure	Bio-PM	Structure
glycerol		(S, R, R)-xylitol	
3-hydroxy propionic acid		L-glutamic acid	
L-aspartic acid		itaconic acid	
fumaric acid		levulinic acid	
3-hydroxy butyrolactone		2,5-furan-di-carboxylic acid	
L-malic acid		glucaric acid	
succinic acid		sorbitol	

Figure 1.2 Top 14 biomass platform molecules

## 1.2 Biomass

According to EU and national legislation on incentives for renewable sources (Directive 2001/77 / EC and Legislative Decree 387/2003, modification from Directive 2009/28 / EC and Legislative Decree 28/2011), the term biomass must be understood as "the biodegradable fraction of products, wastes and wastes of biological origin from agriculture (including plant and animal substances), forestry and related industries, including fishing and aquaculture, mowing and pruning existing from public and private green areas, as well as the biodegradable part of the industrial and urban waste " [13].

The biomass (Figure 1.3) derives from photosynthetic processes in which simple molecules like water, CO<sub>2</sub>, N<sub>2</sub>, and O<sub>2</sub> react and are converted into more complex substances like carbohydrates, proteins, and lignin. Plants absorb about 1% of the solar radiation that reaches the Earth, which is stored by plants as chemical bonds in natural polymers that represent biomass [6].

This stored solar energy can be exploited through the reverse process: combustion, with which the same stored energy can be obtained. Through this process, the net contribution of CO<sub>2</sub> is null, since it captures the same amount used by plants for their growth [14].

Among these natural polymers, starch and wood are the most abundant. Starch is the main constituent of foods, like potatoes, rice and corn. Instead, wood is mainly composed of cellulose, hemicellulose, lignin, and a lesser extent: fats, oils, proteins, and mineral components.

Given the great variety of composition, the uses of biomasses depend strongly on their provenance, which influences composition and properties. Therefore, not all biomass can be used in the same ways; as such, biomass can be classified according to three different criteria:

- Water content: fresh or dry biomass
- Biomass origin: vegetable or animal
- Vitality: the presence of live or dead organisms inside

Considering the Biomass origin criteria, biomasses can be distinguished in:

- Phytomass: originating from plants
- Zoomassa: originating from animals
- Microbial biomass: originating from microorganisms

The most frequent and most used phytomasses are listed below:

- Forest and wood industry residues: These materials derive from the processing of the sawmills, transformation of the wood product and the maintenance of the forest.
- Agricultural products: Straw, sticks, pruning branches.
- Agro-industrial residues: Pomace and other products from the food industry
- Zootechnical waste
- Dedicated energy cultures: These are finalized for the production of biomasses for energy use or the production of biofuels. The most exciting species are sunflower, rapeseed, sugar cane.
- Urban waste: Residues from public greenhouse maintenance operations and only the organic fraction of municipal solid waste [15].



Figure 1.3 Examples of biomasses exploitable for the production of energy and chemicals.

### *1.2.1 Lignocellulosic biomass composition*

The lignocellulosic matrices are composed mainly of cellulose, hemicellulose, lignin, and to a lesser extent from fats, lipids, proteins, and mineral components.

#### **Cellulose**

The lignocellulosic matrices are composed of a percentage of cellulose of 40-50%.

Cellulose has a molecular weight of about 1000000g/mol, and it is a structural polysaccharide consisting of repeating units of D-glucose linked together by linear  $\beta$  (1,4) glycosidic bonds.



In water solution, D-glucose in the extended form (with reducing end) assumes a more stable hemiacetal structure, forming a six cycle, defined as a pyranosic cycle due to the structural similarity with the pyran.

To do this, the hydroxy located on carbon 5 binds with carbonyl carbon in position 1 (called anomeric carbon), which becomes a new stereocenter. At the end of the cycle, the –OH group linked to the anomeric carbon can be in two alternative positions: axial or equatorial.

Two different isomers are thus obtained, defined in this case as  $\alpha$  and  $\beta$  anomers. In particular, the  $\alpha$  anomer represents the structure in which the-OH is in the axial position, while the  $\beta$  anomer, the one in which the-OH is in the equatorial position (Figure 1.4).

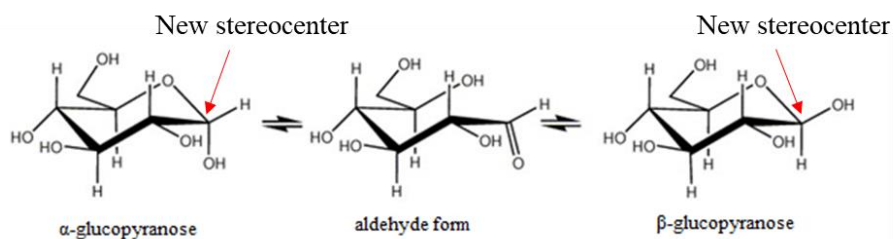


Figure 1.4 Mechanism of mutual-rotation<sup>1</sup> of glucose in an aqueous solution.

The linear  $\beta$  (1,4) glycosidic bonds (Figure 1.5) that unite the D-glucose molecules involve the hydroxide in site 1 of a glucose unit in pyranosic form  $\beta$  and hydroxide in position 4 of the next glucose unit in pyranosic form  $\alpha$ .

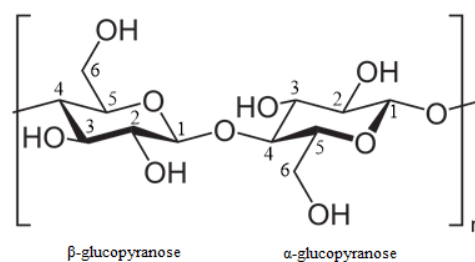


Figure 1.5 Representation of the  $\beta$  (1,4) glycosidic bond that binds the glucose units of cellulose. The subscript “n” indicates that the unit in brackets repeats n times in the cellulose.

The glucose chains thus formed are arranged parallel to each other and bind together by hydrogen bonds, forming the fibrils. These polymeric structures are long, ordered, and difficult to dissolve. Thanks to the order, cellulose reaches a crystal structure alternating with amorphous areas. The difference between these two areas is that the first one is not coordinated with water, but the second one is. The amorphous areas are impact-resistant thanks to the water.

<sup>1</sup> Continuous interconversion between the extended and the pyranosic ( $\alpha$  and  $\beta$ ) forms of monosaccharides in an aqueous solution.

Cellulose is insoluble in common solvents but, it is soluble in concentrated solutions of zinc chloride, in ionic liquids, and ammonia copper hydroxide solutions [6].

## Hemicellulose

In lignocellulosic matrices, there is a percentage of hemicellulose equal to 20-30%, and this has a lower molecular weight than cellulose (50-200 units) and has multiple branches.

Hemicellulose is composed of monosaccharides with five carbon atoms ( $\beta$ -D-xylose and  $\alpha$ -L-arabinose, of which xylose is the most abundant) and six carbon atoms ( $\alpha$ -D-galactose and  $\beta$ -D-mannose are the main ones) (Figure 1.6). There are several hemicellulose conformations, but monosaccharides are always held together by  $\beta$  (1,4) bonds.

This part of the lignocellulosic matrix is characterized by a low degree of polymerization and short ramifications, which lead to low protection of the functional groups; this allows more facile hydrolysis by acids, bases, and enzymes compared to cellulose [6].

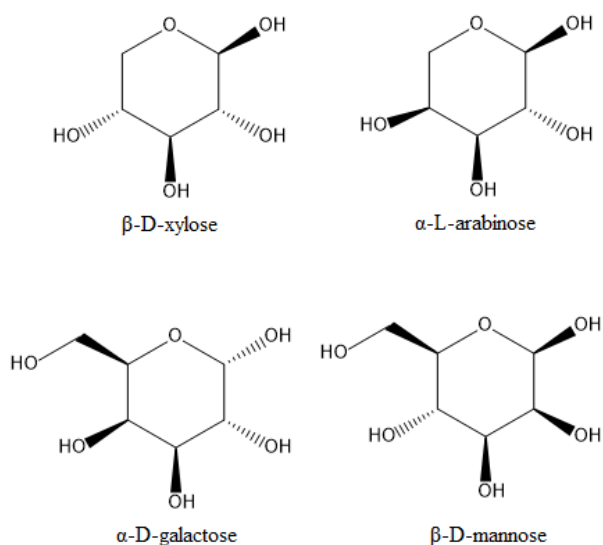


Figure 1.6 Main monosaccharides in pyranosic form which constitute the hemicellulose.

## Lignin

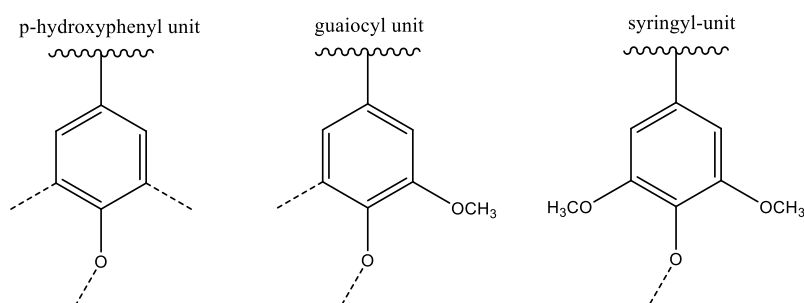
Lignin accounts for about 15–30% of the total biomass content in plants, annually about 150 billion tons of lignin is produced by plants, which makes it the most abundantly available natural polymer next to cellulose.

The critical function of lignin in the cell wall is to provide rigidity by reinforcing the strength of crystalline cellulose that enables the erect growth of plants.

With the empirical formula of  $C_{31}H_{34}O_{11}$ , lignin contains about 95 billion tons of carbon in the Earth's crust, which illustrates the unexploited high carbon energy reserve.

Lignin has an extensively branched three-dimensional chemical structure with various functional moieties: carboxyl (COOH); carbonyl (C=O), and methoxy (CH<sub>3</sub>O) [16]. It is a macromolecule made up of repeating phenyl propane-based monolignols subunits (Figure 1.7):

- Syringyl-(S)
- Guaiacyl-(G)
- P-hydroxyphenyl-(H)



These are the main structural units in lignin, which correspond to the following monomers

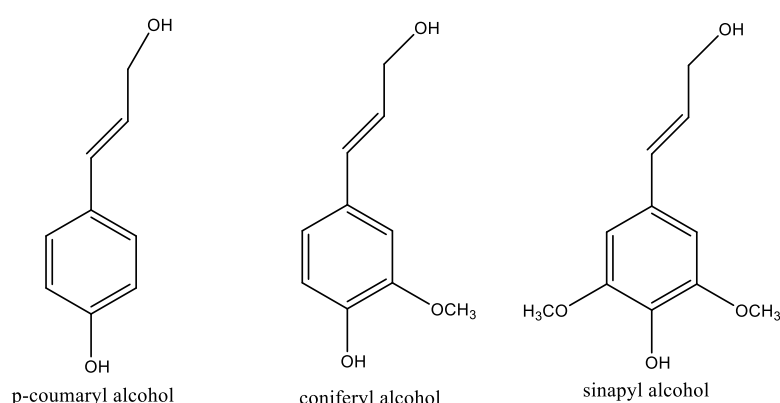


Figure 1.7 Chemical structure of monolignols and the corresponding building blocks in lignin.

These are linked either by ether or carbon-carbon bonds. The percentage content of monolignol subunits varies among different plant species.

Common linkages found in heterogeneous, high molecular weight lignin are  $\beta$ -O-4;  $\beta$ -5;  $\beta$ - $\beta$ ;  $\alpha$ -O-4; 5-5; 4-O-5;  $\beta$ -1 (Figure 1.8). The  $\beta$ -O-4 linkage is the most abundant one representing about 50% of all interunit linkages.

A variation in the linkage's percentage regarding plant species is also similar to the monomer's content.

The variation in linkages and monolignols content with plant species make the actual structure determination of lignin rather complicated [17].

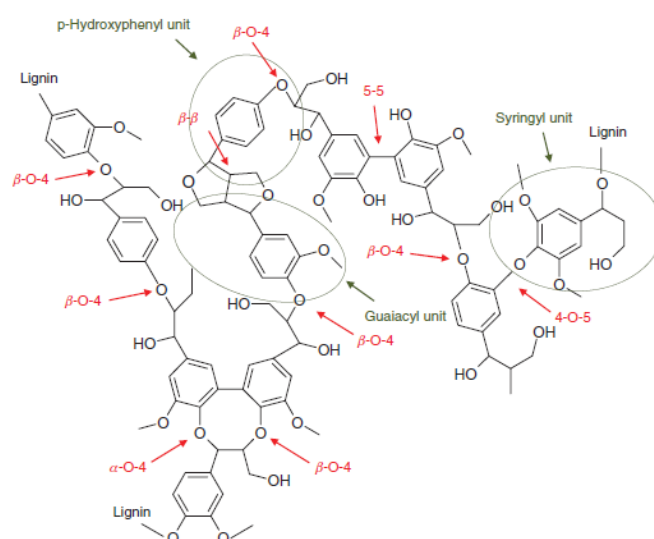


Figure 1.8 Schematic representation of a hypothetical lignin structure, including principal linkage types and building blocks.

In addition to cellulose, hemicellulose, and lignin, low molecular weight compounds such as terpenes, fats, waxes, phenols, and inorganic salts of Si, K, Na, S, Cl, P, Ca, Mg and Fe are also present in a reduced percentage. These cause ash deposition during combustion.

The internal structure of the lignocellulosic biomass (Figure 1.9) is organized into cellulose microfibrils packed together, stabilized by hydrogen bonds, and connected by hemicellulose and other amorphous polysaccharides. The outermost layer instead is formed by lignin [1].

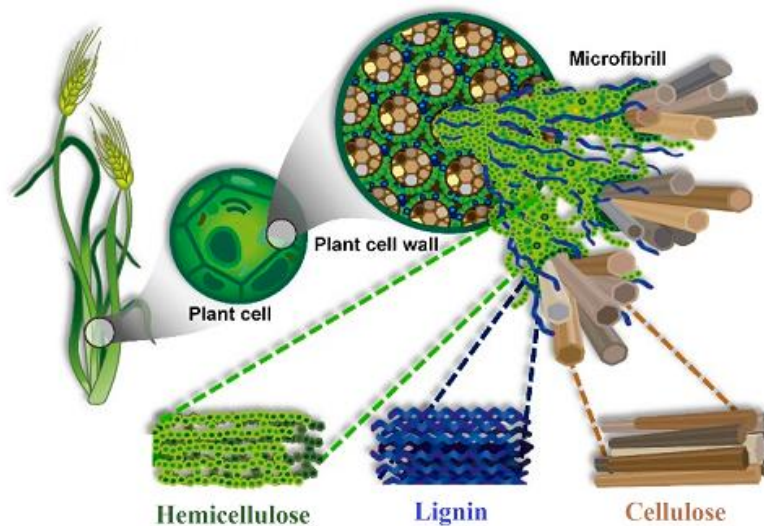


Figure 1.9 Lignocellulosic biomass structure

### *1.2.2 Lignocellulosic biomass treatments and lignin extraction*

The content of lignin varies considerably depending on the species of plants considered, usually decreasing from softwood to hardwood to grasses [18]. Moreover, approximately 50 million tons of lignin is produced annually by the chemical processing of pulp in bioethanol refineries and the paper industry [19].

The isolation of lignin from lignocellulosic biomass is achieved under different conditions, where the lignin is chemically degraded to low molecular weight fragments, with different physicochemical properties.

Therefore, the isolated lignin's properties do not depend only in the source, but also on the extraction's method. Generally, acid or base-catalyzed reactions are commonly used in the extraction of lignin [16].

At an industrial scale, four methods are generally employed for lignin extraction; these can be further categorized into two classes based on the presence or absence of sulfur.

The lignin-containing sulfur is extracted through the Sulfite and Kraft processes. On the other hand, the lignin without sulfur is isolated from Soda and Organosolv processes [20].

## **Sulfite process**

Sulfite-pulping process is a commonly used method for the production of commercial lignin. This involves the utilization of aqueous solutions containing different concentrations of sulfide or bisulfide salts of ammonium, magnesium, sodium, or calcium with a pH range of 1-13.5.

The reaction temperature is usually maintained between 140 and 160 °C. The lignin isolation with the sulfite-pulping process involves sulfonation of the aliphatic chain of the lignin and the cleavage of the  $\alpha$ -O-4-ether bond.

The liginosulfonates produced through this process are water-soluble and so easily dissolved in pulping liquor in an aqueous medium [16], [20].

## **Kraft process**

The most commonly used method for lignin pulping is the Kraft process, which produces lignin-containing sulfur.

Large fractions (98%) of lignin produced through the Kraft process are utilized for energy purposes through combustion, and merely minor fractions (2%) are used for material or chemical synthesis [19]. The Kraft process should be an advancement of the soda process; in fact, it involves the heating of pulping liquor with sodium-sulfide in addition to sodium hydroxide at a temperature between 150 and 180 °C [20].

The process of lignin depolymerization with the Kraft method is the same as in the soda process; the reaction proceeds with the cleavage of  $\alpha$ -O-4 and  $\beta$ -O-4 ether linkages and results in soluble fragments of lignin [19].

A minor fraction of resultant lignin is sulfated due to the presence of anions of hydrosulfide. A large fraction of lignin produced is sulfate-free and isolated via acidification and precipitation method [16].

## **Soda process**

The first pulping process applied for the isolation of lignin was the soda process, introduced by Watt and Burgess in 1854 [16].

The soda process involves heating the biomass in an alkaline aqueous solution (sodium hydroxide solution) at a temperature of around 160 °C [20].

The reaction proceeds with the protonation of phenolic hydroxyl moieties of lignin with simultaneous cleavage of  $\alpha$ -O-4 and  $\beta$ -O-4 bonds [19]. The lignin produced through the soda process is soluble in water, and due to acidification, it is isolated from pulp liquor through precipitation reaction [20].

## **Organosolv Process**

The most recent process used for the extraction of lignin at an industrial scale is the Organosolv process. This technique involves heating the biomass with a mixture of organic solvents for isolating lignin. Polar organic solvents such as methanol, acetone, ethanol, acetic acid, and formic acid are commonly used for the extraction process. The nature of the solvent used significantly determines the structure and properties of the isolated lignin [20].

### **1.3 Lignin properties and applications**

Native lignin is colorless, but acid-alkali treatment changes its color to dark brown [21]. The physical and chemical properties of the lignin vary with the extraction procedure and the monolignols content.

The functional moieties of lignin like carboxylic, phenolic hydroxyls, methoxy, aliphatic, and carbonyl groups depend on the monomeric linkages. Moreover, these moieties significantly contribute to the chemical modification of lignin [20]. The ether (C-O) and alkyl (C-C) bonds present in lignin are not sensitive to hydrolytic attacks, and therefore lignin is highly resistant to degradation [22].

The molecular weight of lignin ranges between 1000 and 20.000 g/mol. Since lignin always degrades during the extraction process, it is, therefore, difficult to predict the degree of polymerization attributed to the random repetition of subunits.

Consequently, its glass transition temperature ( $T_g$ ) differs from moisture content, molecular weight, extraction method, cross-link density and measurement method.  $T_g$  generally increases with the increase in molecular weight, and it usually falls between 70 and 170 °C [16].

Analogous discrepancies have been observed for the decomposition temperature; lignin source, extraction method and measurement techniques influence lignin decomposition processes, it has been observed in the range of 360–480 °C [23].

Among all the fractions of biomass, lignin is the one that is least reused due to its complex structure, recalcitrant nature, and heterogeneity that make its valorization relatively challenging.

Lignin comprises 30% of all the organic carbon present in the biosphere [24]; furthermore, the industry for the production of paper as well as the production of bioethanol produce copious amounts of waste lignin. Now, this is mainly exploited for heat production through combustion. In fact, out of 50 million tons of lignin produced by the paper industry in 2010, only 2% was utilized for the production of chemicals. However, the high aromaticity of lignin makes it a potential precursor for the production of a significant number of compounds [20].

In addition to the generation of added-value chemicals, lignin can be used for manufacturing high-performance materials like high-value polymeric materials, supercapacitors to adsorbents and electrode materials for biomedical application [20].

In 2014, the overall lignin market around the globe was valued at approximately US\$775 million; it has been predicted that this market will have an annual average growth rate of 2.5% [16].

Lignin is a great candidate for the fabrication of composite materials thanks to its several remarkable features such as bio-degradability, antioxidant activity, antimicrobial activity and reinforcing properties. Recently, composites based on lignin gained much attention, like high-performance composites [25].

Adding lignin to the materials, the degradation temperature and oxidation induction time of the composite increase considerably, but the tensile strength is not affected by the presence of lignin.

This goal is achieved either through chemical modification of lignin through esterification, phenolation, and oxypropylation reaction, or partial substitution of traditional materials by lignin.

Therefore, lignin has shown promising features for the preparation of phenol-formaldehyde resins, epoxy resins, polyurethanes, and graft copolymers [19].

Lignosulfonate and Kraft lignin, if combined with activated carbon, can be used in direct carbon fuel cells for the production of electricity.

Lignosulfonate showed better performance than Kraft lignin in these cells thanks to its higher hydrophilicity. High wettability of lignosulfonate also enhances electrochemical reactivity and electrical conductivity in fuel cells [16].

Moreover, a study reported the production of highly nanoporous carbon for supercapacitors using low-cost renewable lignin as a precursor [26].

A better control over the surface functional groups, pore structure and electrical conductivity of lignin-based carbon materials would enhance the electrocapacitive performance of electrodes for supercapacitors [27].



However, there are some problems associated with lignin for its use in energy storage devices, such as low electrical conductivity that make the active sites of lignin electrochemically inaccessible.

The solubility of some types of lignin like lignosulfonates in an aqueous medium can provoke the degradation of some active materials in an electrochemical device. The solution could be to manufacture hybrid capacitors using lignin in combination with metal oxides and conductive polymers; this would be a better approach to improve the electrode capacitance of supercapacitors [16].



Figure 1.10 Summary of current main applications of lignin

Therefore, lignin valorization may play a vital role in the context of sustainability; there is a need to focus on the development of efficient, economical, and green methods for the reuse of this green raw material (Figure 1.10) [28].

## 1.4 Lignin depolymerization products

At first, biomass must be processed in a way that effectively separates its significant fractions from each other: cellulose, hemicellulose, and lignin. The fractionation in this context does not refer to physical separation, as is the case of fossil crude oil distillation, but to a chemical disintegration process (for example, acid or basic treatment). These fractions must be purified and further reacted by chemical or biochemical processes in order to obtain higher-value products.

The utilization of only the carbohydrate fraction (cellulose and hemicellulose) of biomass for fermentation applications, for example, for the production of ethanol, neglect the beneficial synergetic effects of integrating lignin conversion into a biorefinery concept [29].

Therefore, the utilization of lignin in a useful way is essential; in particular, identifying products from lignin, through depolymerization, was more challenging because of lignin's complex nature as a feed. Often, rather than listing discrete chemicals, classes of chemicals were identified based on functionality.

The possible products have been evaluated based on several parameters, including currently available technology for their use with the degree of difficulty to develop it and likely acceptance in the products marketplace (known market or unknown market).

The compounds have been classified as high, medium, or low using the following criteria.

- **Technology degree of difficulty**

This evaluation considers the potential number of steps required in order to obtain the products and the relative difficulty of the same. For many of these compounds, there is not industrial experience; therefore, assessments according to this criterion are based on information from open literature.

- **Market**

This criterion evaluates both potential market size and product value using standard reference sources.

- **Market risk**

The market risk evaluation considers the potential risk of bringing a lignin-derived product into the market. An example of a risk considered "low" would be the introduction of a lignin-based source of BTX or syngas. A risk considered "high" included compounds currently not recognized as chemical building blocks (i.e., eugenol).

- **Building block utility**

This criterion assessed the potential of a candidate compound to serve as a starting material for a larger group of derivatives.

- **Mixture**

This criterion evaluates if a product could be derived from lignin as a single compound or instead as a complex mixture [30].

In general, the depolymerization products of lignin are classified into three main categories: power, fuel and syngas; macromolecule; aromatics and miscellaneous monomers.

Concerning the last category, lignin is the leading renewable source of an essential and high-volume class of compounds, the aromatics [30].

Therefore, direct and efficient conversion of lignin to obtain high-volume, low-molecular-weight aromatic molecules is an attractive goal, but among all the uses of lignin is the most challenging from a technological point of view [29].

Considering that lignin has different structures depending on the biomass from which it derives, two main technology categories of lignin degradation have been developed, leading to two different compound classes.

1. The first compound class arises from aggressive and non-selective depolymerization in the form of C-C and C-O bond rupture; it is composed of aromatics in the form of BTX plus phenol. This class also includes aliphatics in the form of C1 to C3 fractions (Figure 1.1). Moreover, there is the possibility of forming some C6-C7 cycloaliphatics as well.

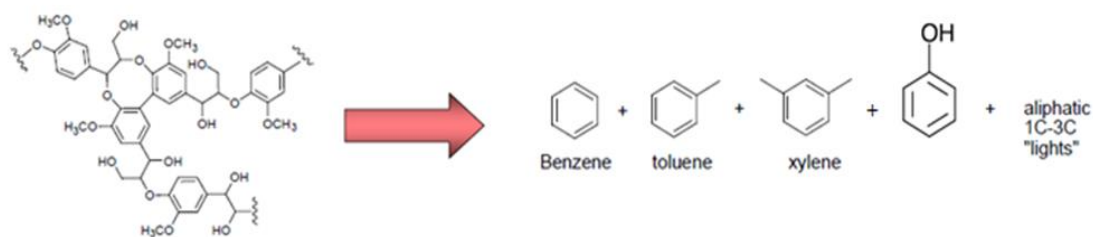


Figure 1.11 Conversion of Lignin to BTX chemicals, phenol and aliphatic fractions.

Conventional petrochemical processes could easily and directly produce all these products. This kind of depolymerization is part of the long-term opportunity but is likely to be achievable sooner than highly selective depolymerizations [30]

Regarding xylene, the most likely form of xylene that could be produced from lignin is the meta isomer. However, isomerization of meta xylenes to para-xylene is commercially done today; the latter isomer is critical for the polyester markets.

For each of the compounds obtained from aggressive lignin degradation, several industrial processes to obtain derived chemicals are known (Figure 1.12; Figure 1.13; Figure 1.14; Figure 1.15). This proves the enormous potentiality of the non-selective depolymerization [30].

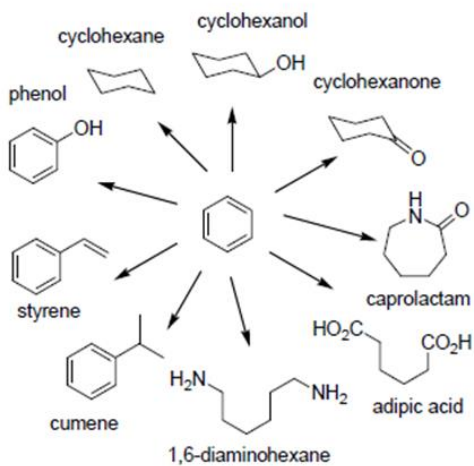


Figure 1.12 Examples of Benzene Derived Chemicals

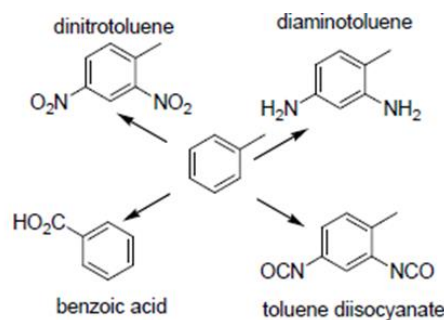


Figure 1.13 Examples of Toluene Derived Chemicals

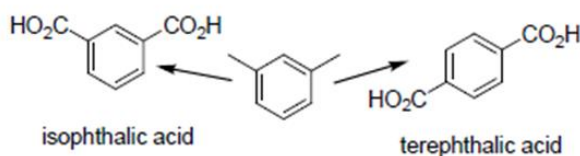


Figure 1.14 Examples of Xylene Derived Chemicals

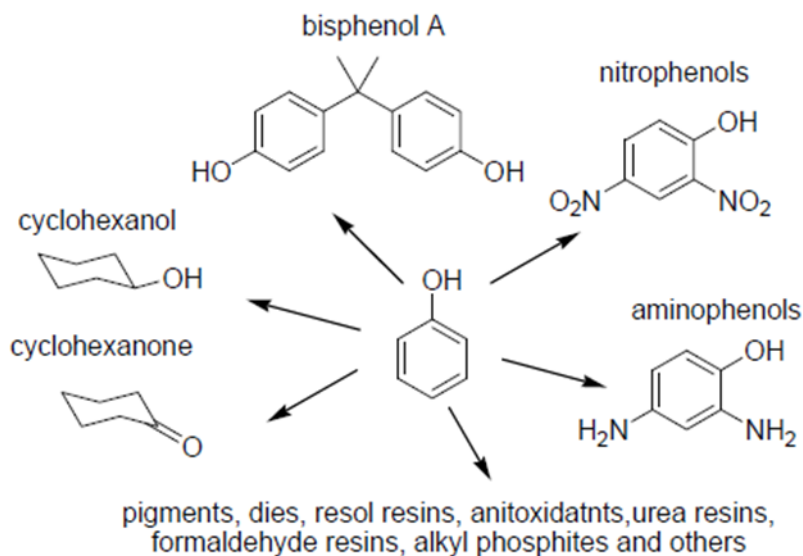


Figure 1.15 Examples of Phenol Derived Chemicals

The low-molecular-weight aliphatics (C1-C3, etc.) products may include formic or acetic acids as well as aliphatics and olefins. Such low-molecular-weight materials could be applied to syngas (reforming), alkylated gasoline or propane (LP) fuels. Alternatively, this material could be dehydrogenated to provide low-molecular-weight olefins, which could be applied to power or heat production to provide the energy to drive the lignin degradation process [30].

2. The second class of compounds derives from very selective lignin depolymerization, also this invokes C-C and C-O bond rupture. In this case, the result is a complex aromatics mixture that is difficult to make via conventional petrochemical way (Figure 1.16). These compounds may be highly desirable if they can be produced in reasonable commercial quantity [30].

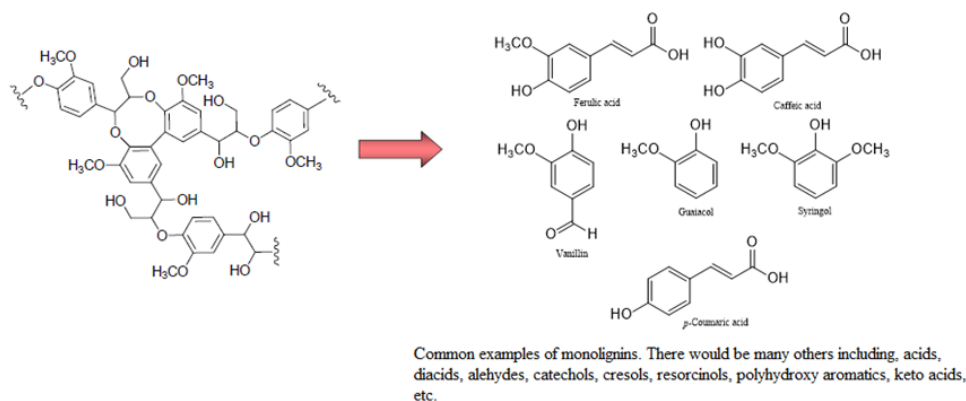


Figure 1.16 Conversion of lignin to the complex aromatics mixture.

However, two barriers would need to be overcome.

- In order to obtain the monomeric lignin building block structures, a technology which can allow highly selective bond-scission must be developed. The development of this technology will be more complicated than the more aggressive one.
- Markets and applications for monomeric lignin building blocks would need to be developed.

For the reasons listed above, this process is longest-term and currently has an unknown market for large-scale use. Most of the chemical industry uses raw materials constituted from pure-molecules; instead, lignin is composed of a mixture of products; this is the main challenge for lignin processing. Therefore, a new/improved separation technique for aromatic lignin monomers constitutes a related challenge.

In general, phenols are extremely interesting as building blocks of new synthetic bioplastics, phenol/epoxy-formaldehyde resins and polyurethane materials. These are just a few options for sensible exploitation of the natural lignin polymer. Moreover, phenols also can help with improving the physical properties of fuels, since certain alkylphenols are being used as antioxidants in diesel at present.

However, the precise chemical depolymerization pathways are still not completely clear, which is mainly due to the very complex nature of natural lignin, resulting in an unpredictable reactivity and complex reaction products.

Furthermore, lignin conversion to high molecular weight molecules was evaluated, for example, the production of compounds obtained through the lignin chain extension using propylene oxide or ethylene oxide. Chain extension can significantly alter the physical property of lignin, even transforming solid kraft lignin into a wax or a viscous fluid [30].

## 1.5 Degradation processes of lignin.

The depolymerization of lignin is considered one of the most critical challenges in lignin utilization. The choice of the type of treatment to depolymerize lignin will depend on the desired final applications (Figure 1.17).

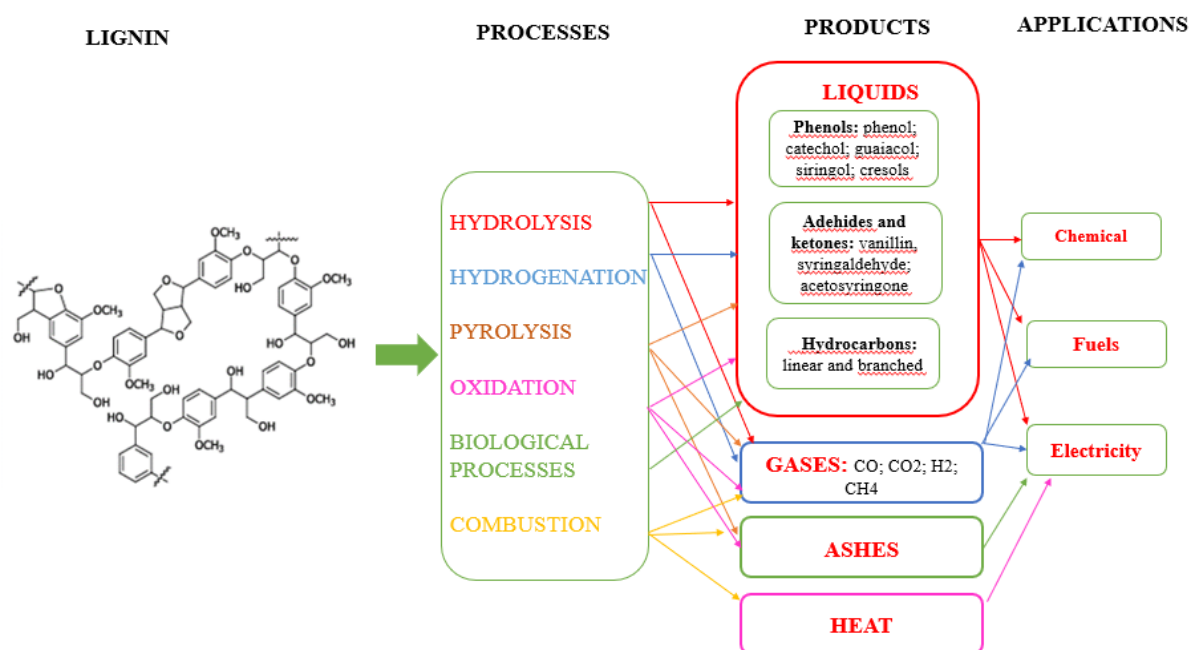


Figure 1.17 Flowchart of processes for the transformation of lignin and its potential products.

Many methods for depolymerizing lignin have been analyzed, and the main ones are:

- Thermochemical treatment:
  - I. Thermal pyrolysis
  - II. Microwave pyrolysis
- Hydrolysis
- Hydrogenolysis/hydrogenation

- Biological treatment
- Oxidative lignin depolymerization

### *1.5.1 Thermochemical methods for lignin treatment*

It is known that increasing temperature is a standard and effective treatment for destroying chemical bonds. Thus, thermochemical methods have been studied in great depth. These treatments may or may not require the utilization of catalysts [31].

#### **Pyrolysis**

Pyrolysis is one of the most widely utilized methods for lignin conversion. This is a thermal treatment of organic substance without or under a limited amount of oxygen, due to the absence of oxygen, the lignin is degraded but does not further convert to carbon dioxide [31].

After the pyrolysis process, lignin is decomposed in gaseous products and solid residues at high temperature. The latter consists of brown tar containing compounds of high molecular weight [31]. This fraction is called bio-char, and it is used to produce carbon-based materials [32].

Instead, the gaseous products, that in general includes substances of lower molecular weight are divided into two categories:

- The condensable is constituted from monomeric phenolic compounds. Some products examples are guaiacol, catechol, syringol, phenol, 4-vinyl phenol, 2-methoxy-4-vinyl phenol, and 2,6-dimethoxy phenol [31]. This fraction is called bio-oil and is the most desired, as it can be used to produce fuels or other chemicals of interest. The phenolic compounds, when they are in the form of gas, can further condense to other dimers and oligomeric products [32].
- The non-condensable, which remain in the gas phase, represents what is called the pyrolytic gas. The main constituents of this fraction are carbon monoxide and hydrogen that can be processed to produce syngas for other applications [32].

The pyrolysis products contain vast amounts of various aromatic monomers, and for that reason, pyrolysis can be an effective method for converting lignin into other biomaterials [32].

In general, increasing the severity of the reaction conditions can lower the molecular weight of the depolymerized lignin fragments. Moreover, the depolymerized products change based on several factors: the source of lignin, the solvent, the catalysts, and the reaction times.

Lignin depolymerization through pyrolysis usually starts with the cleavage of weak linkage at low temperatures, breaking the stronger ones at higher temperatures, which usually reach up to 450 °C.

An essential problem of this method is the formation of coke and polycyclic aromatic hydrocarbons (PAHs); these compounds lower the yields of the monomer.

It is known that the methoxyl and methyl groups of the lignin are one of the main reasons for the coke formation so, due to the high percentage of the methoxyl group presented in the syringol unit, syringol has a higher chance of forming coke during pyrolysis.

A solution would be to increase the pyrolysis temperature from 300 °C to 700 °C; in this way, 60% of the char formation could be suppressed, and the yields of monomers could be increased [31].

Nowadays, pyrolysis is commonly combined with various catalysts and solvents for improving its performance; one of the well-known catalysts is zeolite [22]. Toluene and p-Xylene were the most abundant hydrocarbons produced when micro-porous zeolite catalysts were used in the reaction [33].

The low-selectivity and the severe conditions of the reaction limited its application in the production of specific chemicals.

## **Microwave-assisted depolymerization**

Microwaves can be an alternative method for heating, and it has been widely applied in lignin thermochemical conversion [31].

The microwave exposes the lignin molecule to a high level of electromagnetic radiation; this radiation causes the rotation of the polar molecules resulting in a generation of a massive amount of heat, which causes the final lignin degradation.

Therefore, compared with traditional heating, microwaves can prevent physical contact between the heat source and the biomass, which can avoid the surface overheating and reduce the reaction time [34].

The results indicated that the use of microwaves could specifically cleave the linkages C $\alpha$ -C $\beta$  below 160 °C, and it can increase the soluble proportion from 67% to 86% compared to ordinary thermal pyrolysis.

The microwaves are also proposed as an economical method for biomass heating. Furthermore, microwaves can be accurately controlled during the operation.

It is essential to consider that metal salt as a catalyst can improve the reaction selectivity of this method [31].



A study about the microwave-assisted acid pre-treatment of alkali lignin showed that this method can increase the yields of phenolic compounds like catechol, 2- methyl phenol and decreases the yields of guaiacols like creosol, eugenol [35].

### *1.5.2 Depolymerization by hydrolysis*

Many researchers have focused on this lignin depolymerization method, which tries to break the main C-O bonds present in lignin with water at high temperature (and usually also within acid or base catalysts). Various parameters that influence the hydrolysis process are studied:

- Thermochemical matrix transformations that determine the thermal stability of the different lignin bonds (intramolecular and intermolecular)
- Lignin solubility in the reaction system
- Morphological changes underwent by lignin during the hydrolysis process

At the end of the hydrolysis process, a mixture of products with different molecular weights is obtained, a detailed method for the separation of the primary monomers generated during this process is elaborated. This comprises many techniques, including liquid-liquid extraction, distillation, chromatography, and crystallization [36].

A critical issue for this technique is to minimize the formation of char and avoid lignin repolymerization, and capping agents can be used for such purposes. Capping agents also enhance the yields of low molecular weight liquid products by stabilizing the present phenolic compounds. Phenol was the most used capping agent, its action is reported by Yuan et al [37].

The activity of different catalysts, both homogeneous (acids and bases) and heterogeneous (metal catalysts), has been evaluated. It has been noted that the yield of monomers is directly proportional to the concentration of the catalyst [22].

1. **HOMOGENEOUS CATALYSTS:** In this case, at the end of the hydrolysis reaction, both an aqueous fraction (60% by weight), which contains monomers and oligomers, and a solid fraction (30% by weight) that is composed mainly of ashes are obtained. The reaction has been studied at different temperatures, and it has been noted that the yield of monomers grows with increasing temperatures [22].
  - Among the basic catalysts, the best returns have been achieved with sodium hydroxide. In fact, for example the depolymerization of Kraft lignin into polyols of moderately high hydroxyl number was successfully obtained by Mahmood et

al. without using any organic solvent or capping agent but only direct hydrolysis using NaOH as a catalyst at 250°C [38].

By using this catalyst, unfortunately, also unwanted re-polymerization reactions take place. These cause a residual lignin amount that can even reach 45%.

- Acid catalysts are mostly Brönsted acids and play a dual role:
  - I. Participation in the depolymerization of lignin.
  - II. Stabilization of the monomers that are forming. In this way, re-polymerization is also avoided [22].

2. HETEROGENEOUS CATALYSTS: The utilization of heterogeneous catalysts has only recently been investigated for hydrolysis. For example, nanoparticles of Ni<sup>(0)</sup>, Fe<sub>3</sub>O<sub>4</sub> (NiMgAlO)<sub>x</sub> and nanofoils of NiO<sup>(111)</sup> have been used, the best results with these catalysts showed yields of about 45% for a liquid fraction with molecular weights between 100-500 (monomers and dimers) with conventional thermal heating [39].

Another kind of heterogeneous catalysts applied to this process are the carbonates. In this case, lignin was treated by liquefaction in a basic medium in the presence of carbonate-type catalysts, such as RbCO<sub>3</sub> and CsCO<sub>3</sub>. The main products have proven to be 2-methoxyphenol and 1,2-benzenediol (or catechol) [40].

All the catalysts reported a higher selectivity towards catechols and of all the monomers obtained, catechol and guaiacol proved to be the majority products.

Of course, the lignin depolymerization can be realized even without catalysts [22]. The thermal process **without the catalysts** gives as main products 4-methyl-phenol, 2-furan carboxaldehyde and 2-methoxy-phenol [33].

### *1.5.3 Depolymerization by hydrogenolysis*

During the depolymerization process by hydrogenolysis/hydrogenation, lignin is subjected to a reduction reaction (at moderate or high pressures and temperatures) in the presence of H<sub>2</sub>, water, and a catalyst with hydrogenating properties.

The hydrogen needed for this process can be generated in situ by promoters (or donors) such as formic acid or methanol [22].

It is a process usually catalyzed by acids, and highly hydrogenated aromatic and aliphatic hydrocarbons are obtained.

Yan et al described a two-stage hydrogenolysis process for the conversion of the lignin in hydrocarbons and methanol.

- The first stage provides the lignin transformation into an aqueous or organic acid medium (solvent: dioxane), using catalysts Pt/C or Rh/C at 474K and 4 MPa of H<sub>2</sub>. The best results are obtained using H<sub>3</sub>PO<sub>4</sub> (1% in water) in dioxane (50%) and as a catalyst Pt/C. In this way yields of 46% and 12% respectively for monomers and dimers are obtained.
- In the second stage, the products obtained in the previous step are converted in alkanes and methanol with almost quantitative yields, using H<sub>2</sub> and a Pd/C catalyst. Finally, the yields obtained from alkanes (C<sub>8</sub>-C<sub>17</sub> hydrocarbons) and methanol were 90% and 95% molar, respectively [41].

#### *1.5.4 Biological depolymerization*

Various chemical and thermochemical treatments have shown great potential for highly efficient lignin depolymerization. However, both of them require relatively severe reaction conditions, including high temperature and pressure.

Furthermore, these processes usually have some environmental risk factors which may cause damage to the environment and require a massive amount of energy for operation.

Therefore, the use of biocatalysts has been considered as an alternative method for lignin depolymerization; this is usually considered as an environmentally friendly catalyst because the enzymes or microbes involved in the biological treatments are usually from nature and they are not harmful to the environment.

Several enzymes can specifically catalyze specific reactions; thus, the use of biocatalysts can improve the reaction selectivity and suppress undesired side reactions such as repolymerization. Moreover, the biocatalyst required relatively milder reaction conditions when compared to others; thus, it lowers the formation of char.

Biocatalysts are still not close to actual application in industry, and there are many challenges to be solved before applying the enzyme or bacteria in lignin valorization. The major problem is the low efficiency of converting lignin polymer to monomers or even other chemicals [31].

## **Biocatalyst types:**

- **ORGANISMS:** Numerous organisms have developed an effective metabolic system and methods to degrade and convert lignin to aromatic compounds and further convert these compounds to energy via multiple pathways [42].
- **BACTERIA:** Bacteria are considered less effective than fungi in lignin degradation, and one of the reasons is that there are fewer species of bacteria which are able to degrade lignin. However, several strains of bacteria have been identified that are suitable for the depolymerization and conversion of lignin [43].
- **FUNGI:** The fungus is one of the most studied microbes for lignin depolymerization and degradation. They show a higher conversion rate and depolymerization efficiency when compared to bacteria. Due to strong ability in degrading lignin, white-rot fungi have been used in various industrial applications. White rot fungi are the most effective microbe for degrading the native lignin in the wood [31].
- **ENZYMES:** Enzymes that can effectively degrade lignin have been isolated from fungi or bacteria, and these enzymes have been applied in several vitro experiments for lignin depolymerization or conversion study. Using in vitro enzymatic reaction can avoid several drawbacks, including reducing the culture time and the direct encounter between microbe and substrate [44].

Biological depolymerization of lignin will yield a range of substituted phenols and propyl phenols, as well as oligomers of these [33].

The biocatalytic conversion, as an alternative to the chemical one, to obtain commercial products like vanillin has been of considerable interest.

Concerning the vanillin production, a potential starting point would be ferulic acid, and a possible conversion is a two-step enzymatic conversion starting with a decarboxylation giving 4-vinylguaiacol, which is subsequently oxidized to vanillin. This aim can be achieved by a whole-cell catalyst in a suitable host (e.g. *Escherichia coli*) which overexpressing the two enzymes [45].

Vanillin can, in turn, be reduced to vanillyl alcohol or oxidized to vanillic acid.

Purified ferulic acid may be more valuable than the products that can be obtained from it, therefore, the economics of the process to obtain vanillin depend on the availability of a low-cost source of ferulic acid [33].

Rosazza et al. reviewed possible bioconversion routes of ferulic acid, including, apart from vanillin, also products such as caffeic acid, 4-vinylguaiacol, guaiacol, dihydroferulic acid, and polymers derived from ferulic acid [46].

In particular, initial demethylation of ferulic acid, which is a rather common microbial reaction, yields caffeic acid, which is a starting point for new product family. In fact, in the absence of oxygen, caffeic acid may be further converted through dehydroxylation to cinnamic acid, and then reduced to phenyl propionic acid. The latter can in turn, subsequently be converted to phenyl acetic acid [33].

The main challenge when a specific monomer from the lignin depolymerization mixture must be used is no doubt separation. A different approach is, therefore, to work with the entire mixture as a carbon source in a complete biological conversion. In the “sugar-platform” biorefinery concept, the depolymerized mixture of carbohydrates is fermented into a wide range of desired end-products (e.g. alcohols, carboxylic acids, polyols) using genetically engineered microbes such as yeast [47].

### *1.5.5 Oxidative lignin depolymerization*

Oxidation is one of the most common methods for lignin depolymerization and degradation [31]. This alternative method involves treating lignin at moderate pressures and temperatures in the presence of an oxidizing agent, preferably O<sub>2</sub> or air, and a catalyst. [22].

Hydrogen peroxide and potassium permanganate are also widely used as oxidants for chemical oxidation in industry or the laboratory due to their high availability, low cost, and ease of production that lower the reaction time and temperature and may enhance the reaction selectivity [48].

Unfortunately, hydrogen peroxide also causes over-oxidation, which leads the aromatic or ring-opened phenolic compounds to become alkylic compounds.

Excessive oxidation makes the product non-specific and difficult to control; this could increase the complexity of the mixture produced [31].

Several aldehydes (vanillin, syringaldehyde, p-hydroxybenzaldehyde) have been obtained by lignin oxidation in a basic solvent and using perovskites as catalysts. Perovskites which presented the best yields of the mentioned aldehydes are La<sub>0.8</sub>Sr<sub>0.2</sub>MnO<sub>3</sub> e LaSr<sub>0.2</sub>Mn<sub>0.8</sub>O<sub>3</sub> [49].

Also, the oxide type perovskite  $\text{LaCoO}_3$  was studied as catalyst for the lignin oxidation (120 °C, 20 bars of  $\text{O}_2$  reaction and 3 hours), aldehydes in the following selectivity order syringaldehyde > vanillin > p-hydroxybenzaldehyde were produced. The analysis of the reaction mechanism involves the reaction of lignin molecules with oxygen molecules adsorbed on cobalt. This catalyst showed reusability five times without showing a significant reduction in its activity [50].

pH plays an essential role in the oxidative depolymerization process of lignin: in fact, the reaction seems favored at low pH when high ionic forces are present [51].

Vanillin is one of the most important aromatic aldehydes on an industrial level, and it can be obtained through lignin oxidation. Several tests for vanillin production have been conducted in different reactor types, namely: fixed bed reactors that use ion exchangers, continuous reactors with packed columns, and discontinuous suspended reactors [22].

## **Electrochemical oxidation**

Electrochemical oxidation (EO) could be another alternative for lignin degradation, which can be controlled by the manipulation of the electrode potential, which can target the cleavage and formation of specific bonds. Other relevant parameters for electrochemical depolymerization are the current density, the electrolyte, and the electrode material.

Electrochemistry has met the growing need to develop sustainable chemical processes, EO, uses mild temperature and pressure conditions, contrariwise the processes described so far require high T and P. Electrochemistry avoids the use of toxic and difficult to dispose of oxidants; moreover, these reactions can be supported by electricity obtained from renewable sources.

The challenges of EO include:

- High cost of electrode materials such as noble metal electrodes like Pt
- Noble metals possible deactivation during the reaction
- Low yields of monomers

Lead dioxide is one of the common active catalysts for lignin EO; however, environmental regulations limit the use of lead, so other metallic catalysts are being sought to replace it, for example Ni and Co [17].

## 1.6 Lignin depolymerization catalysts

Almost all lignin degradation methods also require a catalyst. The chemical catalysts used for lignin depolymerization can generally be divided into five different categories:

- Acid-catalyzed
- Base catalyzed
- Metallic catalyzed
- Ionic liquids-assisted catalyzed
- Supercritical fluids assisted catalyzed.

Different chemical catalysts can be combined at the same time or applied at a different stage of the depolymerization process to improve efficiency and obtain the desired products. Reactions involving the use of a catalyst provide milder conditions and higher selectivity, but environmental damage is also greater using chemical catalysts [31].

### **Acid catalysts**

Acid-catalyzed depolymerization is widely studied, but there are several disadvantages which have to be overcome: the depolymerization process requires relatively severe reaction conditions like high temperature, high pressure, long reaction time and involves the use of corrosive chemicals; the waste products from the depolymerization process are considered environmental pollutants; the intermediates of depolymerized products could condense together and form macromolecules which could lower the yields of the desired products [52].

The most used acid catalyst is hydrochloric acid; other common acids have also been investigated. The products of depolymerization under these conditions contain a high amount of hydroxyl and carbon content [31].

### **Base catalysts**

The most used base catalyst is sodium hydroxide, and it is indicated that its use can increase the yield of depolymerized lignin; this catalyst is also widely utilized due to its low cost.

Using strong bases, like KOH, NaOH, can convert and produce more depolymerized products rather than the weak bases, like  $\text{Ca}(\text{OH})_2$ , LiOH. The strong base can also reduce char formation.

Repolymerization is also observed during base-catalyzed depolymerization, and this could lower the depolymerization efficiency and increase the amount of residual lignin [53].

## **Metallic catalysts**

The use of acid or base catalysts mainly focuses on the cleavage of the ether bonds. However, with these methods, it is difficult to produce specific products. Furthermore, base or acid-catalyzed degradation usually requires relatively severe reaction conditions, like high temperature and high pressure. Thus numerous studies are looking for methods or catalysts, which can catalyze the reaction under a mild condition [31].

Several metals have been selected as potential catalysts for further study. The most analyzed is nickel that can be a potential metallic catalyst to produce phenolic chemicals; in fact, it is able to hydrolyze the carbon-hydroxyl linkage. Moreover, nickel can catalyze the depolymerization process under a mild reaction temperature, and if it is combined with another metal, it can form bimetallic alloy Ni-M which can increase reactivity and selectivity due to the synergistic effect [54].

However, there are several limitations of using the nickel bimetallic catalyst:

- The noble metals used in the bimetallic alloy are expensive. Using them could increase the cost of the depolymerization.
- Noble metallic catalysts also cause over-hydrogenation of the aromatic compounds, which decreases the yield of the phenolic products.

## **Ionic liquid assisted catalysis.**

Ionic liquid is widely defined as salts with a melting point of less than 100 °C. They can potentially be used in an industrial process because: they have flexible characteristics that can be modified by changing the cation and anion in the salts; it is possible to control the degree of oxidation; they are able to stabilize the intermediates during the lignin depolymerization.

Other properties like low volatility, non-flammability, and high thermal stability also favor industrial application [55].

Ionic liquid is usually used as a solvent and cooperates with other catalysts to depolymerize lignin.

The high cost of ionic liquid restricts its application in industrial operation; besides, ionic liquid usually interacts with the aromatic compound derived from lignin; thus, it causes the difficulty in separating the ionic liquid from the monomeric products [31].



## Sub- or supercritical fluid assisted catalysis

When solvents are subjected to high temperature and pressure, they become sub- or supercritical fluids and exhibit several different properties than when they are at room temperature, in particular, supercritical fluids usually contain both liquid and gas properties. Moreover, low viscosity and high diffusivity allow the fluids to permeate into the lignin molecule structure.

For example, water under supercritical conditions exhibits a low dielectric constant, which is similar to a non-polar organic solvent; thus, water in these conditions can solubilize several organic compounds effectively [56].

It has been indicated that the repolymerization of lightweight molecules is observed in the supercritical condition; for this reason, phenol can be added to lignin to inhibit char formation and repolymerization. In particular, phenol can react with the decomposed fragment derived from lignin and block its active site to prevent the cross-linking reaction and repolymerization. However, the use of phenol for suppressing repolymerization is expensive, which would increase the cost of the overall process.

In conclusion, the high cost and severe reaction conditions restrict the application of supercritical fluids. Moreover, the rapid hydrolysis of lignin in supercritical fluid enhances the difficulty of mechanism study and intermediate detection; thus, the chemical conversion pathway needs further study in order to improve selectivity and product separation [31].

## 1.7 Electrocatalysis

The redox reactions which involve charge transfer are defined electrochemical reactions (1.1).



The primary function of the electrocatalysis is to allow the charge transfer and thus speeding up the redox reaction. The catalytic activity of the material, which depends on electronic, geometric and intrinsic surface properties of the catalyst itself, influences the final rate of the reaction; the efficiency of the process and the selectivity of the desired product.

The degree to which an electrode will influence the reaction rates is different for different electrochemical reactions and for different materials from which the electrode is made. In complex electrochemical reactions having parallel pathways, such as a reaction involving

organic substances, the electrode material might selectively influence the rates of specific individual steps and thus influence the selectivity of the reaction [57].

The electrode could be “inert” towards the electrochemical reaction; this means that it is not consumed and that there is no stoichiometric involvement of the metal of which the electrode is made in the electrochemical reaction. In this case, the electrode has the sole task of allowing the transport of electrons necessary for the reaction to take place between the species dissolved in solution, called electrolytes, which are the substances that actively participate in the reaction. In electrocatalysis, the working electrode, which also acts as an electrocatalyst, is not inert in the full meaning of the term. As it is not only needed to feed the current through the electrolyte but actively intervenes in the reaction influencing its stoichiometry [58] [59].

Electrocatalyst can be deposited on the surface of the electrode or act as the electrode itself (bulk electrode); for this reason, in general, the reaction happens on the electrode surface. In particular, the catalyst adsorbs reactant on its surface to form the adsorbed intermediate; in this way, the charge transfer between the electrode and reactant is facilitated.

The exchange of interfacial charge during an electrochemical reaction can involve two types of mechanisms:

1. **Mechanism of the external sphere:** the interaction between the reagents and the electrocatalyst is direct but very weak or almost absent. For this reason, charge transfer kinetics and thermodynamics are not related to the electrode structure.
2. **Mechanism of the internal sphere:** the interaction between the species involved in the reaction and the electrode is intense and often involves breaking or bonding. Therefore, interfacial charge transfer and the rate of the reaction are extremely sensitive to the characteristics of the surface of the catalyst. Sometimes, the adsorption phase can take place simultaneously with the electronic transfer phase; in this way, the intermediates formed can be subjected to further complex electrochemical and chemical mechanisms, before the final product is formed.

The second type of mechanism is much more interesting as regards electrocatalytic applications [58].

The electrocatalytic science has been developed investigating the cathodic hydrogen evolution. This reaction has been chosen as several metals can catalyze it. In particular, several studies have been founded at the end of the nineteenth century, which investigated this reaction at a given potential. It has been noticed that the rate of the reaction varies by several orders of magnitude among the various metals. Further tests were made with the purpose to observe the

current differences generated for the same reaction with different electrodes, always at the same applied potential.

The processes and the electrocatalytic phenomena are substantially studied in aqueous solutions at temperatures that generally do not exceed 150 °C [1].

### *1.7.1 Evaluation of the performance of the electrocatalyst*

Many electrocatalytic kinetic parameters are utilized to evaluate the performance of electrocatalysts fairly. These parameters are crucial and can offer insightful information with regards to the mechanism of the electrochemical reaction.

- **Overpotential ( $\eta$ )** is one of the essential descriptors to evaluate the performance of target electrocatalysts. The applied potential value, E, depends on the thermodynamic contribution deriving from Nerst's law (eqn. 2), and also on a kinetic contribution which is a function of the dissipated energy which is called overvoltage  $\eta$  (eqn.1).

In an ideal world, the applied potential for driving a specific reaction should be equal to the potential of the reaction at equilibrium. In reality, it is never the case, in fact, the applied potential commonly is much higher than that at equilibrium in order to overcome the electrode kinetic barrier (eqn.1), which is composed of the following contributions:

1. Cathodic overpotential  $\eta_{Cat}$ : It corresponds to the overvoltage in the half-cell where the reduction half-reaction takes place.
2. Anodic overpotential  $\eta_{An}$ : It corresponds to the overvoltage in the half-cell where oxidation half-reaction takes place.
3. Ohmic drop  $\eta_{\Omega}$ : corresponds to the potential drop determined by the electrical resistance of the homogeneous phases (electrodes and electrolyte bulk).

$$\eta = \eta_{Cat} + \eta_{An} + \eta_{\Omega} \quad (1)$$

According to the Nernst equation (eqn.2), the equilibrium potential ( $E_{eq}$ ) can be expressed as eqn. below, where  $E^{0'}$  is the formal potential of the overall reaction. T denotes absolute temperature, R is the universal gas constant, F is Faraday constant, n is the number of transferred electrons in the reaction, and  $C_O$  and  $C_R$  are the

concentrations of oxidized and reduced reagents, respectively.  $E_{eq} = E^{0'}$  when the solutions have a concentration of 1M and solids have activity equal to one.

$$E_{eq} = E^{0'} + \frac{RT}{nF} * \ln \frac{C_o}{C_r} \quad (2)$$

The overpotential ( $\eta$ ) is a difference between the applied potential under current conditions (with any circulating current intensity value) and potential under equilibrium conditions (i.e. in the absence of current circulation) (eqn.3). It is essential to try to reduce this value to a minimum so that we can work as close as possible to the thermodynamic equilibrium conditions. Through the electrocatalyst utilization, it is possible to reduce to the minimum this dissipation of energy  $\eta$ .

$$\eta = E - E_{eq} \quad (3)$$

Notably, the overpotential ( $\eta$ ) is commonly referred to a value that has to be applied to achieve a specified current density, and a lower overpotential of an electrocatalyst in the system indicates its superior electrocatalytic ability for the target reaction.

- **Exchange current density ( $i^0$ ):** Another critical indicator for electrocatalytic kinetics is the current exchange density ( $i^0$ ). For a given reaction, the overall current ( $j$ ) (eqn.4) is the sum of anodic ( $j_a$ ) and cathodic ( $j_c$ ) currents and the contributions from each anode and cathode ends are shown in eqn.5 and 6, respectively.

$$j = j_a + j_c \quad (4)$$

$$j_a = nFk_a[C_r] \exp\left(\frac{\alpha_a nFE}{RT}\right) \quad (5)$$

$$j_c = nFk_c[C_o] \exp\left(-\frac{\alpha_c nFE}{RT}\right) \quad (6)$$

$K_a$  and  $\alpha_a$  represent the rate constant of the anodic-half reaction and anodic transfer coefficient, respectively.  $K_c$  and  $\alpha_c$  have the same meaning in the cathodic-half reaction.

At equilibrium ( $\eta=0$ ;  $E=E_{eq}$ ) conditions, the anodic ( $j_a$ ) and cathodic ( $j_c$ ) currents are equal to each other, but with opposite sign, which results in a zero total net current ( $j=0$ ).

The magnitude of intercepts (the value of the cathode and anode current at equilibrium) at  $\eta=0$  refers to exchange current ( $j^0$ ), it is customary to divide exchange current ( $j^0$ ) by

the area of the electrode (A), and the exchange current becomes exchange current density (eqn.7).

$$\frac{j_0}{A} = i_0 \quad (7)$$

The magnitude of exchange current density ( $i^0$ ) reflects the intrinsic bonding/charge transferring interactions between electrocatalyst and reactant. A high exchange current density ( $i^0$ ) is usually a good indication of being an excellent electrocatalyst for the target reaction.

Although the exchange current density ( $i^0$ ) is a good approach to evaluate the electrocatalytic ability of a catalyst, it is a great challenge to directly find the exchange current density ( $i^0$ ) since we can only obtain overall current density ( $i$ ) from the experiment ( $i=0$  when  $i_a = j_c = j^0$ ). One can still calculate the exchange current density from the Tafel equation.

- **Tafel equation and Tafel slope (b).** For practical purposes, is required to apply a high overpotential ( $\eta$ ) in order to have a significant magnitude of current density ( $i$ ). In general, a smaller overpotential ( $\eta$ ) with a faster increase in corresponding current density ( $i$ ) is desired. The current density ( $i$ ) and the applied overpotential can be described according to the well-known Butler–Volmer equation (eqn.9).

From the Butler–Volmer equation, under high anodic overpotential conditions, the overall current is mainly attributed to the anodic end while the contribution from the cathodic part is negligible. Accordingly, the Butler–Volmer equation can be simplified in what is called Tafel equation (eqn.8).

$$i \approx i_0 \exp\left(\frac{\alpha_a n F \eta}{RT}\right) \quad (8)$$

$$i = i_0 \left[ \exp\left(\frac{\alpha_a n F E}{RT}\right) + \exp\left(\frac{\alpha_c n F E}{RT}\right) \right] \quad (9)$$

By translating the Tafel equation to logarithm function the eqn.8 can be re-written as eqn.10, where the exchange current density ( $i^0$ ) and Tafel slope (b) can be calculated accordingly. The Tafel slope (b) can be expressed as eqn.11, and from this one can understand that the definition of Tafel slope (b) is “how fast the current increases against overpotential (Z)” and its value mostly depends on the transfer coefficient ( $\alpha$ ).

$$\log(i) = \log(i_0) + \frac{\eta}{b} \quad (10)$$

$$b = \frac{\partial \eta}{\partial \log(i)} = \frac{2.303RT}{\alpha F} \quad (11)$$

A smaller Tafel slope (b) indicates that current density can increase faster with smaller overpotential ( $\eta$ ) change which implies functional electrocatalytic kinetics. Besides, Tafel slope (b) provides valuable and insightful information toward the mechanism of the reaction, especially for elucidating the rate-determining step. This information can be beneficial for understanding the fundamental behaviour between electrocatalyst and reactant [59].

### 1.7.2 Electrocatalytic kinetics

The increase in the speed of a catalyzed reaction compared to one that is not is due to the rapid formation and decomposition of intermediates that derive from the reaction between two or more reagents and the catalyst itself. Considering Arrhenius integrated kinetic law, we can say that the speed of the catalytic reaction,  $v$  (eqn.12), is:

$$v = \frac{k_b T}{h} \Pi_i^n a_i^p \exp\left(-\frac{E}{k_b T}\right) \quad (12)$$

Where:  $\Pi$  represents the product of the reactant activities of the reaction of order  $p$ , in the limiting stage;  $E$  is the activation energy of the reaction;  $T$  the absolute temperature;  $K_B$  represents the Boltzmann constant and  $h$  the Plank constant.

So that an electrocatalytic reaction can take place, there must first be the formation of the electrolyte/surface complex and then a rapid charge transfer in the complex itself. In this way, the reaction product is formed on the electrode surface and with its subsequent detachment there is the reformation of the active site on the surface of the catalyst.

What determines the speed in the formation of the electrolyte/surface complex is the speed of mass transfer, which is usually a process that takes place in a short time. Instead, the speed with which electrons are exchanged through the complex interface is often a slow process, which therefore will represent the kinetically determining stage on which the speed of the entire reaction will depend. To ensure that the electronic transfer rate is optimized, electrically conductive active phases, such as metal particles, can be used or an already conductive matrix can be used as a support for the active phase, in the event that the latter it is not.

The expression of the reaction rate,  $v$  (eqn.13), for an electrocatalytic reaction can be written like below:

$$v = P\rho\Pi_i^n a_i^p \exp\left(-\frac{E(\varphi)}{k_bT}\right) \quad (13)$$

Where:  $E(\varphi)$  is the activation energy of the reaction at a specific potential  $\varphi$ ;  $P$  is the probability integral for the charge transfer;  $\rho$  is the electrons concentration on the electrode surface better known as the density of states.

It is essential to consider the temperature effect on the reaction; in fact, this is a parameter which can influence the rate of a catalytic reaction. Based on the activation energy which each reaction has, the temperature is able to change the reaction speed of many units. However, the rise in temperature is a problem when there is a solid/liquid interface because there is the possibility that the solvent will evaporate. Therefore, an alternative in the electro-catalytic reaction is to change the potential on the working electrode to modify the reaction rate, because this parameter is more comfortable to modify. Moreover, by choosing the potential to be applied, it is possible to impart a specific selectivity to the reaction [60] [61].

## 1.8 Theoretical notes on electro-catalytic oxidation

The study of the electrocatalytic processes as promising methods for wastewater treatment, allowed to collect useful information regard the electrochemical oxidation mechanism of organic substances (pollutants or waste products). These studies also provided models for analyzing the reaction course and these models allowed to optimize the method from the laboratory scale to the construction of pilot plants [62].

The catalytic tests were conducted in an electrochemical glass cell with three thermostat compartments (Figure 1.18):

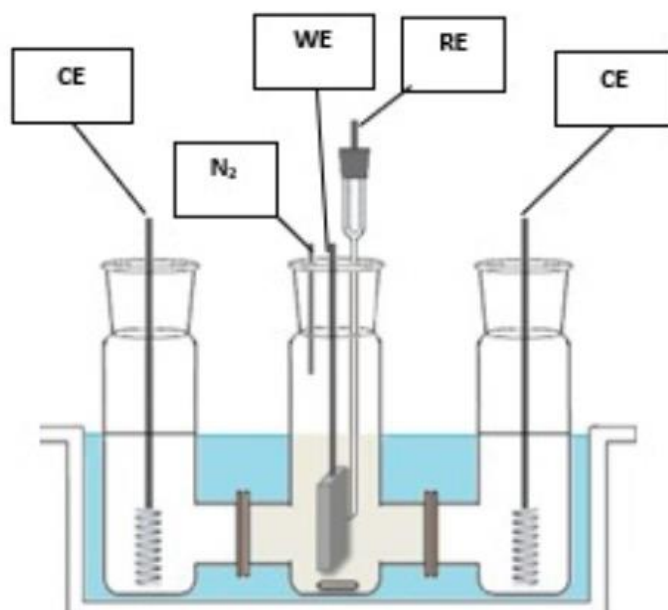


Figure 1.18 Electrochemical glass cell with three thermostat compartments

In the central compartment, the working electrode and the reference electrode were inserted. In the two lateral compartments were inserted instead of the counter-electrodes. The reference electrode is held in electrolytic contact with the working electrode by insertion in a capillary of Luggin.

At first, it was thought to treat these pollutants with biological treatments, but these procedures are impossible due to the bio-refractory character of the treated organic substrates. Consequently, the oxidation through chemical agents was studied, some examples are ozone and chlorine dioxide. This method is effective, but the transportation and storage of these reagents was a problem in designing safe treatment [58].

The advantages in using an electrochemical oxidation are generally numerous. In fact, it is not necessary to remove chemical oxidants or products derived from them, this means that the procedure most of the time provide the removal of the solvent only, this shows that it is a very practical process. The electrochemical oxidation is a low-cost process if we neglect the initial cost of the equipment, in fact the cost of the power fed stably is lower than the chemical reagents used in the classic oxidations. Moreover, this type of oxidation presents a yield that it is often adequate [63].

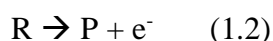
The organic pollutants can be removed by a direct or indirect electro-oxidation procedure. In the first case, the organics are oxidized directly through transfer of electrons from the anode. In the second case, electro-active species are generated and these act as intermediates to carry on the degradation reaction of the organics. Therefore, during the indirect EO, some strong



oxidizing agents are produced starting from the reactions that take place at the anode. The nature of the intermediates depends on the type of material the electrode is made of and on the system conditions. The reactions that happen during the indirect electro-oxidation can be reversible or irreversible [62].

### **Direct electro-chemical oxidation**

First of all, the organics must diffuse from the bulk of electrolyte to the anode surface, where they get adsorbed. Subsequently, the organics are oxidized on the anode surface through the electron transfer (1.2).



Where R is the targeted organic pollutant and P is the organic pollutant oxidized.

This type of EO is possible if the electro-chemical system operates at potential values lower than those necessary for the oxygen evolution reaction. The reaction rate of a direct EO is usually lower than that of the indirect one, but the rate depends a lot on the electro-catalytic activity of the electrode material.

The process efficiency depends on the rate of the mass transfer. The major drawback in this mechanism is the formation of a polymer layer over anode surface exhibiting “poisoning effect” to the electrocatalytic property of anode material. The probability of electrode fouling by polymer layer formation depends upon adsorption properties of anode material, concentration and properties of the targeted organics [63] [64].

### **Indirect electrochemical oxidation**

The indirect electrochemical oxidation is carried out in the potential region where the oxygen evolution reaction takes place, therefore to the potential in which the water is oxidized. Starting from this reaction some intermediate species are created that act as oxidants on the anode surface. The mechanism efficiency of degradation depends on the selected materials for the electrode and on the experimental conditions.

Conducting electro-oxidation in the OER potential range leads mainly to the formation of hydroxyl radicals ( $\bullet$  OH defined as active oxygen). These radicals are adsorbed over anode surface and they push the oxidation of the organic substance to take place, these are also reported like excellent oxidizing agent of aromatic substances, like lignin (1.3; 1.4). This is an

important discover since the aromatic matters are particularly recalcitrant towards biological treatments.



Where S represents the site over the electrode surface where the hydroxyl radical is adsorbed; R is the targeted organic compound and RO is the oxidized organic substance.

A drawback associate with the degradation of organics through the electro-oxidation is the reduction in current efficiency as one portion of applied energy is used for oxygen evolution [63] [64].

### **Electrochemical conversion by ‘active’ anodes**

There are some metals which present higher oxidation state leading the reaction forward the formation of superior metals oxides  $MO_{x+1}$ , in this way the  $\bullet OH$  amount which remains fisisorbed on the anode surface is nearly nothing. In fact, almost all  $\bullet OH$  formed by OER reacted with the metal forming the  $MO_{x+1}$  species, that is defined as “chemically adsorbed active oxygen” (1.5; 1.6).



Therefore,  $MO_x$  is the symbolic representation of the anodic metal oxide and  $MO_{x+1}$  represents the intermediate which allows the partial oxidation of the organic compound (1.7).



Since the oxygen chemically adsorption took place on the electrode active sites, the “active metals” cannot be considered inert.

These metals have low oxygen evolution overpotential and thus they are good electrocatalysts. For this reason and for the low amount of  $\bullet OH$  adsorbed over the electrode, the degradation reaction of the organic compound is disadvantaged and takes place only partially, but it is very selective.

Carbon, graphite, Pt,  $IrO_2$  and  $RuO_2$  are some examples of these kind of electrode [63] [64].

## Electrochemical combustion by “innert” anodes

Metals which doesn't have a high oxidation state doesn't react chemically with the hydroxyl radicals physisorbed over electrode surface, so they do not lower their concentration. In this way, the •OH can be utilized to degrade totally the chemicals substances up to CO<sub>2</sub> and H<sub>2</sub>O (1.8). The complete combustion is favoured on the “non-active anode” without the need for further treatments.



These materials do not provide for any type of chemical adsorption either for oxygen or even less for polluting substances or degradation products and therefore acts as an inert substance.

The “non-active anodes” have high oxygen evolution overpotential, therefore they are not very active towards this reaction. For this reason and for the presence of the •OH adsorbed on the electrode surface, the complete organic substances oxidation is favoured.

These electrodes result to be the best version for the organics degradation, but not for selective oxidation of the reagents.

On the basis of these statements, finally, the activity of the species •OH is dependent on the strength of the M- •OH interaction [63] [64].

Some examples of ‘inert’ anodes are PbO<sub>2</sub>, SnO<sub>2</sub> and boron-doped diamond (BDD) [63].

### *1.8.1 Experimental approaches for the electro-oxidation of organic substances*

The electro-oxidation of organic substances can be carried out with two different experimental approaches:

#### **Galvanostatic Electrolysis**

A constant current density shall be applied during the test in galvanostatic electrolysis. In this type of approach, the potential (U) of transformation is not controlled. However, at low current densities, the bonds with the lower characteristic redox potential are oxidized first, over time, the starting material is thus consumed, and its concentration decreases while the product is forming (figure 1.19). At some point, mass transport of the reagent from the bulk solution to

the double electrochemical layer on the electrode surface, becomes insufficient, despite always being induced by agitation.

If the electrolysis continues to this point, the galvanostat, to ensure the same initial current density, must increase the applied potential. In this way, bonds with higher characteristic redox potential will oxidize (figure 1.17). Unfortunately, with these reaction conditions, the formation of collateral products is practically unavoidable, which may result from unwanted degradation of the reagent, but also partial oxidation of solvents or other components, such as additives. This will be a problem because the more sub-products there are, the more complex the post-electrolysis separation process will be [65].

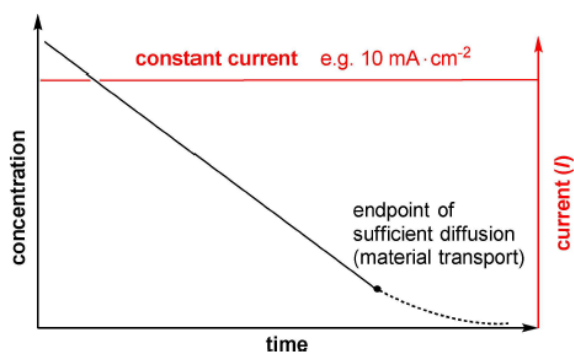


Figure 1.19 Concentration profile of a galvanostatic electrolysis

## Potentiostatic Electrolysis

The use of this technique requires that the reference electrode is in a separate compartment from the working electrode. The former will provide a constant reference potential as a fixed point as long as the concentrations in its compartment remain unchanged. For this purpose, materials such as ceramics are used to prevent the spread of organic solvents in the reference electrode enclosure.

The precipitation of salts on the materials that separate the two electrodes can be problematic because it could cause clogging and the consequent loss of the point of attachment of the electrode of reference that will cause the oscillation of the potentiostat and will determine therefore uncontrollable electrolysis conditions.

The applied potential ( $E$ ) is set to the desired value and is applied to the surface of the working electrode, the ratio of the applied potential ( $E$ ) to a reference electrode makes the reaction reproducible.

To perform the electrolysis, it is necessary to know the redox potential of the starting material in the solvent system. When the cyclic voltammetry is applied to measure the redox potential

of the source material, the redox potential is set to a value 10-20% higher than the base (start) of the peak.

When these conditions are applied, and the concentration of the starting material is high, a constant transport of the starting material to the electrode will ensure a more or less constant flow of charge through the solution. Sooner or later, the starting material is consumed, and the mass transfer to the electrode becomes the limiting factor. At this point, the current will decrease because the potentiostat will keep the applied potential constant (figure 1.20). The endpoint of electrolysis is reached when the current is less than 5% of the initial current. At this point, the starting material will have been consumed (> 98%) and through this technique will avoid the formation of unwanted collateral products because the potential is not altered by electrolysis [65].

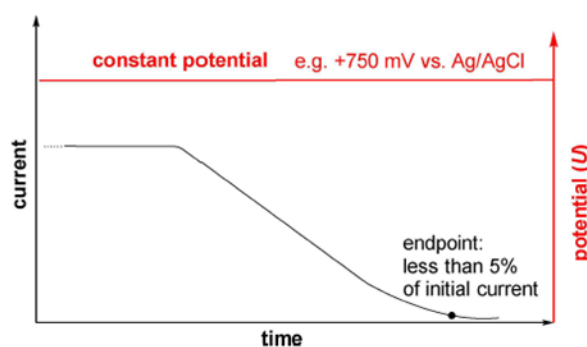
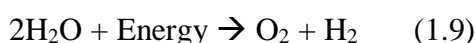


Figure 1.20 Current profile of a potentiostatic electrolysis

### *1.8.2 Electrolysis of water and evolution of oxygen and hydrogen*

The general process of electrolytic splitting of water can be represented as follows (1.9), with individually generated molecular hydrogen and oxygen, on cathode and anode respectively of an electrolytic cell.



This energy, in the form of operating voltage  $E_{\text{eff}}$ , depends on the kinetics of splitting reactions and on the design of the electrocatalytic unit. Theoretically, it is possible to obtain the energy necessary to guide the reaction from a series of renewable sources such as the photovoltaic and/or the use of wind turbines [66].

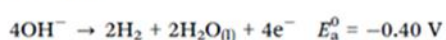
It is known that the reactions of splitting of water at cathode and anode are different for acid or alkaline conditions (figure 1.21). Many research groups proposed possible mechanisms for the reaction of oxygen evolution at anode both in acid and alkaline conditions, some disparities and some similitudes are present among these proposed mechanisms. Many of these include the intermediate MOH and MO formation (where M represents the metal electrode), while the major disparities are found for the oxygen formation reaction.

### Alkaline conditions

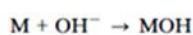
Cathode reaction:



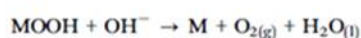
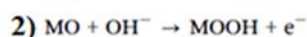
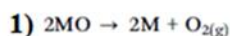
Anode reaction:



Proposed MO formation mechanism

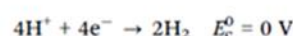


Proposed O<sub>2</sub> formation mechanisms

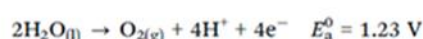


### Acidic conditions

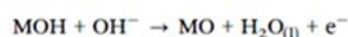
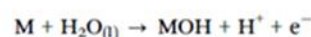
Cathode reaction:



Anode reaction:



Proposed MO formation mechanism



Proposed O<sub>2</sub> formation mechanisms

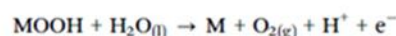
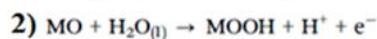
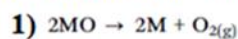


Figure 1.21: Proposed mechanisms for the reactions of splitting of water in acid or alkaline conditions

It is known that there are two different approaches to create oxygen starting from the reaction intermediate MO.

The first goes through the direct combination of 2MO to produce gaseous molecular oxygen (green route in the figure 1.22 below), the second proceeds among the intermediate MOOH formation which subsequently decomposes to give O<sub>2</sub> (black route in the figure 1.22 below). Both are shown in the figure 1.21 above, both in acid and basic environments.

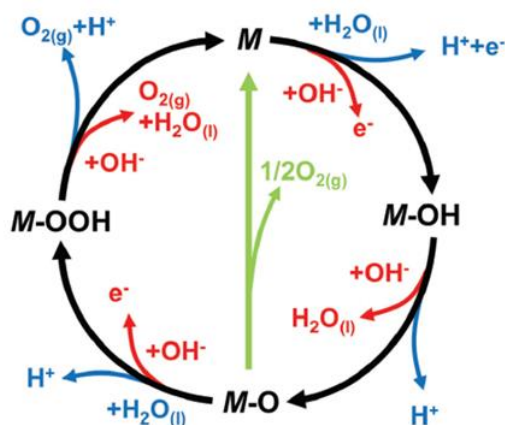


Figure 1.22 The OER mechanism for acid (blue line) and alkaline (red line) conditions. The black line indicates that the oxygen evolution involves the formation of a peroxide (M-OOH) intermediate (black line) while another route for direct reaction of two adjacent oxo (M-O) intermediates (green) to produce oxygen is possible as well.

Despite this difference, the common result is that the OER is a heterogeneous reaction in which the M-O bond, with the respective intermediates (MOH, MO and MOOH), is a crucial point for the whole reaction.

The OER is the main competitor for the electrolytic oxidation process of organic compounds, in fact, this affects the efficiency of selective electronic transfer for product training. Moreover, the consequent formation of bubbles of O<sub>2</sub> at the anode leads to a reduced electrolyte-electrocatalyst interaction, disturbing in this way the outcome of the reaction and decreasing its efficiency.

How much OER is favoured depends on the energy with which the formed oxygen is adsorbed on the electrode surface, metals that show adsorption energies too strong or too weak are not very active for the reaction [59].

## 1.9 Electrocatalytic oxidation of lignin

As has been mentioned in paragraph Lignin depolymerization products, the lignin oxidation consists of its depolymerization through the breakdown of inter-monomeric bonds to simpler and low molecular weight molecules. The most abundant bond in lignin is the β-O-4, from whose break it is expected to obtain molecules like phenols, aldehyde, ketone and carboxylic aromatics [67].

The degradation processes described in the paragraph “Degradation processes of lignin” often presents solid residue like char and the catalytic processes usually are challenging to control, and the commercial profitability has not been demonstrated [68].

The electrochemical paths instead provide a series of measures for the control of lignin oxidation, first of all, through the choice of the potential (therefore, the energy provides to the reaction) one can restrict the range of products obtainable until a specific interval of molecular weights. The same thing can be done controlling the time of the reaction [68].

Moreover, the electrode structure has to guarantee the accessibility of the macromolecule to the catalyst. Therefore, it is appropriate that the electro-catalysts for lignin degradation have a high surface area. In this way it will be a high catalytic activity due to the presence of numerous active sites, metal foams are excellent candidates for this type of reaction [69].

The lignin degradation by electrochemical way is potentially more environmentally friendly since the reaction happens in moderately alkaline solutions at low to moderate temperature and pressure, the electrons that guide the reaction can be described as non-polluting reagents [68].

Lignin, having an incredibly complex structure, can depolymerize in several ways, consequently in most cases from its oxidation a mixture of numerous products is obtained.

In particular, when the characteristic reduction potential of fracture of a specific bond is reached and overcome, the reaction is unlocked, and the oxidation in question happens.

Through the choice of the potential to apply to the reaction, the electro-oxidation can be made more or less selective for specific reactions. Given the countless number of degradations that lignin can go through, the several oxidation ways, often, have energy values very close to each other, which generally makes the selectivity of the process very low.

Therefore, since the electro-catalytic depolymerization suffers from these problems of poor selectivity and the meagre yields of the products, research has recently moved towards replacing aqueous electrolytic solutions with solutions that are not, such as ionic liquids or deep eutectic solvents [70].

The advantages of these innovative electrolytic solutions are the enlarged electrochemical windows, the decrease of parasitic water electrolysis and the possibility to perform the electrochemical depolymerization in wood fractionation downstream [70].



Lignin is depolymerized through indirect electro-catalytic oxidation by “active” anodes. These catalyze the formation of the hydroxyl radicals  $\bullet\text{OH}$  physically absorbed on their surface, which by chemically reacting with the anode create oxidized metal species that are active in the depolymerization of the organic compounds present in solution when they come into contact with the anodic surface. Catalyzing in this way the degradation reaction of lignin, the polymer can be oxidized to lower potentials than would be used in the absence of the catalyst.

Omar Movil-Cabrera et al. reported the study of the electrochemical oxidation of lignin using Co alloy with a partial Pt shell as an anode. In this study, the probable electro-oxidation mechanism of lignin through the  $\bullet\text{OH}$  radicals have been discussed.

Considering recent knowledge about the reaction mechanism, an electro-catalyst which is capable of readily forming these  $\bullet\text{OH}$  radicals should be chosen, Pt and Co have both been noted as catalysts for this reason.

The proposed reaction mechanism in this paper indicates that oxidation, mediated by radicals, is probably driven by the transfer of a single electron from the anode, as shown below (figure 1.23):

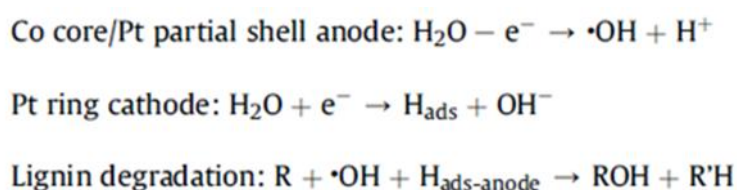


Figure 1.23 Probable electro-oxidation mechanism of lignin through the  $\bullet\text{OH}$  radicals

Where R represents the lignin biopolymer or its partial degradation products [68].

The success of the reaction can be verified through pre-and post-reaction cyclic voltammetry tests. By analyzing these tests, the catalyst activity can be evaluated and consequently, the best potential to react to can be studied.

Taking as an example always the study cited above, in fact, from the cyclic voltammetries made on lignin in alkaline solution it is evident that the characteristic peaks of the depolymerization reactions are quasi-reversible or completely irreversible. From this, can be guessed that there are many species which participates to electrochemical processes, which means that the degradation mechanism is complex [68].

The irreversibility of the reaction also indicates that the oxidation products are not present for a possible reduction, which may be due to two phenomena:

1. The oxidation products, once formed, are promptly transported away from the electrocatalyst surface before they can be reduced.
2. Homogeneous chemical reactions consume oxidation products on time scales similar to charge transfer processes.

From this, one can also guess that the complex structure of lignin and its oxidation products leads to significant limitations in mass transport, which affect the electrochemical mechanism.

Omar Movil-Cabrera et al. analyzed non-oxidized Aspen lignin and the post-electrolysis Aspen lignin in an alkaline 1M solution of KOH via GCeMS. The only volatile compound identified at an appreciable concentration (greater than 0.01 ppm) in the unreacted lignin sample was vanillin; this indicates the presence of this molecule in the purchased lignin samples.

Here lignin has been oxidized at a constant potential of 0,598V compared to SHE (Standard Hydrogen Electrode) and the reaction products have been analyzed with GC-MS periodically. It is seen that the oxidation products and also their concentrations depend on the reaction time; in Table 1.1, the molecules obtained at various times are reported. Heptane is present at all oxidation times, and its concentration is growing. Moreover, its concentration is always higher than 0,01 ppm. This behaviour suggests that heptane is a stable product and that it may not participate in an appreciable speed to other reactions, also 2,4-dimethyl-1-heptene and 1,3-bis (1,1-dimethyl ethyl) benzene have the same growing trend.

Some products show decreasing concentrations; these could form as oxidation products and then participate as reagents in other reactions which can be electrochemical or homogeneous. For example, vanillin, at first increases its concentration and then decreases and re-increases at specific times. Therefore, the generation rate of vanillin increase at long oxidation times when there has now been significant degradation of the biopolymer, this indicate that the electrochemical generation rate of vanillin at long times compensates and exceeds the conversion rate of vanillin to other products.

In general, it is evident that the concentrations of the oxidation product are low, usually, less than few ppm, especially if we consider the initial concentration of lignin (10 g of lignin per litre, corresponding to 10,000 ppm) [68].

Oxidation product	Oxidation time (min)		
	83	1200	2700
2,4-dimethyl-1-heptene	0.07	0.12	0.26
Heptane	0.42	0.49	0.50
2-methoxy-phenol	0.60	0.54	0.73
Phenol	0.08	–	–
2,6-dimethyl-nonane	0.06	–	–
Vanillin	8.45	7.43	9.83
Apocynin	1.96	1.62	2.49
1,3-bis(1, 1-dimethylethyl)-benzene	0.14	0.21	0.41
2,4-di-tert-butylphenol	0.18	0.47	0.44
1-(4-hydroxy-3,5-demethoxyphenyl)-ethanone	0.23	–	0.23
4-methyl-benzaldehyde	–	0.17	–

Table 1.1 Lignin oxidation product concentrations (ppm) at different reaction times.

Di Marino et al. speculated that the low yields associated with aromatic products obtained by electrochemical oxidation could be due to the further oxidation of the aromatic rings to products such as carboxylic acids.

This kind of electrochemical breakdown of monomers and dimers has been widely studied, and di-carboxylic acids like maleic acid; fumaric acid; oxalic acid and other products such as carbon dioxide have been identified as the main products of this further oxidation.

Succinic acids, for example, could be a useful product since it is an essential precursor for polyesters and also the oxalic acid could be an essential catalyst for the fractionation of biomass [70].

The results reported in Table 1.2 refers to the Di Marino et al. study, in particular, the reaction was made with Ni foam as a catalyst, and the starting lignin was of the Kraft type [70].

product	Y 0.8 V [%]	Y 2.5 V [%]	Y 3.5 V) [%]
vanillin	1.04	0.03	0.01
oxalic acid	0.43	6.36	10.26
malonic acid	0.02	0.33	0.38
succinic acid	0.03	0.17	0.31
malic acid	0.02	0.17	0.16
formic acid	0.00	26.8	9.10
acetic acid	0.00	4.20	4.10
<b>total</b>	<b>1.54</b>	<b>38.06</b>	<b>24.32</b>

Table 1.2 Yields (wt% referred to the initial amount of used lignin) for the identified products coming from the electrochemical depolymerization at 0.8, 2.5 and 3.5V.

In the Omar Movil-Cabrera et al. experiment the reason why the concentrations of aromatic products are only in the order of magnitude of ppm is that the current is shallow, that indicates that the reaction is slow. This is due to the load of small electro-catalyst (25mg catalyst) which leads to a consequent small current (in the order of several mA).

The prevalence of carbonyl groups in oxidation products suggests that the guaiacyl units of lignin have degraded under these conditions. In the flow of products, there are also medium-length branched hydrocarbons; these are an indication of the fact that significant destruction of the aromatic rings has occurred.

Some of the identified products are known for being important in the industrial processes or the research laboratories. For example, heptane is a non-polar solvent commonly used in the research laboratories. Apocynin can be used as an antioxidant in endothelial cells, while 2,4-di-tert-butyl-phenol has been studied as an antifungal relevant for agriculture and is commonly used as a UV stabilizer and antioxidant.

Likely, separation and purification of the product of interest from the post-reaction mixture would be required to use the products industrially [68].

### *1.9.1 Electro-deposition methods*

Open-cell metal foams are promising supports for the development of structured catalysts that are formed through the deposition of an active metal phase. Deposition means the process of applying a thin film or particles of more or less reduced size on support. The cellular foam structure is formed by interconnection channels that create a high geometric surface, low-pressure drops and a more excellent transfer of mass and heat.

The performance of structured catalysts does not depend only on the properties of the deposited material (loading, composition, size, dispersion of active species and textile characteristics) but also by the level of adhesion of the layer deposited on the surface of the foam [71] [72]. Generally, the adhesion begins with the formation of single nucleation germs on the working electrode, which aggregating form a continuous and dispersed layer.

The morphology and thickness of the layer of deposited material vary according to various factors such as time of application of the pulse, concentration of the electroactive species, applied potential, the material used as a support, the temperature of the solution, agitation of the solution and purity of the electrolyte. Given the enormous number of factors involved, controlling the size and distribution of deposited particles is not easy.

Recent studies comparing the performance of 2D supports (metal plates) with 3D supports (metal foams) showed that the resistance to electronic transfer offered by the catalysts prepared on the two different systems, from the same material, is more or less the same. However, H<sub>2</sub> bubbles that form at the cathode during electrodeposition tend to accumulate more on 2D planar supports, leading more easily to the detachment of the deposited phase. Instead, the use of 3D

macro-porous substrates, facilitates the dispersion of bubbles in the solution, without causing their accumulation on the surface of the electrode, which allows a better deposition of the active phase.

The methods commonly used to adhere the active phase to the medium are chemical, spontaneous or electrochemical deposition techniques [72].

The most used techniques are the one that uses catalyst sludge; the deposition on catalytic supports through the impregnation of active phase and in situ synthesis of the active phase on the metallic foam.

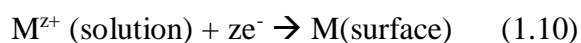
The coating, in general, can have some drawbacks such as the modification of the properties of the catalyst or the blockage of the pores, in fact, usually are used foams that have medium or large pores to avoid this problem.

An alternative synthesis route would be the deposition of catalytic species by hydrothermal treatment; this offers some advantages such as the absence of additives and binders and is the most straightforward and fastest procedure.

Electrochemical deposition is an easy way to coat supports in a single step at room temperature. Both electrically conductive metal particles and hydroxides, oxides or a combination of these can be deposited.

These electrochemical depositions can be performed by applying a cathodic potential in a continuous or pulsed way to a working electrode, which represents the substrate to be coated [71].

**For the deposition of metallic particles**, the applied potential and the electrolytic solution shall be chosen in such a way that direct electrochemical reduction of metallic precursors occurs (1.10).



In contrast, **the electro-basic generation method** is applied in the deposition of hydroxides and oxides.

Metal cations that need to be electrodeposited by this technique are usually found in solution in the form of metallic nitrates [71]. A cathodic potential is applied to the nitrate solution in which several reactions occur, leading to the disappearance of  $H^{+}$  ions and the generation of  $OH^{-}$  ions at the electrode-electrolyte interface. In this way, a basic environment is formed as a result of the increase in pH at the interface which thus causes the precipitation of metallic hydroxides on

the electrode surface. The reactions involved in the consumption of H<sup>+</sup> ions are as follows (figure 1.24) [1]:

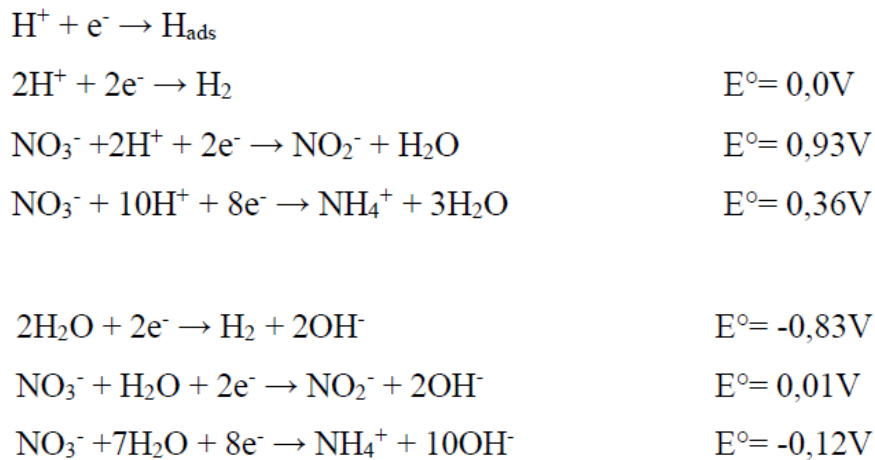
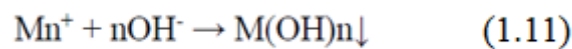


Figure 1.24 Reactions involved in the consumption of H<sup>+</sup> ions and in the generation of OH<sup>-</sup> ions at the electrode-electrolyte interface.

All these reactions contribute to the formation of metal hydroxide (1.11) on and near the electrode surface, according to the reaction:



Among the reactions listed above, it is difficult to determine which ones influence the evolution of pH at the surface of the electrode.

This kind of electrochemical synthesis can be conducted by galvanostatic or potentiostatic conditions.

In the first case, synthesis can be carried out in which the speed of the reduction reactions involved can be carefully controlled, allowing the obtaining of films with excellent adhesion and with the desired morphology. The control of the working current corresponds to control the flow of electrons passing through the electrode necessary for the reduction of the concerned species.

However, synthesis of this type can lead to considerable variations in potential, which could encourage 'parasitic' reactions, such as the direct reduction of the metals considered, which would lead to the production of undesirable phases.

The potentiostatic synthesis is conducted in a classic three-electrode cell by applying a suitable potential to the working electrode, measured in relation to the reference electrode used.

In this case we generally have a decrease in current, mostly due to the decrease in the rate of diffusion of ions from bulk to the electrode surface over time. Depending on the applied potential it is, in this way, possible to deposit single phases with a reasonable degree of purity.

Electrochemical deposition, in general, offers several advantages over other deposition techniques. First, all reactions occur close to the electrode and the products are deposited in the form of thin layers whose thickness can be easily varied from about 100 nm to a few  $\mu\text{m}$  acting on the synthesis time. Secondly, the solid/liquid interface allows the growth of homogeneous coatings on any support, without limits of shape, provided that the material of which the support is constituted is an electric conductor.

The use of a suitable counter-electrode allows to obtain a uniform polarization on the working electrode, in this way is also standardized the start of electrochemical reactions on the entire surface of the catalyst.

Electrochemical depolymerization is also a technique that requires little time to obtain hydroxide films, also allows the kinetic control of the reaction through the control of the current passing through the electrodes and the thermodynamic control through the application of a suitable potential.

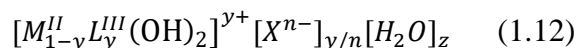
There are, however, some disadvantages, such as the fact that at room temperature electrochemical techniques lead to the formation of little crystalline phases that are difficult to identify [1].

Although cathodic electrodeposition has been studied since the 1990s, the coating of complex-shaped foams with active phases for the preparation of structured catalysts was new and not simple. First, the coating layer must reach a certain thickness (e.g. 20  $\mu\text{m}$  or even thicker) to provide sufficient catalyst loads; this is a much higher value than those present in the state of the art that is about a few microns. Besides, to have specific properties, sometimes it is necessary to make simultaneous electrodeposition of multiple components, this is a challenge for the control of the composition [71].

In conclusion, we can, therefore, say that the success of this synthesis method depends on different parameters, the choice of electrodes, the type of cell, the electrochemical technique used, the composition and concentration of the solution, the working temperature and pH, both the first working solution and the one developed at the surface of the electrode [1].

The electrodeposition of hydroxides was originally developed for the modification of small and straightforward electrodes with simple hydroxides such as  $\text{Ni}(\text{OH})_2$ . This technique was subsequently extended to the deposition of more complex hydroxyl compounds such as

hydrotalcite (HT) (1.12), which are also called double-layer LDH hydroxides, with the general formula:



The deposited Hts with Ni/Co, Ni/Fe and Co/Fe formulations have been used as sensors, redox supercapacitors and, more recently, as electrocatalysts, mainly for the reaction of the evolution of oxygen [71].

### 1.9.2 Choice of Ni-Co catalyst for lignin electro-oxidation

As has already been discussed in the previous paragraphs, there are various types of lignin, but since Kraft lignin is a vital waste material of the typical Kraft process to obtain cellulose, there is a tendency to use this type of lignin for electro-oxidations, intending to enhance it. This type of technical lignin is characterized by its inertia and stability to degradation [73] [74]. Moreover, its structure has not yet been fully understood, and it is for this reason that it is difficult to associate with certainty the degradation mechanisms intuited by the depolymerization of the model compounds to lignin Kraft [74].

Electrochemical degradation of Kraft lignin in alkaline media is usually performed on Nickel anodes. This is because Ni electrodes show high corrosion stability due to the formation of an electro-catalytic surface layer (NiOOH) (figure 1.25) that is stable in the electrolytic solution [73]. This surface layer is electro-catalytically active for the lignin degradation reaction, which means that NiOOH is the relevant oxidizer in this conversion [74]. This specie regenerates during the oxidation of the bio-polymer in question [73].

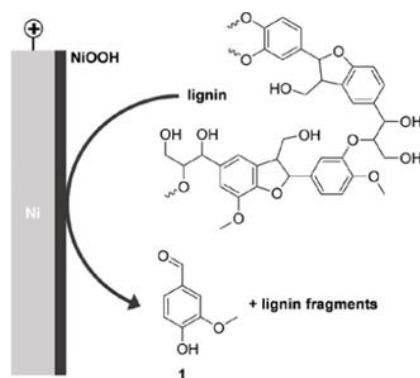


Figure 1.25 Schematic representation of the electrocatalytic degradation of lignin to vanillin at NiOOH.



Mechanistic studies of a lignin dimer model have revealed that using NiOOH as an electro-catalyst leads to oxidative splitting of the aryl-ether  $\beta$ -O-4 bond. In particular, oxidation affects the aromatic system of the bond and initially leads to the formation of a quinone structure, after a second phase of oxidation is obtained the corresponding aldehyde. This series of electrochemical oxidation reactions led selectively to the vanillin molecule, which is a prized product of fine chemistry [74].

In particular, Schmitt et al. and Zirbes et al. have demonstrated the excellent performance of Ni-based electrodes for the electrochemical degradation of lignin obtaining vanillin yields up to 1% by weight. These yields are not optimal, but there is the advantage that the corrosion phenomena are not observed [73] [74].

In these studies, three-dimensional electrodes have been used, as they increase the effective anodic area leading to a better space-time yield [73] [74].

The electrochemical degradation of lignin has been performed successfully and selectively also using Ni and Co-based materials in alkaline electrolytes [74].

It has been shown that Co-based materials can achieve higher yields of vanillin, but suffer from corrosion which therefore limits technical application. In particular, carbon oxides are formed on the electrode surface, and this causes the presence of a dark coating. Due to corrosion, these species are also found in suspension in the electrolytic solution, although in small quantities.

The corrosion is why the electro-catalytic activity of Co-based catalysts decreases dramatically after a series of electrolysis cycles [73] [74].

The idea of using alloys composed of both Ni and Co was born from the intuition of being able to combine the stability of Ni to corrosion with the higher electro-catalytic activity of cobalt. Moreover, these two metals are inexpensive and non-toxic [17]. Movil-Cabrera et al. (2015) showed that Ni and Co alone are insufficient electro-catalysts and also show a rapid deactivation [68]. Unfortunately, Zirbes et al. reported that the desired combination of properties was not observed [74].

Although no catalyst corrosion has occurred, the vanillin yield remained below 1% by weight; this is comparable to that obtained from regular Ni-based materials [74].

An advantage of the electrochemical oxidative degradation of lignin using these Ni-Co-based materials is that usually a good selectivity, regarding the formation of low molecular weight phenolic compounds, is obtained [74].

Zirbes et al. reported that the Kraft lignin pre-electrooxidation contains traces of phenolic derivatives, such as vanillin, acetovanillon, guaiacol and 4,4'-dihydroxy-3,3'-dimethoxy stilbene. These compounds are already observed after that the lignin sample is dissolved in alkaline solution, acidified and finally, after that, the aqueous phase is subjected to liquid-liquid extraction. After the electrochemical treatment guaiacol and the stilbene derivative disappear and the only products observed are vanillin and traces of acetovanillone. These last two products are the only ones present in determinable quantities, and therefore the process can be considered quite selective [74].

Differences in electrochemical performance between catalysts with and without Co can be attributed to charge transfer processes involving lignin or its derivatives. It has been found that incorporating Co in electro-catalysts causes a decrease in the potential at which the oxidation of lignin begins. In other words, by inserting Co into the catalyst, the energy required for lignin electro-oxidation has been reduced [17].

A high percentage of Co in Ni-Co electro-catalysts promotes a better electron transfer during the oxidation process. This effect is due to an increase in surface area, as structural defects of Ni hydroxide caused by doping with Co will be created. The higher the surface area of the catalyst, the faster the lignin electro-oxidation rate will be [17].

Raziyeh Ghahremani et al. carried out the oxidation reaction of Kraft lignin at room temperature, at a constant potential of 0,598V and with an electro-catalyst containing both Nickel and Cobalt in the proportion of Ni<sub>2</sub>-Co<sub>8</sub>. The current density that is reached is high, and this shows that with a high amount of Co also, the speed of the reaction will be high. Through the use of this particular catalyst, a high yield of specific aromatic compounds has been achieved. In particular, vanillin and apocinine arise from the rupture of the G unit of Kraft lignin, while 3-methyl-benzaldehyde and 1,2-Dimethoxy-4-(1-methoxy-1-propenyl) benzene arise from the fragmentation of the  $\beta$ -O-4 bond [17].

Schmitt et al. carried out the electro-oxidation of lignin always with a bi-metallic catalyst Ni-Co, but at 80°C and it was shown that at temperatures higher than the environmental one, the vanillin yield increases to a value of 2.0% by weight. Although the temperature has a positive influence on the efficiency of the reaction, processes must always be economically reasonable and therefore use mild conditions. For this purpose, it is necessary to try to use environmental pressure and temperatures that do not exceed 100 °C [73].

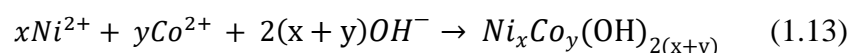
In addition to the temperature and the applied anode materials, the current density also has a strong influence on the obtainable vanillin yield. In particular, applying rather low current densities,  $< 2.0 \text{ mA/cm}^2$ , it has been shown that vanillin yields are high regardless of the material of which the electrode is made [73].

Especially Co-based materials are susceptible to this parameter, and even a slight increase in current density would lead to a drastic drop in vanillin yield [73].

The problem, however, is that low current densities are very unfavourable from a technical point of view due to the long electrolysis times they need [73].

Bi-metallic electrodes have been often obtained through electro-deposition to co-deposit hydroxides of Ni and Co in the form of nano-sheets on the surface of the electrode [75]. Electro-deposition is a powerful tool for modulating the properties of electrode materials [74].

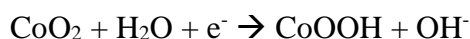
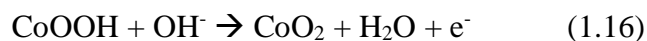
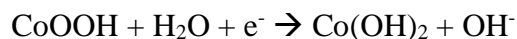
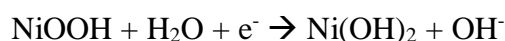
In particular, in aqueous solution, nickel (II) and cobalt (II) nitrates deposit as hydroxides through the electro-basic generation (a process already described in the previous paragraph) through which the metal double hydroxide nanosheets (Dhs) Ni-Co are created on Ni foam according to the following reaction (1.13) [75]:



Ultrathin Ni-Co Dhs has at least three advantages:

1. They are vertically aligned on the porous 3D Ni foam and form a well-defined nano-layer hierarchical structure, which can provide a very high specific surface and be useful for sound mass diffusion and good electron transport.
2. Amorphous Ni-Co Dhs have an electrical capacity comparable to crystalline Dhs, but have a much higher power density as well as better cyclability and are therefore often selected.
3. No binders are needed for their production as the active materials are created directly on the porous Ni substrate, thus avoiding the decay of the electrical conductivity caused by the strength of the binder.

The electro-catalytically active species in these Dhs, as well as in all bi-metallic Ni-Co catalysts, are NiOOH and CoOOH, which are the oxidizing species for lignin. In Dhs, these two species are formed according to the following reactions (1.14; 1.15; 1.16) [75]:



## 1.10 Parameters affecting electrocatalytic oxidation of lignin

### *1.10.1 Influence of the nature of the metal*

The metal electrodes are easily usable at the cathode, both at the laboratory and at the industrial level, since it is only necessary that they can conduct electrons in the electrochemical reactions.

Instead, at the anode, the situation is more complicated because the metal electrodes should only be used at potentials where the metal undergoes neither dissolution nor oxidation. In the latter case, the electrode would be covered with an oxide layer that would prevent electronic transfer.

The catalytic activity of the metals depends strongly on the electronic structure of the metal atom; a high activity has been found in transition metals which present the d shell empty. A lower activity has been noticed in sp metals, but since they present a high hydrogen overpotential (and therefore a low rate of evolution of the hydrogen itself), they are commonly used as materials for the cathode.

Platinum and other metals of the platinum group are the most used catalysts for many electrochemical reactions, as they are stable in a wide range of potentials in many solutions. Although they cost a lot, they are still used as they are very efficient.

In alkaline solutions, the Ni electrode is quite common as it is a material that resists corrosion under these conditions.

The catalytic activity of the electrode is determined also from the composition and the structure of the surface where the electrocatalytic reaction will take place. These parameters depend on factors as: method with which the electrode was prepared; method with which the surface was treated and others.

The factors that characterize the structure and the state of the catalyst surface are the crystallographic orientation of the surface and individual segments; the presence of structural defects or the presence of active sites that have unique characteristics and finally the presence of accidental or consciously added traces of foreign matter.

This classification is very relative as far since the degree of activity also depends on the nature of the electrochemical reaction [57].

The efficiency of an electro-oxidation, therefore, depends also on the nature of the anode material. The choice of electro-catalytic material is a crucial issue, and the electrode must have the following properties:

3. High chemical and physical stability.
4. High resistance to erosion, corrosion and passive layer formation on the catalyst.
5. Relatively high electrical conductivity.
6. High selectivity and catalytic activity.
7. Low cost and high durability

The anode material determines not only the percentage of organic material that is oxidized in the bulk solution but also the efficiency of the faradic current.

Faradaic efficiency (FE) (eqn.14) corresponds to the electrons involved in the reaction and is an essential parameter for the evaluation of the reaction, especially in the case of non-quantitative or non-selective reactions. FE is obtained from the ratio:

$$FE = \frac{n \cdot \beta \cdot F}{Q} \quad (14)$$

where  $n$  represents the amount in moles of the product,  $\beta$  is the number of electrons involved in the reaction,  $F$  is the Faraday constant and  $Q$  is the total charge exchange [76].

### *1.10.2 Effect of current density and potential applied*

The current density used for oxidation or the potential applied to the system are critical parameters since they can be controlled directly. The current density (understood as current per unit area of the electrode) is the term that is most frequently referred to since it controls the reaction rate and consequently defines the efficiency of the entire process.

For low current values (where EO is not kinetically limited by the mass transport of reagents to the electrode surface), an increase in current leads to oxidation of a large amount of organic material. For high current values (when the process is controlled by mass transport) from an increase in current one expects more significant molecular oxygen formation, which leads to a decrease in the efficiency of the faradic current and an increase in energy costs. For intermediate current values (when the process is under a mixed kinetic regime), an increase in current should cause an increase in oxidation of the organic material but also a decrease in efficiency.

For a given anode material, the effect of current density also depends on the characteristics of the effluent to be treated.

Unsuitable hydrodynamic conditions may cause the appearance of additional mass transport limitations that would negatively affect the action of current density on the EO. The stirring rate is one of the most critical parameters, especially when using batch cells, because proper agitation minimizes the appearance of concentration gradients in the electrolytic cell, ensuring homogeneous conditions. Besides, it promotes the movement of generated ions, the removal of oxidation products from the surface of the catalyst and the transport of oxidants, such as radical •OH, from the surface of the anode towards the solution [76].

### *1.10.3 Influence of the temperature*

The effect of temperature on the efficiency of the EO process is not a parameter that has been extensively studied. However, some studies have shown that temperature changes have a slight influence on the EO that occur by oxidizing effect of the hydroxyl radicals. Some authors have suggested that an increase in temperature causes higher mass transport to the anode due to the decrease in average viscosity.

It has been suggested that the positive effect of the temperature increase can be mainly attributed to improved anode activity. However, this is a wrong conclusion because, in reality,

the improved efficiency of the oxidation reaction is due to an increase in the speed of the indirect reaction of organic substances with electro-oxidizing agents generated by electro-oxidation, such as hydroxyl radicals. However, there is a risk that at high temperatures, the thermal decomposition of some oxidants takes place.

Despite the positive effects, room temperature operation is usually still preferred as it provides electrochemical processes with lower energy requirements than their non-electrochemical counterparts. These results confirm the need to optimize the configuration of the electrolytic system and parameters such as pH and temperature to achieve maximum oxidation capacity with minimum energy consumption [76].

Zirbes, Quadri et al. have shown that there is a relationship between the electrolysis temperature and the observed vanillin yield (figure 1.26) [77].

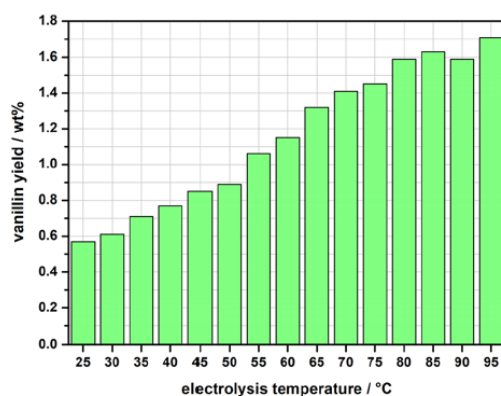


Figure 1.26 Influence of the electrolysis temperature onto the yield of vanillin in the electrodegradation of Kraft lignin

Due to the complex experimental configuration, the temperatures used in electrolysis so far have been limited to a maximum of 95°C. But, the application of temperatures above 100°C should lead to better performance with regard to vanillin yield, for which the following reaction scheme has been assumed (figure 1.27) [77].

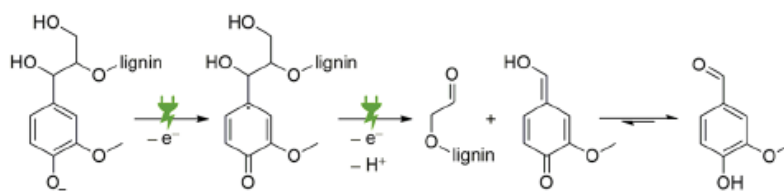


Figure 1.27 Proposed mechanism for the electrochemical degradation of Kraft lignin to Vanillin

However, working at temperatures > 100°C using an aqueous electrolyte requires a specific and challenging experimental configuration. For this purpose, in this experiment, a simple and

undivided electrolysis cell was designed, which allowed efficient operation in these severe conditions.

In particular, the experiment involves the electrolysis of Kraft lignin at 8 bar, 160° C, at constant current density (12 mA/cm<sup>2</sup>) up to a charge of 1418 C and using as the electro-catalyst foam of Ni.

In order to optimise electrolysis at high temperature relative to vanillin yield, linear screening experiments were conducted by variation of current density (geometric), and the amount of charge applied (figure 1.28) [77].

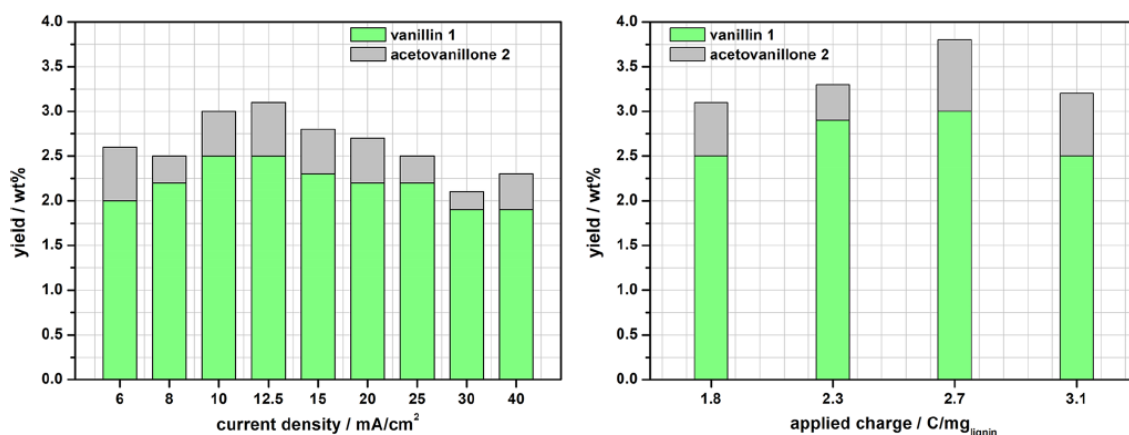


Figure 1.28 Optimization via linear screening of the lignin electro-degradation using nickel foam electrodes under variation of geometric current density with 1.8C per mg lignin and under variation of applied charge with a geometric current density of 12,5 mA/cm<sup>2</sup>

The data provided suggest that current densities (relative to the geometric surface) in the range of 10.0 to 12.5 mA / cm<sup>2</sup> are favourable, compared to the formation of vanillin and acetovanillon. Due to the shorter electrolysis time associated with higher current density, 12.5 mA/cm<sup>2</sup> were used for investigations. As for the amount of charge applied, 2.7 C per mg of lignin led to the maximum observed vanillin yield, so this is the value that was selected.

On the one hand, quantities higher than 2,7 C/mg of applied lignin feed are correlated with longer reaction times, which would also lead to undesirable consumption of vanillin due to over-oxidation, resulting in lower yields of the aldehyde itself.

On the other hand, lower amounts of this charge value are insufficient for depolymerisation.

By applying the optimised reaction conditions, vanillin is obtained with a good yield (3.0% by weight, related to lignin used). Besides, acetovanillon was obtained as a secondary product at a yield of 0.8% by weight [77]



### 1.10.4 Effect of the nature and concentration of the organic reagent

In general, the higher the concentration of organic material that needs to be removed, the higher the energy efficiency of the process will be (figure 1.29).

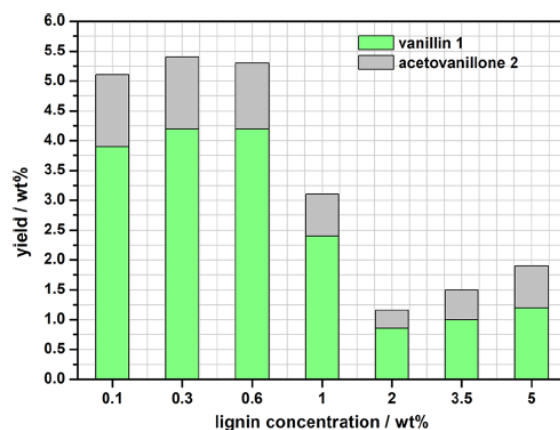


Figure 1.29 Electro-degradation of Indulin AT lignin to vanillin by variation of the initial lignin concentration in 3M NaOH using nickel electrodes applying 10 mA/cm<sup>2</sup> and 2,7 C per mg lignin at 160°C.

However, it must be considered that, at high initial concentrations of lignin, the phenomena of re-polymerization are favoured, representing parasitic reactions in the depolymerization process. The re-polymerization is a problem because part of the potential applied to the system to provide low molecular weight products is consumed to create bonds. Therefore, in order to eliminate depolymerization, but at the same time to guarantee excellent energy efficiency, we must use a concentration that is a middle way [76], [77].

### 1.10.5 Influence of the pH

The pH of the solution is an essential operating parameter in the EO. The pH effect on the efficiency of EO depends on the chemical structure of the material to oxidize because according to this, the reagent will be more or less electro-active in alkaline solutions rather than in acidic ones. The pH also influences the concentration of OH hydroxides in the bulk solution [76].

Zirbes et al. have shown that the Kraft lignin electro-oxidation system tolerates a wide range of values regarding the basicity of the system (figure 1.30). The maximum vanillin yield is obtained by using a NaOH concentration of 3 M. Higher concentrations, up to 5 M, have led to a reduction in yield even if not significant.

A negative influence was also noted by choosing a lower concentration of 3M of NaOH. Decreasing concentrations up to 1M led to a continuous decrease in the yield in weight. A further reduction in NaOH concentration to 0.5 M resulted in a substantial drop in yield.

These data suggest that the basic nature of the solution is of great importance for the solubility of lignin and also influences the accessibility of potential active degradation sites on the surface of the electrode [74].

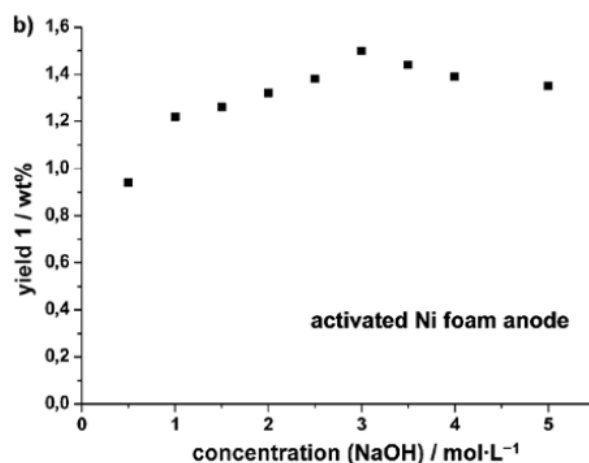


Figure 1.30 influence of the basicity on the electrochemical degradation of lignin using Ni foam electrodes Smith, Utle & Hammond et al. also reported that sodium hydroxide concentration influences lignin conversions. They stated that a poor conversion was achieved with sodium hydroxide solutions of 1 M and 6 M compared to those obtained using 3M solutions [78].

## 2. Experimental part

### 2.1 Material and reagents used.

The list of materials and reagents used for the synthesis of electrocatalysts; their use in catalytic tests; the purification of reaction products and their analyses are given in Table 2.1.

Compounds	Physical state	PM(g/mol)	Purity	Producer
NaOH	Pellets	40	98	Sigma-Aldrich
Kraft Lignin	Fine brown powder	60000	96	Sigma-Aldrich
Nickel metal foam	Macroporous solid	-	-	Alantum
Ni (NO <sub>3</sub> ) <sub>2</sub> *6H <sub>2</sub> O	Green solid	290.81	99.8	Alpha-Aesar
Co (NO <sub>3</sub> ) <sub>2</sub> *6H <sub>2</sub> O	Red solid	182,94	99.9	Sigma-Aldrich
HCl	Water solution	36.46	-	Sigma-Aldrich
Sulfuric acid	Liquid	98.08	96	Sigma-Aldrich
Isopropanol	Liquid	60.09	100	Sigma-Aldrich
Chloroform	Liquid	119.38	98	Carlo Erba
Ethyl acetate	Liquid	88.10	99.8	Sigma-Aldrich
Ethanol	Liquid	46.07	99.8	Sigma-Aldrich
DMSO deuterated	Liquid	84.17	99.8	Eurisotop
Chloroform deuterated	Liquid	120.38	99.8	Eurisotop

Table 2.1: List of reagents and materials used.

All the aqueous solutions have been prepared using ultrapure water obtained with Milli-Q plus system (Millipore Co, resistivity 18,2 MΩ cm).

## 2.2 Electrocatalyst preparation

The catalysts used for electrochemical testing are based on open-cell, 3D nickel-metal foams (Figure 2.1). These supports have been tested both as and with an active phase of  $\text{Ni}(\text{OH})_2$  and  $\text{Co}(\text{OH})_2$  deposited. The support used for the foams is obtained from macro-porous nickel sheets of 300 mm x 200 mm x 1.6 mm with a cell size of 450  $\mu\text{m}$ , from which 10 mm x 10 mm foams have been obtained.

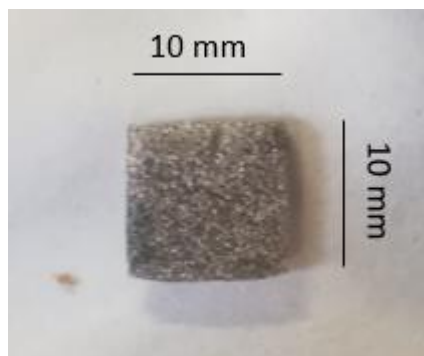


Figure 2.1: Open-cell, 3D nickel-metal 10mm x 10mm foams

These are fixed to a glass rod employing platinum contacts, which are secured by the application of a parafilm layer so that they are stable and immobile and the contacts are not exposed to the solution. The glass rod is then connected to the instrument via clamps.

Before any operation, the supports are pre-treated by washing with water UPP and isopropanol for about 1 minute, to remove possible contaminants present on the surface, then a wash in HCl 1M for 5 minutes, in order to eliminate surface oxides. Finally, rinse thoroughly with water to remove traces of acid. At this point, the support is ready for active phase deposition and/or for electrochemical tests.

## 2.3 Electro-deposition of the active phase

### *2.3.1 Electrochemical cell used for electro-depositions*

The synthesis of the catalysts was conducted using a three-electrode system in a flow cell consisting of two separate compartments (Figure 2.2). An AUTOLAB PGSTAT12 potentiostat controlled with a computer through the GPES software was used for the syntheses.

The three electrodes used are:

- **The working electrode (WE)** is constituted by the Ni foam on which the deposition will take place, and this is connected to the potentiostat utilising two platinum wires;
- **The reference electrode (RE)** is a saturated calomel electrode (SCE), positioned in the upper part of the cell, in contact with the main compartment of the WE through a Luggin capillary. The capillary is positioned at a distance of about 1 mm from the WE. In this way, there is better control of the applied potential;
- **The counter electrode (CE)**, is a platinum wire (0.4 mm diameter, 40 cm long), located in a second compartment separated from that of the other two electrodes by a porous glass septum.

The electrolytic solution is made to flow both inside the main compartment, using a peristaltic pump, able to regulate the flow, and in the counter-electrode compartment. It was decided to conduct the syntheses using a flow of 2 mL/min [79].

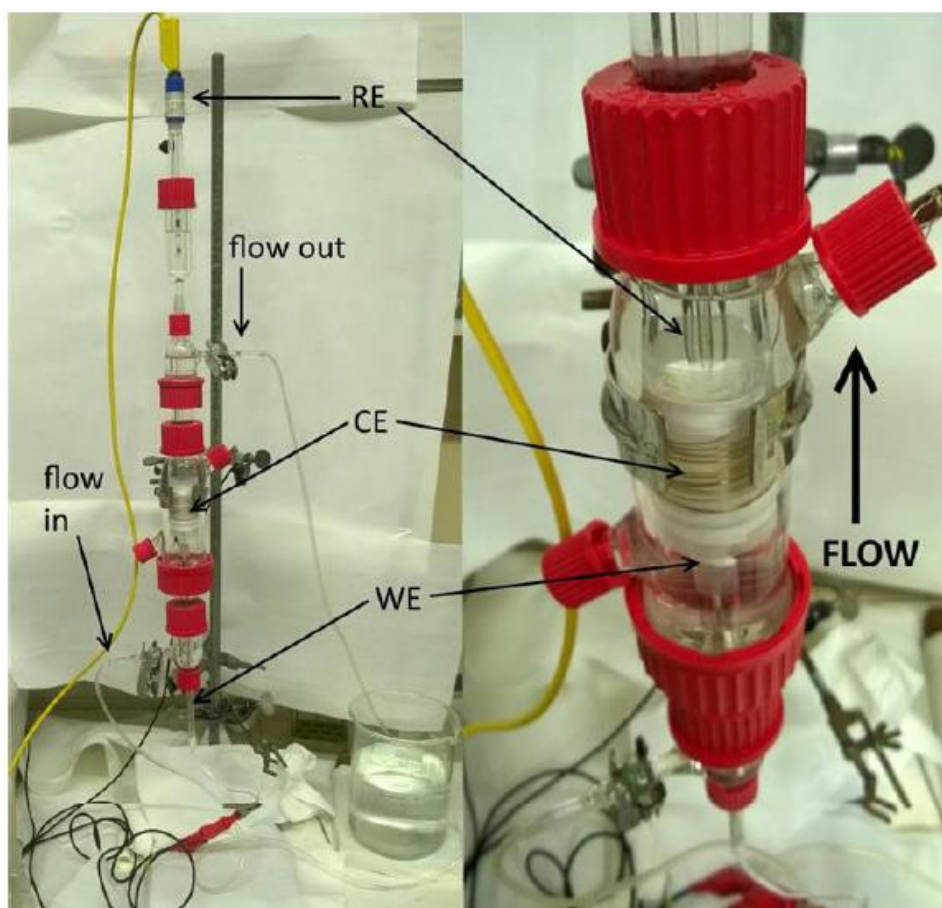


Figure 2.2 Flow cell used for catalyst synthesis

### 2.3.2 Preparation of solutions

Ni and Co hydroxides were deposited in equimolar ratio and Co hydroxides only on Ni foams, as regards the former, three types of solutions were tested at different concentrations and in different synthesis conditions (Table 2.2) [75]. The combination that led to obtaining a coating with the desired molar ratio, thickness and morphology (-1.2V, 100s and 0.06M) was chosen. The same optimal conditions of concentration, potential and time were then used for the deposition of the hydroxides of Co.

Catalyst	Voltage (V)	Time (s)	Concentration (M)
Ni(OH) <sub>2</sub> / Co(OH) <sub>2</sub>	-1.2	50	0,1
Ni(OH) <sub>2</sub> / Co(OH) <sub>2</sub>	-1.2	100	0,06
Ni(OH) <sub>2</sub> / Co(OH) <sub>2</sub>	-1.2	200	0,01
Co(OH) <sub>2</sub>	-1.2	100	0,06

Table 2.2: Different concentrations and synthesis conditions for the Ni(OH)<sub>2</sub>-Co(OH)<sub>2</sub>/Ni and Co(OH)<sub>2</sub>/Ni deposition.

The solutions were prepared with the respective nitrates, Ni(NO<sub>3</sub>)<sub>2</sub> \*6H<sub>2</sub>O and Co(NO<sub>3</sub>)<sub>2</sub> \*6H<sub>2</sub>O.

### 2.3.3 Substrate pretreatment

The Ni foams are subjected to a chemical pretreatment for about one minute in UPP water and isopropanol and 5 minutes in 5M HCl. The pretreatment allows the removal of surface oxides and other possible impurities, increasing the surface conductivity of the metal. The foams are then washed with UPP to avoid chlorine residues on the foam.

### 2.3.4 Electro-deposition

Once the cell is trimmed, the synthesis parameters shown in the Table are set, which guarantee the best synthesis conditions, as already seen in previous works (Figure 2.3; Figure 2.4) [75].

After synthesis, the coated foams are gently washed in UPP to remove surface residues, dried overnight at 40 ° C and weighed again, to check the amount of material deposited.



Figure 2.3: Ni foam with electro-deposited Co hydroxide layer.



Figure 2.4: Ni foam with electro-deposited NiCo hydroxides layer.

## 2.4 Characterisation of catalysts

### 2.4.1 SEM-EDS Analysis

SEM (Scanning electron Microscope) (Figure 2.5) analyses were carried out to study the morphology of the catalysts, while to determine the composition of the surface an EDS (Energy Dispersive X-Ray Spectroscopy) analysis was carried out. The electron microscope SEM bases its operation on electron beams collimated, called primary electrons, which affect different areas of the sample through a scanning mechanism. The primary beam-sample interaction generates various signals that are acquired by appropriate detectors. This technique allows to reach greater depths and resolutions in comparison to standard optical microscopes.

At the same time, EDS can be used to obtain semi-quantitative elementary results on specific areas of the surface under analysis. When the primary electrons hit the surface of the sample, part of them is reflected, while another part is diffused or absorbed. The electron-surface beam interaction of the sample results in four types of phenomena, each translated into an electrical signal using appropriate detectors [80].

- **Emission of secondary electrons (SE)** are low energy electrons ( $< 50$  eV) generated near the surface due to the release of energy by the primary electrons. The detector, through a transducer system, converts these electrons reflected from the sample surface into a highly detailed 3D image. SEM images are grayscale because the detected electrons have wavelengths that do not fall within the visible spectrum. The contrast between the different shades of grey highlights the depth of the image.

- **Retrodiffuse electron emission (BSE)**, the emission of these higher energy electrons (50 eV) results from the interactions of the primary electrons with the nuclei of the atoms of the sample, this interaction results in a reflection and diffusion of the incident electron beam. Not all electrons belonging to this category have the same energy; in fact, it depends on the properties of the surface of the sample that is hit. Generally, heavier atoms exhibit higher intensities, as they can reflect primary electrons more strongly than light atoms. This results in different shades of grey, in which samples composed of heavier atoms (e.g. silver, gold) give more or less light grey, while surfaces characterised by lighter atoms give a dark grey (e.g. copper, nickel, iron) until black when no reflection takes place. For these reasons, BSE does not provide any information on the topography of the sample, but on its composition.
- **X-ray emission**, electrons belonging to the innermost electronic shells are excited by the bombardment of the incident beam and torn to the attraction of the nucleus. As a result, to restore the equilibrium condition, the outermost electrons move to cover this gap. The decay produces an excess of energy on the core. The energy excess is disposed of with the propagation to the outside of X-rays, characteristic for each element. With the EDS analysis, these radiations can be used to obtain information on the composition of the microvolume in question.
- **Emission of electrons Auger**, are electrons arising from surface emissions (5-75 Å) and possess low energy, provide compositional and chemical information on the bond of excited atoms. The mechanism of emission is similar to that of X-rays. They differ for the fact that to restore the equilibrium condition, after the bombardment of the incident beam, an electron is released from the outer orbitals [80].



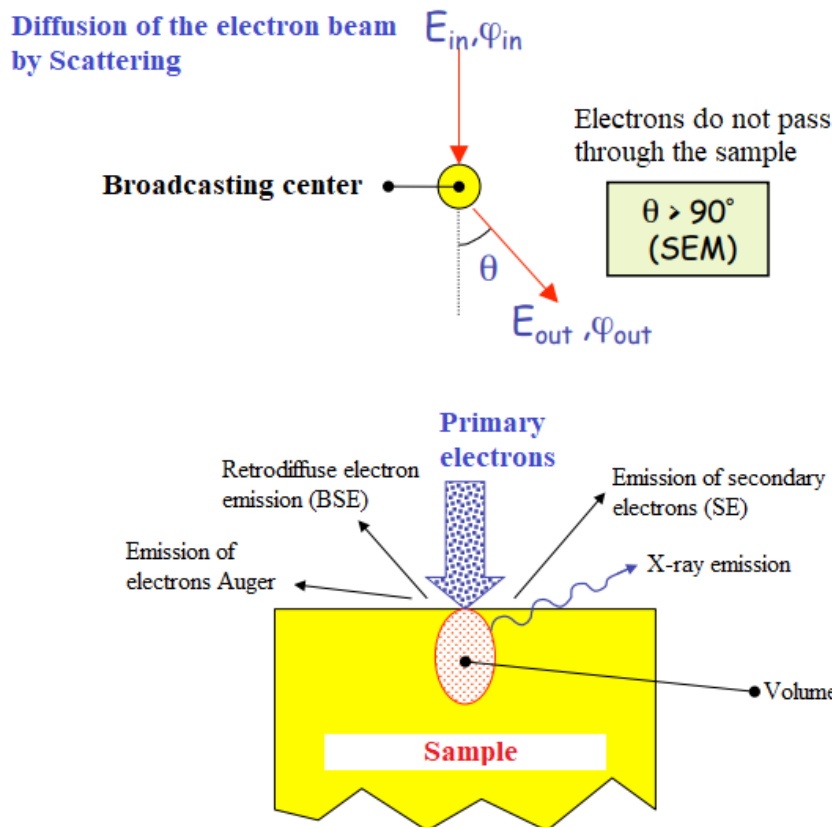


Figure 2.5 Main types of emissions from an SEM analysis

The scanning electron microscope used for our analyses was an EVO 50 EP (LEO ZEISS), with Oxford Instruments INCA ENERGY 350 microsonda (EDS) equipped with an INCASmartMap system. The potential difference applied for electron acceleration was 20 kV and the spectral acquisition time for EDS analysis was 60 seconds.

### 2.4.2 Raman spectroscopy

When monochromatic radiation is cut on a surface, a part of it is absorbed, a part is reflected and finally a small is diffused. The latter, in part, is diffused with an elastic collision mechanism, that is without energy variation (Rayleigh scattering), maintaining the same frequency of impact. The remaining fraction, by inelastic collision, is diffused with variation in energy and therefore also in frequency (Raman scattering). This phenomenon is due to the polarizability variation of the atoms that make up the sample, induced by vibrational transitions caused by the laser radiation (in the field of visible) incident.

The polarizability measures the capacity of the charge distribution of molecules (electronic cloud) to deform, compared to nuclear positions, due to the effect of the electric field.

Polarizability is an intrinsic property of a molecule and is usually anisotropic; in fact, a molecule will be active Raman only if it is polarisable. In both elastic and inelastic interactions, one can imagine that the affected molecules start from a virtual energy state  $h\nu_0$  from which they decay emitting photons. Inelastic interaction can evolve into two distinct paths [81] (Figure 2.6):

- The molecule decays to an excited vibrational energy state emitting a photon of lower energy than that of the incident (Stokes shift, towards red).
- The molecule, already present in an excited vibrational state, decays from the virtual state to the fundamental state, emitting a photon of energy more significant than that incident (anti-Stokes shift, towards the blue).

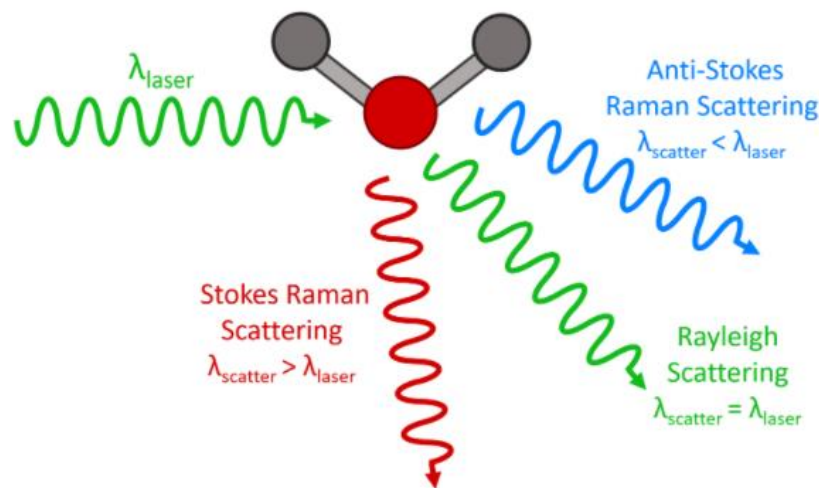


Figure 2.6: Rayleigh and Stokes anti-Stokes Raman scattering in comparison [82].

However, since at room temperature, the most populated vibration level is the fundamental one, anti-stokes movements are less frequent than Stokes ones. What is ultimately measured is, therefore, the difference between the frequency of the incident radiation and the diffuse radiation.

Raman analysis falls into the category of vibrational spectroscopies, just like infrared (IR) spectroscopy the two techniques provide similar results (in terms of recorded frequency) but obtained in a completely different way and based on different selection mechanisms and rules. If the dipole moment of a molecule changes with the vibration, then the IR will be active, if instead to change is the polarisation, then the Raman will be the active technique. Therefore, these two techniques can be used in a complementary way [81].

The instrument used is a Renishaw RM1000 micro spectrometer. The experiment is conducted focusing on the objective a 50x magnification in the area of interest, proceed by having the laser engraved and making the measurement. A green laser (Ar + 514.5 nm) with 10% power is used. Spectra were recorded between 4000 and 100 cm<sup>-1</sup>, for the analysis of Ni electrodeposited foams and between 2000 and 100 cm<sup>-1</sup> for bare foams, with four accumulations and an acquisition time of 10 seconds.

### 2.4.3 X-Ray diffraction spectroscopy

X-ray diffraction spectroscopy is a widely used technique for the study of the mass properties of solids such as catalysts, as it allows to determine the crystallinity of a solid or one of its components; the estimate of the crystallite size; the type of phases present; the size of the cell unit and the type of atoms that compose it.

The technique is based on the diffraction phenomenon that is created when a monochromatic X-ray beam interacts with atoms of a sample through which it propagates (Figure 2.7).

There will therefore be constructive interference, given a specific wavelength of the incident radiation and a particular arrangement of the atoms, only for certain angles of incidence, as can be deduced from Bragg's law (15).

$$\lambda n = 2d \sin(\theta) \quad (15)$$

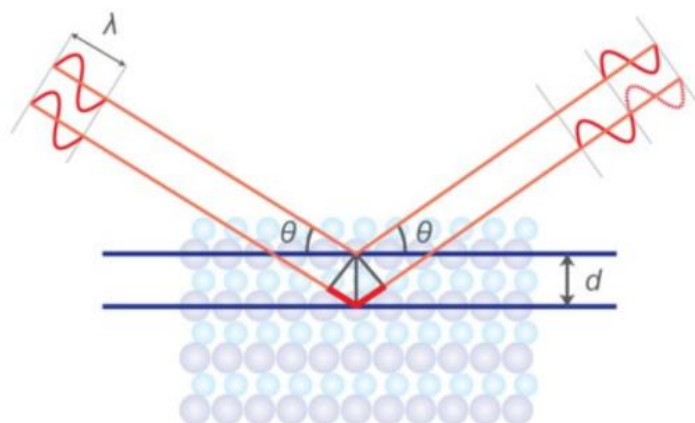


Figure 2.7: X-ray diffraction phenomenon

Where  $n$  is the order of diffraction,  $\lambda$  is the wavelength of the incident radiation,  $d$  is the distance between the points of the grating,  $\theta$  is the angle of incidence of the beam on the grating.

In the diffractograms, the intensity is reported as a function of  $2\theta$ . This is because, in practice, the angle between the incident and refracted ray is measured, which is twice the angle of incidence with the reticular plane.

The electrocatalysts were studied with X-Ray diffraction spectroscopy, before and after the reaction. In this way, any morphological changes that occurred to the electrocatalyst, are studied [83].

For this work, XRD analysis were performed with a Bragg-Brentano X'pertPro Penalytical diffractometer using a copper anode ( $K\alpha$  radiation at  $\lambda = 1.5418 \text{ \AA}$ ) as source of X-radiation with  $0,08^\circ$  step size and acquisition time of 1300s per step in  $36 - 41^\circ 2\theta$  range.

## 2.5 Electrochemical study of electro-catalysts

The catalytic tests were conducted in an electrochemical glass cell with three thermostat compartments (Figure 2.8).

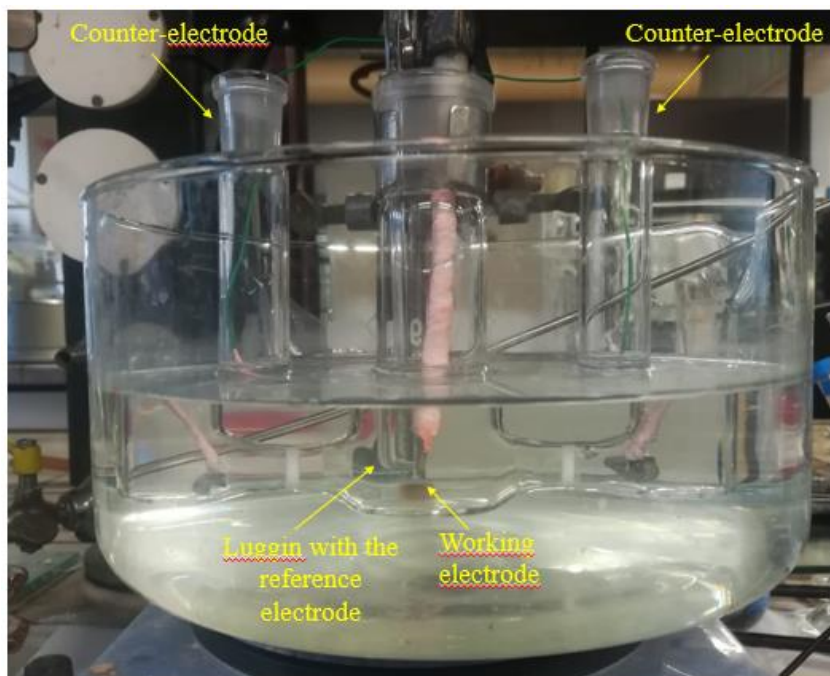


Figure 2.8 Electrochemical glass cell with three thermostat compartments

In the central compartment, the working electrode and the saturated calomel reference electrode (SCE) were inserted. In the two lateral compartments were inserted instead of the counter-electrodes, consisting of 12.5 cm long platinum wires, coiled.

Each compartment is separated from the adjacent compartment through a porous sintered glass septum. This is used to prevent any unwanted or harmful reaction products in the counter-electrode from coming into contact with the reaction products of the working electrode. Besides, the porous septum allows the passage of the ions necessary to ensure the flow of current within the electrolytic cell. The reference electrode is held in electrolytic contact with the working electrode by insertion in a capillary of Luggin, positioned about 2 mm from the same, which allows the reference electrode to be as close as possible to that of work, in order to reduce possible ohmic falls.

The electrocatalyst represents the working electrode, therefore by the foams, on which the reaction of interest takes place, this plays the role of electrode ideally polarisable. The reference electrode has a stable and well-known electrode potential, so it is used as a guide for measuring the potentials in the electrochemical cell. Being a calomel electrode with saturated KCl the redox potential is +0.2444 V vs SHE at 25°C, and it is an electrode ideally not polarisable.

Since the current cannot pass through the reference electrode, which must remain at equilibrium, a third electrode called counter-electrode is used, which is inserted to facilitate the passage of current to the working electrode. Usually the counter-electrode does not participate in the reaction. The cell has been connected to a potentiometer/galvanostat, Metrohm Autolab PGSTAT204, which carefully controls the potential that is established between the counter-electrode (CE) and the working electrode (WE) so that the potential difference between the working electrode (WE) and the reference electrode (RE) is well defined and corresponds to the chosen value.

The electrochemical tests were carried out using unmixed aqueous solutions of NaOH 1 M (pH=14) and lignin Kraft 10 g/L in NaOH 1M. In order to remove dissolved oxygen, N<sub>2</sub> gas flowed into each solution before use.

## 2.5.1 Cyclic-voltammetry

The electrochemical tests involve the execution of a voltammetry cycle in NaOH 1M solution to study the activity of the catalyst for the oxidation reaction of water. Then a voltammetry cycle follows in a 10 g/L lignin kraft solution in NaOH 1M, to study the activity of the catalyst concerning the electrochemical oxidation of lignin. Cyclovoltammetry (CV) or cyclic voltammetry is an electrochemical potentiodynamic technique based on the application of potentials, between the working electrode and the reference electrode, whose values have the shape of a triangular wave [84] (Figure 2.9).

So cyclovoltammetry is a technique of voltammetry where the potential is made to vary linearly over time, within a defined range of potentials. The rate of variation, called scanning rate, is constant throughout the range of potentials and is generally between 2 and 50 mV/s. As it increases, a decrease of the diffusive layer occurs, with a consequent increase of the intensity of the redox peaks. What is recorded is a current of variable intensity according to the electrochemical processes involved, which vary according to the applied potential. With the variation of the potential, the analyte can meet oxidation or reduction, through an exchange of electrons with the working electrode. This results in a peak in the voltammogram, positive in the case of oxidation and negative for reduction processes.

If there are reversible processes, when the voltage returns to the value where the already oxidised/reduced analyte in the first scan is reduced/oxidised respectively, a new peak is recorded. The shape will be similar to the previous one, but with opposite polarity and peak torque. In the case of a single electronic transfer reaction, will be separated by a maximum potential difference  $\Delta E$  of 57 mV. From this, it is possible to derive the oxide-reductive potential of a redox torque overvoltages caused by the system and information about the speed of the reaction (Figure 2.9). In the case of an analyte in solution, if the electronic transfer the electrode is fast and the process is limited by the diffusion of species on the surface of the electrode, the current intensity will be proportional to the square root of the scanning speed and described by **Cottrell's law** (16):

$$I = (nFAC_{oj}D_j^{\frac{1}{2}})/(\pi t)^{1/2} \quad (16)$$

Where n is the number of electrons exchanged, F the Faraday constant, A the active surface of the electrode, CO the initial concentration of the analyte of the species j-esima, D the diffusion coefficient of the species j and t the scanning time [84].

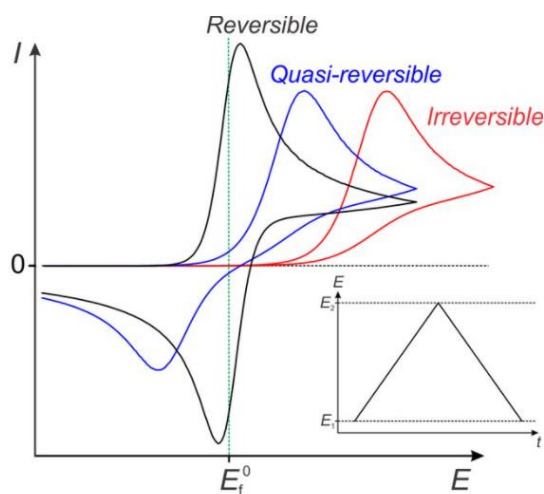


Figure 2.9: A comparison of cyclic voltametric wave-shapes for reversible, quasi-reversible, and irreversible electron transfer process with the same formal potential. The inset shows the triangular potential "ramp" applied to the working electrode during measurements.

## 2.5.2 Chronoamperometry

Chronoamperometry (CA) is an analytical technique in which a current is measured and recorded as a function of time. Between the working electrode and the reference electrode, a potential is applied, which can be constant or follow a programmed, and the current recorded in the chosen time interval embodies the faradic processes that take place.

## 2.5.3 Catalytic cycle

The catalytic cycle is structured as follows:

- Cyclic voltammetry in NaOH 1M (25 ml in the central compartment) between -0,4 V to 1,0 V and return to -0,4 V vs SCE with scanning speed five mV/s, performing three scans.
- Lignin cyclic voltammetry Kraft 10g/L in NaOH 1M (25 ml in the central compartment) between -0,4 V to 1,0 V and return to -0,4 V vs SCE with scanning speed five mV/s, performing three scans.
- Constant potential electrolysis (chronoamperometry) of a 10g/L lignin solution Kraft in NaOH 1M, carried out at 0,5 V, 0,6 V, 0,8 V and 1,0 V vs SCE with a constant agitation

of 1000 rpm, with times between 1 and 5 h.

- Cyclovoltammetry in NaOH 1M (25 ml in the central compartment) between -0,4 V to 1,0 V and return to -0,4 V vs SCE with scanning speed five mV/s, performing three scans.
- Lignin cyclovoltammetry Kraft 10g/L in NaOH 1M (25 ml in the central compartment) between -0,4 V to 1,0 V and return to -0,4 V vs SCE with scanning speed five mV/s, performing three scans.

All tests were carried out at T = 25 C and T = 60 C and P atm. At the end of the tests, the catalysts and the cell are washed with UPP water.

## 2.6 Analysis of the reaction products

At the end of the electrochemical reaction (chronoamperometry) the reaction solution is taken from the cell and placed in two falcons, at this point it acidifies up to pH = 2 by H<sub>2</sub>SO<sub>4</sub> 96 % (ca 1 ml per falcon), and it centrifuges for 20 min at 4500 rev/min. In this way, it separates the reactive lignin, which precipitates. In order to evaluate the best solvents to conduct the extraction, it has been found in the literature that chloroform and ethyl acetate are very well suited for the extraction of aromatic products such as vanillin and acetovanillon, resulting from the depolymerisation reaction of lignin. After testing both of them, it was decided to use only ethyl acetate. The supernatant (S1) present in the two falcons is separated from the solid, filtered with a 0,45 µm filter and extracted with an ethyl acetate solution (16 ml x 3). The resulting organic phase is washed with a saturated NaCl solution (20 ml) and then dried with anhydrous Mgso<sub>4</sub> and filtered through a Gooch filter. The residual solid (L) is extracted with 10 ml of ethyl acetate and centrifuged for 20 min at 4500 rev/min. The solid is separated from the supernatant (S2), the first is filtered on Buckner, lavender with ethyl acetate (15 ml), the organic phase of washing (S3) is then washed with a saturated NaCl solution (10 ml), anhydride with anhydrous Mgso<sub>4</sub> and filtered on a Gooch filter. The S2 supernatant is also washed with saturated NaCl solution (10 ml), anhydride with anhydrous Mgso<sub>4</sub> and filtered through a Gooch filter. The organic phases S2 and S3 are filtered with a 0,45 µm filter, assembled in a flask with S1 and concentrated at the rotary evaporator, in order to eliminate the extraction solvent. An oily substance is then obtained which is dissolved in DMSO or deuterated chloroform (0,7 ml) and, after the addition of para nitro benzaldehyde as an internal standard, analysed by NMR and GC-Massa. Untreated lignin (L) is washed with water and dried in the oven at 50° C throughout the night, then weighed to determine the conversion and analysed via ATR.



## 2.6.1 Nuclear Magnetic Resonance Spectroscopy Analysis

Each sample was analysed by high-field NMR spectroscopy (600MHz), by 1D analysis, proton experiment ( $^1\text{H}$ ); with relaxation times of sixty seconds ( $d1 = 60 \text{ s}$ ) for the quantification of reaction products and 2D analysis using the Heteronuclear Single Quantum Correlation experiment (HSQC) ( $^1\text{H} - ^{13}\text{C}$ ) for the characterisation of lignin post oxidation.

Thanks to this technique, unlike other techniques such as IR and UV, it is possible to obtain a more significant number of structural information, useful for the identification of an unknown compound.

The source of energy used in Nuclear Magnetic Resonance Spectroscopy (NMR) is radio waves, which are electromagnetic waves of large wavelengths and therefore low energy.

When low-energy radio waves interact with a molecule, they can induce a variation in the nuclear spin of certain elements such as  $^1\text{H}$  and  $^{13}\text{C}$ . When a charged particle, like a proton, rotates around its axis, it generates a magnetic field, and it is, therefore, possible to consider the nucleus as a small magnetic strip. Under normal conditions, these nuclear magnets are oriented in space at random, in the presence of an external magnetic field  $B_0$ , they orient in the same direction or the opposite direction concerning the applied field [85]. (Figure 2.10) .

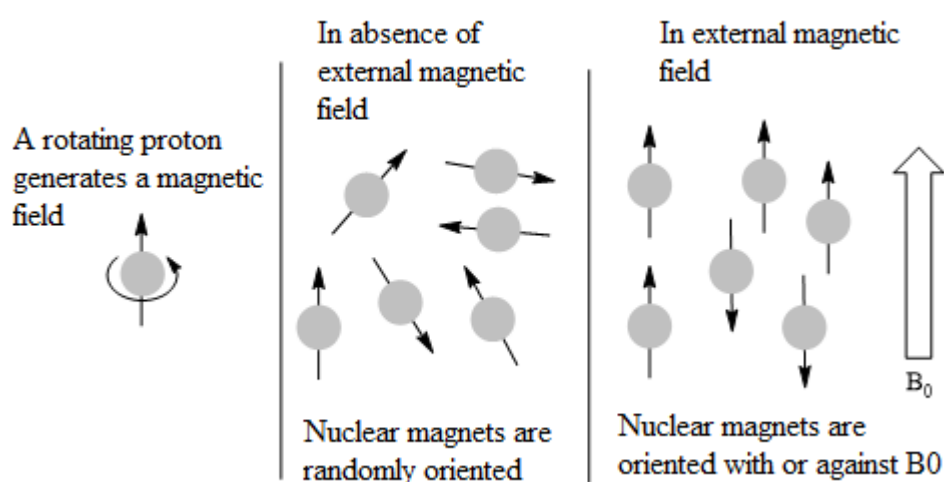


Figure 2.10: Process of alignment of atomic nuclei with the external magnetic field  $B_0$ .

A slight excess of nuclei is oriented in agreement with the applied field because, in this position, it is less energy. The energy difference between the two states is minimal (0.1 cal).

When nuclei are irradiated with an energy source  $h\nu$ , which equals the difference in energy  $\Delta E$  between these two states, an energy absorption occurs, which induces a reversal of nuclear spin from one orientation to another. It is said that the nucleus is in resonance (Figure 2.11). The energy difference between these two spin states corresponds to low-frequency radiation in the RF (radio frequency) region of the electromagnetic spectrum [85].

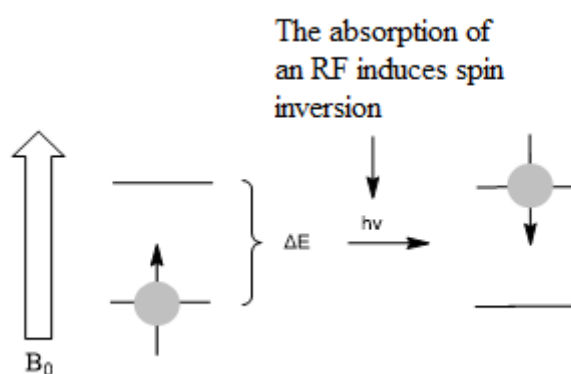


Figure 2.11 Spin transition by radiofrequency (RF) absorption.

Furthermore, it should be remembered that only nuclei that possess a nuclear magnetic moment of spin  $\mu$  are capable of generating this nuclear magnetic resonance phenomenon (17) [85].

$$\mu = I \gamma \frac{h}{2\pi} \quad (17)$$

Where:  $I$  is the quantum number of nuclear spin,  $\gamma$  the gyro-magnetic ratio of the nucleus,  $h$  the Plank constant. Active nuclei are magnetically characterized by having odd protons and even neutrons (odd mass number) or vice versa ( $I = 1/2, 3/2, \dots$ ), is the case of  $^1\text{H}$  (1p),  $^{13}\text{C}$  (6p, 7n),  $^{19}\text{F}$  (9p, 10n),  $^{31}\text{P}$  (15p, 16n), or numbers of odd protons and neutrons ( $I = 1, 2, \dots$ ), is the case of  $^2\text{H}$  (1p, 1n),  $^{14}\text{N}$  (7p, 7n). Nuclei with even number of protons and neutrons are silent nuclei and therefore not observable at the NMR ( $I = 0$ ), and this is the case of the  $^{12}\text{C}$  (6p, 6n),  $^{16}\text{O}$  (8p, 8n). The instrument used to acquire NMR spectra is a Varian Unity INOVA 600 Mhz model spectrometer, the signal of each spectrum was instead processed using Vnmrj software. The deuterated solvents used for our analyses were the deuterated chloroform ( $\text{CDCl}_3$ ), whose signal falls to 7,26 ppm, present as a singlet due to the proton of the species  $\text{CHDl}_3$ , present as

an impurity in the deuterated chloroform. The deuterated DMSO ( $C_2D_6OS$ ); the peak signal falls to 2,50 ppm, present as Quintuplet due to the proton of the species  $C_2D_5HOS$ , present as an impurity in the deuterated DMSO. Remembering that the use of the deuterated solvent not only has the task of solubilising the reaction products but also has the task of stabilising and blocking the magnetic field  $B_0$  of the magnet [85].

## 2.6.2 *Gas Chromatography with Mass Spectroscopy (GC-MS)*

GC-MS is an analytical technique in which a carrier gas, which constitutes the mobile phase, flows through a column in which the stationary phase is placed. The column is located inside an oven, which maintains the temperature at the set value, generally following a ramp. At the exit of the column, a detector signals the passage of the different components of the mixture, transforming the electrical signal into a gas chromatogram. The amount of eluted substance is plotted according to the retention time (the time needed for an analyte to leave the chromatographic column). This time depends on the affinity the analyte has with the latter.

Gas chromatography can be used to analyse gaseous, liquid and solid samples, provided they are suitably soluble and can be vaporised. Detectors, coupled with this technique can be multiple, but one of the most used detectors is mass (MS). Inside the detector the molecules are ionised and fragmented by bombardment by a beam of electrons at about 70 eV, obtaining ions with different charge and mass. The ions obtained are accelerated by an electric field placed in a magnetic field, where they will travel different trajectories depending on their  $m/z$  ratio (mass/charge). The obtained spectrum allows reconstruction of the structure of the molecule through the identification of fragments, according to their atomic mass [86]. The instrument used is an Agilent Gas Chromatograph 6890N series coupled to an Agilent Technologies 5973 Inert mass spectrometer with EI (electrical impact) filament ionisation system and quadrupole mass analyser. The injector is maintained at a temperature of 250°C, and the injection is done manually injecting, through a graduated syringe, two  $\mu$ l of the solution with split ratio 10. The column is capillary, model Agilent HP5, composed of 5% phenyl - 95% dimethyl- polysiloxane, length 30 m and diameter 1.025 mm. Separation takes place by temperature gradient: 3 minutes at 50°C followed by a temperature ramp of 5°C/min up to 270°C. The gas carrier, which carries the vaporised sample inside the column is helium fed with a flow of 1,0 ml/min. The instrument

works under pressure at 52 kPa. At the last part of the column there is a split that directs a known amount of flow to the mass spectrometer. The identification of the peaks obtained from the chromatogram is carried out by the instrument's software, which compares the mass spectra of each peak with those present in the NIST library. The quantification was carried out by constructing a calibration line, reporting the analyte concentration vs the ratio of SI area/ analyte area.

Every sample, after electrolysis, was analyzed at GC-Mass and, through the use of a calibration line, the yield in vanillin was calculated. In particular, the calculation was made by using a calibration line that gives the possibility to relate the area of the peak corresponding to vanillin (retention time of vanillin 23.3 min) and its concentration in the solution.

### *2.6.3 Attenuated Total Reflectance Analysis*

Beyond the classic infrared spectroscopy in transmission, there is a technique that is based on the principle of total attenuated reflectance, called ATR (Figure 2.12). This technique is much used for the analysis of the surfaces of materials and their characterization. In this case, the infrared radiation passes through a particular crystal, with a high refraction index and transparent to the IR, which allows the electromagnetic wave to be reflected within it many times. The surface of the sample is pressed onto the upper surface of the crystal. Then the IR radiation coming from the spectrometer enters the crystal, is reflected through the crystal and penetrates the sample for a few fractions of microns, being partially absorbed (or attenuated). The sample has a lower refractive index than the crystal, so a region is created in the sample where the electromagnetic wave, called an evanescent wave, penetrates the medium for a fraction of its wavelength.

The evanescent wave decays in the sample exponentially relative to the distance from the crystal surface, over a distance of the order of microns. After some reflections, the attenuation of the intensity of the IR ray is sufficient to be detected by the spectrophotometer, giving an FT-IR spectrum in total attenuated reflectance (ATR) [87] .

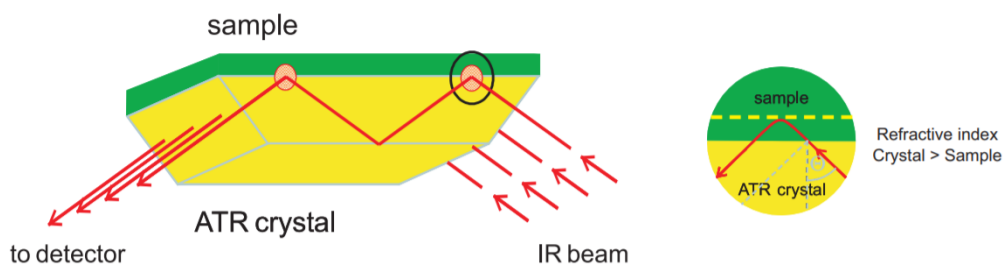


Figure 2.12 Phenomenon of Total Attenuated Reflectance [88]

The analyses were carried out on lignin samples before the reaction and on the precipitated one after the reaction. They were recorded with an Alpha Brucker instrument, with OPUS software. Measurements were conducted between 4000  $\text{cm}^{-1}$  to 360  $\text{cm}^{-1}$  with a spectral resolution of 2  $\text{cm}^{-1}$  operating with the diamond crystal. The background is recorded without a sample and automatically subtracted from the spectrum. The signal-to-noise ratio is increased by recording 20 accumulations for each measurement, both for the samples and the background.

### 3. Results and discussion

In the following chapter, the results of the catalytic electro-oxidation of Kraft lignin, using open-cell 3D Ni foams as electro-catalysts, are elaborated and discussed. These foams have been used as received or as supports for the deposition of active phases.

An initial bibliographic research study has been conducted about catalysts reported in the literature, which moves onwards through the selection of materials active in the oxidation of lignin and in general in the oxidation of organic substrates, as already explained in Chapter 1. Hence, taking into account the data reported in the literature Ni and Co mixed hydroxides and Co hydroxides were deposited through electrodeposition on Ni foams, as described in Chapter 2.

#### 3.1 Catalysts characterization

The SEM images of the Ni bare foam are displayed in Figure 3.1-A; B. A low magnification image (Figure 3.1-A) showed the macroporous structure of the open-cell foam, while in the high magnification image, the grain edges that make up the metal structure of Ni and its characteristic roughness were observed (Figure 3.1-B). EDS analyses in selected regions of interest did not detect the presence of oxygen species on surface.

SEM images of the NiCo and Co samples in Figure 3.1-C and Figure 3.1-D, respectively, showed the deposition of a thin film of hydroxides. EDS spectra confirm the deposition of Co on both foams, it should be noted that the estimation of the content of Ni in the coating is not straightforward since the Ni signal was also related to the Ni foam. During the application of the cathodic potential of -1,2V vs SCE for 100 s, the pH close to the foam surface increased, leading to the formation of the hydroxides. Cracks were present on the surface of both catalysts, which could be related to the drying process or to the evolution of H<sub>2</sub> during electrodeposition. From the inspection of regions of the coating containing cracks, the thickness of the electrodeposited coatings was estimated.

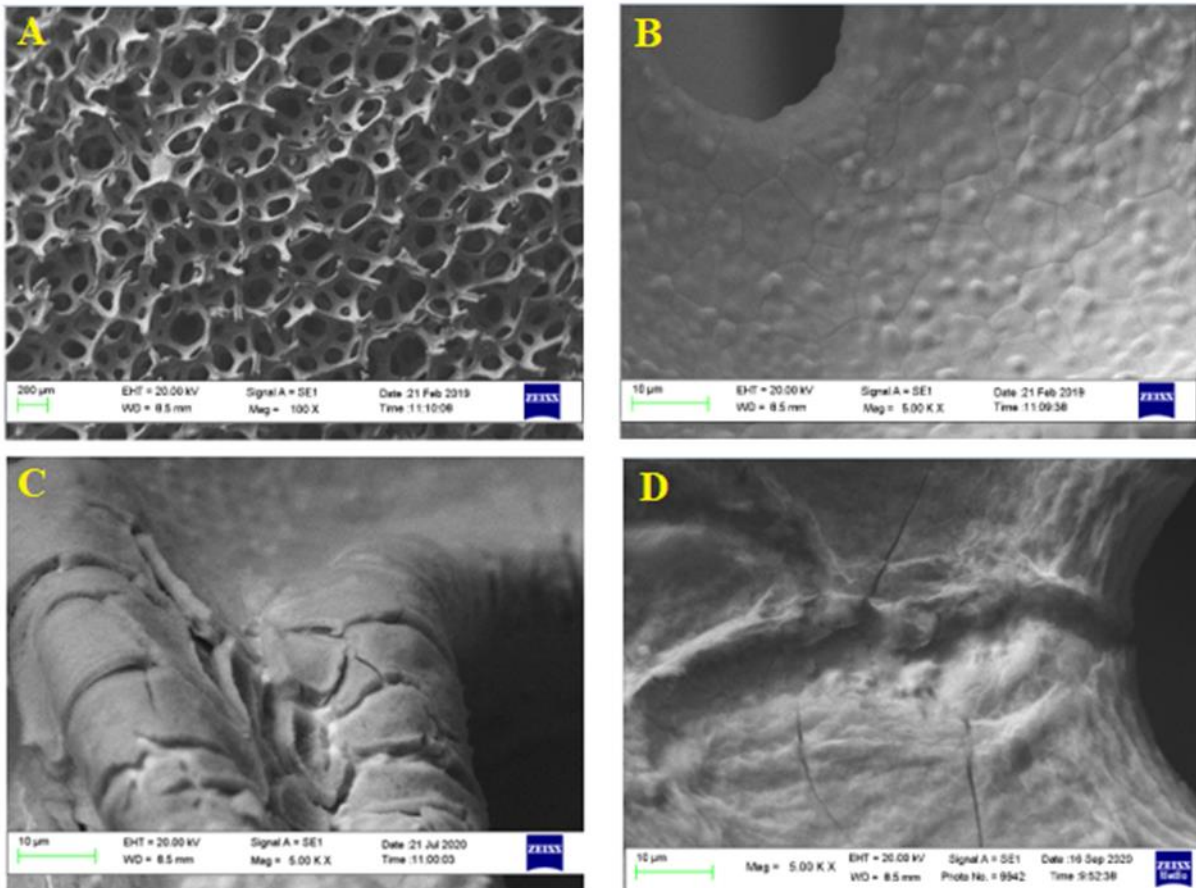


Figure 3.1: SEM images of: open-cell Ni foam at different magnification, A (100x) and B (500x); surface of Ni(OH)<sub>2</sub>-Co(OH)<sub>2</sub>/Ni, C (500x) and of Co(OH)<sub>2</sub>/Ni, D (1000x).

The layer of hydroxides Ni(OH)<sub>2</sub>-Co(OH)<sub>2</sub> deposited was thicker (ca. 4-5 μm) than that of Co(OH)<sub>2</sub> hydroxides (ca. 2-5 μm). Probably, because of this increased thickness, the cracks on the foam coating Ni(OH)<sub>2</sub>-Co(OH)<sub>2</sub>/Ni are more pronounced than those on the Co(OH)<sub>2</sub>/Ni foam coating. Moreover, the coating on the foam surface Co(OH)<sub>2</sub>/Ni is more homogeneous than that for the foam Ni(OH)<sub>2</sub>-Co(OH)<sub>2</sub>/Ni.

The diffraction pattern in Figure 3.2 for Ni bare foam only showed the reflections due to Ni<sup>0</sup>. After electrodeposition of the hydroxides, it was not possible to identify any reflections related to crystalline phases, which could be related to either the low amount of coating or the deposition of poorly crystallized solids.

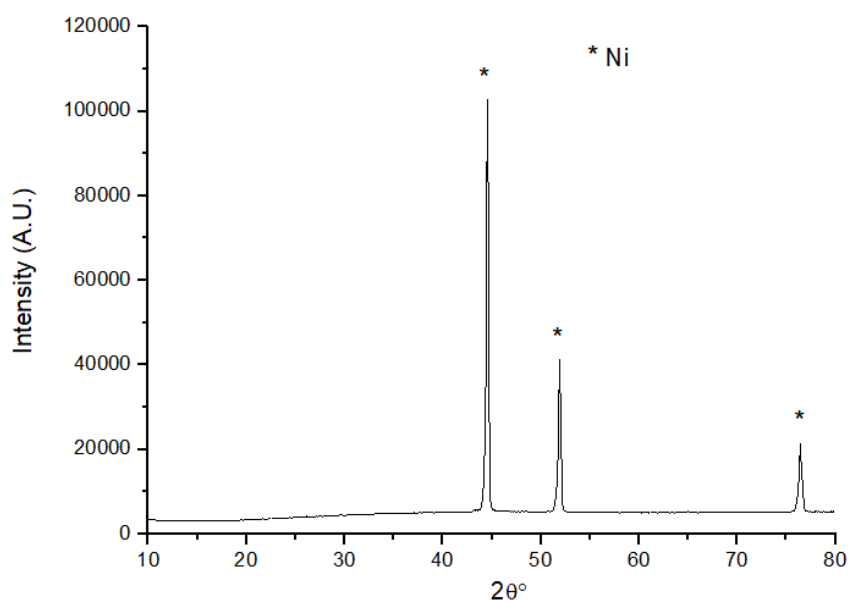


Figure 3.2 XRD pattern of Ni bare foam after pretreatment.

In the Raman spectra of  $\text{Ni(OH)}_2\text{-Co(OH)}_2/\text{Ni}$  and  $\text{Co(OH)}_2/\text{Ni}$  (Figure 3.3-A) four well-defined bands were recorded at 459, 528, 1056, and  $3600\text{ cm}^{-1}$ , which confirmed the deposition of Ni and Co-Hydroxides species. The first two bands were presumably associated with the  $\alpha\text{-Co(OH)}_2$  structure, a layered rhombohedral-type structure (similar to hydroxycalcite) [89]. The intense band at  $520\text{ cm}^{-1}$  could be related to the symmetrical stretching of the CoO bond ( $A_{2u}$ ) and that at  $455\text{ cm}^{-1}$  to the bending mode of the OCoO bond ( $A_{1g}$ ) [89]. The  $1056\text{ cm}^{-1}$  one instead indicated the presence of nitrates embedded in the electrodeposited layers and in particular the symmetrical stretching of the N-O bond of the  $\text{NO}_3$  [90].

The peak at  $3600\text{ cm}^{-1}$  was characteristic of stretching of the OH bond of water into the crystalline forms of  $\alpha$  or  $\beta\text{-Ni(OH)}_2$ . The water may be interspersed between the lattice layers or simply be surface water [91].



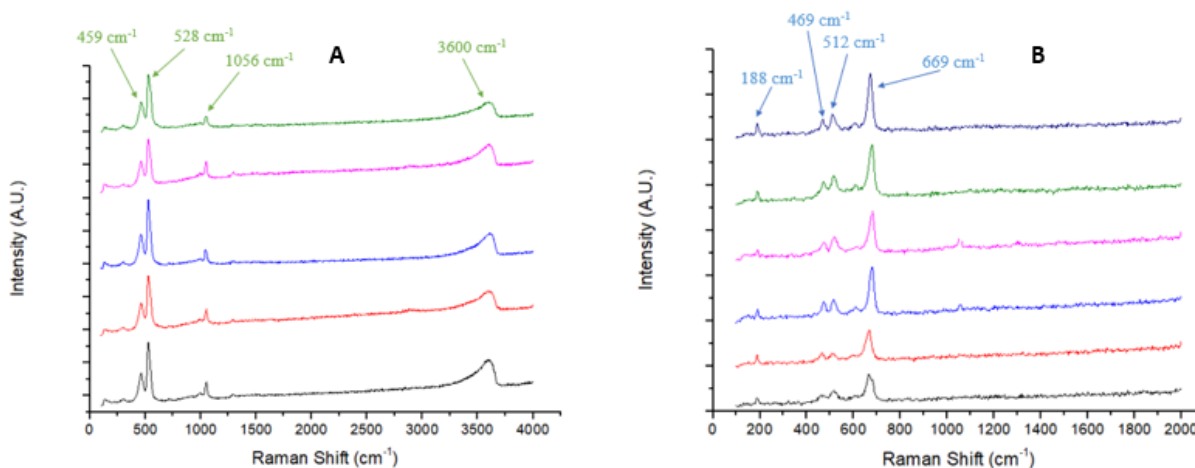


Figure 3.3 Raman spectra acquired in different sections of Ni(OH)<sub>2</sub>-Co(OH)<sub>2</sub>/Ni electrode pre-electrolysis between 100 and 4000 cm<sup>-1</sup> (a) and Co(OH)<sub>2</sub>/Ni electrode (b) pre-electrolysis between 100 and 2000 cm<sup>-1</sup>

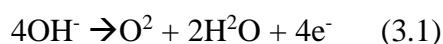
In the Raman spectra of Ni foams deposited with Co hydroxides (Figure 3.3-B) the peaks characteristic of  $\gamma$ -CoOOH are recorded at 469, 512, and 669 cm<sup>-1</sup>. This is a stoichiometric form of Co hydroxide, where cobalt generally has oxidation states of Co (3+). Among the various possible crystalline forms of oxyhydroxide, the  $\gamma$  form is quite common [91]. The peaks at 465 and 510 cm<sup>-1</sup> can be respectively assigned to the Co-O bond (H) and the vibrations mode Eg. Finally, the one at 664 cm<sup>-1</sup> can be associated to the A<sub>1g</sub> mode [89].

The band of 188 is associated with cobalt oxide, Co<sub>3</sub>O<sub>4</sub>, in particular to the F3g mode [92].

### 3.2 Cyclic-voltammetry in NaOH 1M.

In the figure 3.4, the cyclic-voltammeteries in NaOH 1M for the investigated electrocatalysts Ni bare, Ni(OH)<sub>2</sub>-Co(OH)<sub>2</sub>/Ni and Co(OH)<sub>2</sub>/Ni were displayed. This technique permits to study the activity of the electrocatalysts for the oxygen evolution reaction (OER) and the species formed on surface, due to modification of Ni and Co oxidation state. Through the comparison of the current density curves vs potential obtained, it was possible to evaluate qualitatively the catalytic activity of the catalyst for the electrochemical oxidation of lignin and the OER.

At potentials around 0.5-0.6V vs SCE the current density began to increase exponentially, reaching a value of 0.150-0.175A/cm<sup>2</sup>. This sudden increase was mainly due to the OER, which involved the oxidation of OH<sup>-</sup> present on the surface of the electrode to give O<sub>2</sub> (3.1).



The starting potential of the current discharge was here defined as the onset. It should be noted that the onset was not the same for all the three electrodes and this indicated that there were different activities towards the OER. In particular, Co(OH)<sub>2</sub>/Ni displayed the onset at less anodic potential and, while the most anodic value of the onset was observed for Ni bare. From this information, it could be deduced that Co(OH)<sub>2</sub>/Ni was the most active catalyst for OER, conversely, Ni bare had the lower catalytic activity.

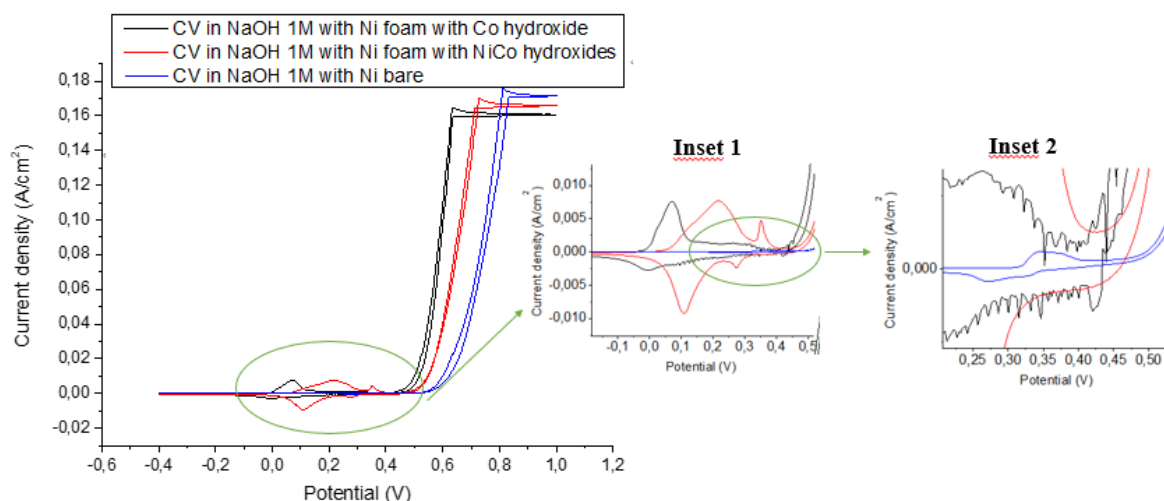


Figure 3.4 Cyclic-voltammeteries for the electrodes (between -0.4 and 1.2V vs SCE with a scan-rate of 5 mV/s, in a NaOH 1M solution): Ni foam with Co hydroxide (black line); Ni foam with NiCo hydroxides (red line) and Ni bare (blue line). **Inset 1**: magnification in the potential range from -0,1V to 0,6V vs SCE. **Inset 2**: magnification in the potential range from 0,2 to 0,5V vs SCE.

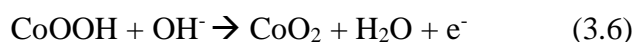
The insets 1 and 2 in Figure 3.4 showed three peaks, related to the Ni<sup>2+/3+</sup> and the Co<sup>2+/3+</sup> redox species in the potential range from -0.10 to 0.50V vs SCE (3.2-3.3 and 3.4-3.7). In the CV of the Ni bare (blue line) a pair of redox peaks at ca 0,35V vs SCE in oxidation and at ca 0.27V vs SCE in reduction are observed, see Figure 3.4-inset 2. These peaks were related to the redox pair Ni<sup>2+/3+</sup> and in particular to the following reactions [75]:



There were no oxidation peaks of Ni<sup>0</sup> to Ni<sup>2+</sup> (we would see them at lower potentials [93], but it is known that Ni undergoes a oxidation effect to Ni(OH)<sub>2</sub> when immersed in alkaline solutions [94]. This accounted for the presence of the hydroxides on the surface of the catalyst. The Ni hydroxides that were formed on the surface of the foam continued to oxidize providing the Ni oxo-hydroxides, and then reduced to give the Ni hydroxides again.

Comparing the CV in NaOH made at Ni bare, with those made at Ni(OH)<sub>2</sub>-Co(OH)<sub>2</sub>/Ni and Co(OH)<sub>2</sub>/Ni, it was evident that redox peaks attributed to the substrate (blue curve) were extremely low in intensity compared to the those for electrodeposited catalysts. Hence, it could be deduced that the substrate had little influence on the total current of these hybrid electrodes [75].

The redox peaks, recorded for Co(OH)<sub>2</sub>/Ni (black line), at 0,07V vs SCE and -0,01V vs SCE, are associated with the Co<sup>2+/3+</sup> species. In literature, the most common interpretation about the phenomena that could occur on the surface of the electrode was illustrated below (3.4-3.7) [73]. Co<sup>2+</sup>, in the potential range from -0.10V to 0.6V vs SCE should undergo two oxidation steps: from Co<sup>2+</sup> (oxidation state in the hydroxides) to Co<sup>3+</sup> (in the oxo-hydroxides) and from Co<sup>3+</sup> to Co<sup>4+</sup> (in CoO<sub>2</sub>), as shown below [75].



Therefore, theoretically, we should be able to see two pairs of redox peaks, but in Figure 3.4-Inset 1, only one pair was visible. This may be related to the fact that the redox processes occurred at very close potentials, and hence the peaks were overlapped, probably this may be also because that the amount of material deposited is quite high.

For Ni(OH)<sub>2</sub>-Co(OH)<sub>2</sub>/Ni sample (red line) the peaks of the Ni and Co redox pairs were observed. The first one was more intense and it was related to Co species (3.4-3.7), with maximum at 0,22V vs SCE in oxidation and at 0,11V vs SCE in reduction. The second one recorded at 0,35V vs SCE in oxidation and at 0,28V vs SCE in reduction was attributed to the Ni<sup>2+/3+</sup> couple (3.2-3.3). Again, it was not possible to detect two pairs of Co peaks, as expected from the number of species involved in the process.

### 3.3 Cyclic-voltammetry in Lignin 10g/L

Firstly, the Lignin concentration used for the catalytic tests was selected. In literature, the two most common concentrations used are 10g/L and 1g/L [17]. However, a low lignin concentration (1g/L) did not allow to identify any oxidation step due to the lignin depolymerization, over the Ni bare foam. Moreover, during the experiments at constant potential the OER was favoured. Hence, the concentration chosen to continue the work was 10g/L

In the Figure 3.5, CVs in Kraft Lignin 10g/L for the Ni bare and the electrodeposited Ni(OH)<sub>2</sub>-Co(OH)<sub>2</sub>/Ni and Co(OH)<sub>2</sub>/Ni catalysts were compared. The peaks, related to the Ni<sup>2+/3+</sup> and the Co<sup>2+/3+</sup> redox species, above explained were observed. However, their slightly lower intensity in comparison to the ones recorded in 1M NaOH suggested the detaching of a small amount of coating.

Adding lignin 10 g/L in solution the onset of discharge increased for each catalyst compared to CVs without lignin. Slightly for Co(OH)<sub>2</sub>/Ni, and around ca 30-50mV for Ni bare and Ni(OH)<sub>2</sub>-Co(OH)<sub>2</sub>/Ni foams. This suggested a higher activity for lignin electro-oxidation of these two latter catalysts.

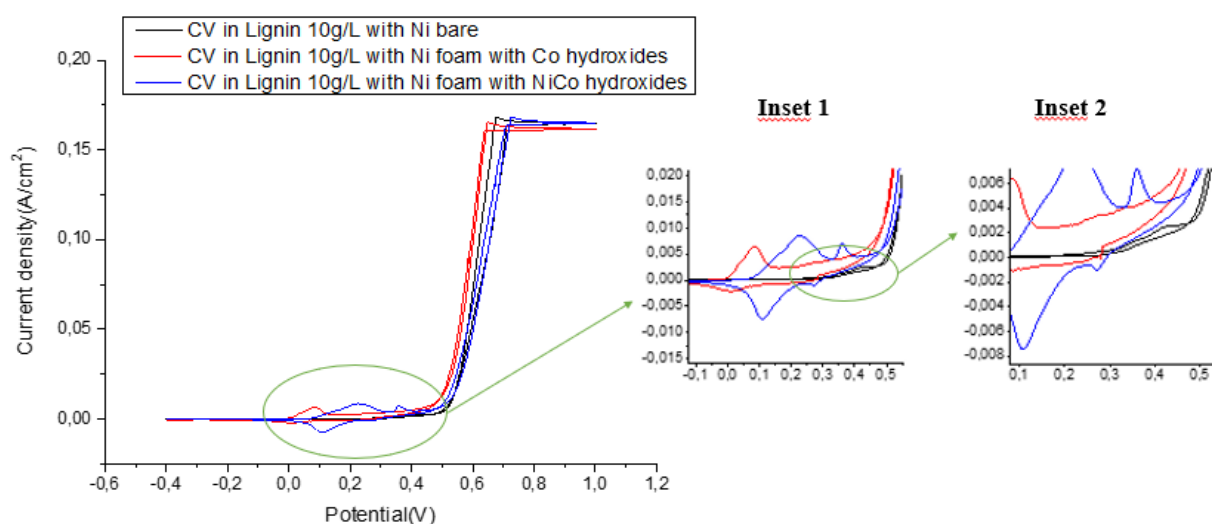


Figure 3.5: Cyclic-voltammeteries for the electrodes (between -0.4 and 1.2V vs SCE with a scan-rate of 5mv/s, in a Kraft Lignin 10g/L solution): Ni foam with Co hydroxide (red line); Ni foam with NiCo hydroxides (blue line) and Ni bare (black line). **Inset 1**: magnification in the potential range from -0,1V to 0,5V vs SCE. **Inset 2**: magnification in the potential range from 0,1 to 0,5V vs SCE.

### 3.4 Electrochemical oxidation of Kraft Lignin

From the comparison of CVs with and without lignin, shown in fig 3.6, it was observed that the current density generated in the presence of lignin was greater than that generated in its absence. Especially, this was true in the range of potential from 0.05V to 0.5V vs SCE, and confirmed that lignin was oxidized in that range of potential.

In order to select the optimal potential to perform the electrooxidation of lignin to vanillin, some preliminary electrochemical tests were performed for 5 h in the potential range from 0.5 V to 0.1 V vs SCE. In fact, the optimal potential for lignin electrolysis could be any value beyond the onset potential, however it should be underlined that the current density was not related to the selectivity, namely a higher current involved an increase in the electroactivity but it could not be stated the type of products obtained.

Hence, the vanillin produced was qualitatively evaluated by  $^1\text{H}$  NMR. The characteristic singlet of the vanillin aldehyde proton at 9.76 ppm was only present in the spectra of the sample obtained after oxidation at 0.6 V (Figure 3.7). Conducting the electro-oxidation of lignin in the OER potential range (above 0.6 V) mainly led to the formation of hydroxyl radicals ( $\bullet\text{OH}$  defined as active oxygen). These radicals were adsorbed over the anode surface and they pushed the oxidation of the organic substance to take place. While at 0.5 V, beyond the OER potential range, there were not enough active oxygen species to promote the degradation of lignin, and in particular the breakage of  $\beta\text{-O-4}$  bond, indeed no Vanillin yield was recorded [68].

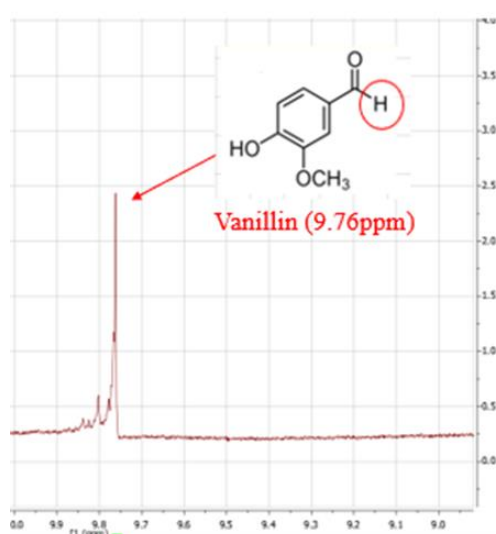


Figure 3.7:  $^1\text{H}$  NMR Spectrum of products mixture post-electrolysis (0,6V, 3h, 25°C with Ni bare as catalyst) of Kraft lignin 10g/L.

To estimate the amount of vanillin produced at 0.6 V, the electrolyte after the reaction was analysed at the GC-MS. A really low yield in vanillin was obtained, i.e. 0.009 wt.%, though the conversion of lignin was ca. 35%. These results could be explained considering the insurgence of repolymerization/recondensation processes or the further oxidation and decomposition of vanillin.

Hence, to limit the effect of the side reactions and therefore increase the Vanillin yield, lower reaction times, i.e. 3 and 1 h, were used for the tests carried out with all the three types of electrocatalysts.

In the Table 3.1 the results obtained from the electrolysis of Kraft lignin with Ni bare; Ni(OH)<sub>2</sub>-Co(OH)<sub>2</sub>/Ni and Co(OH)<sub>2</sub>/Ni electrodes, at a reaction time of 3 hours, were compared. The presence of Ni-Co mixed hydroxide or Co-hydroxide did not enhance the catalytic activity of Ni bare foam in terms of vanillin yield; although, the charge passed during the electrooxidation was comparable for all electrocatalyst. However, both the charge accumulated during the reaction and the conversion of lignin were greater for the Co(OH)<sub>2</sub>/Ni foam, probably due to the occurring of re-polymerization and OER side reaction.

Catalysts	Potential (V)	Time (h)	Temperature (°C)	Charge (C)	Vanillin Yield (% w/w)	Lignin Conversion (% w/w)
Ni bare	0,6	3	25	2794	0,065	25
Ni(OH) <sub>2</sub> /Co(OH) <sub>2</sub>	0,6	3	25	2770	0,015	15
Co(OH) <sub>2</sub>	0,6	3	25	3526	0,005	66

Table 3.1: Lignin conversion and Vanillin yield obtained from the electrolysis of Kraft lignin with Ni bare; Ni(OH)<sub>2</sub>-Co(OH)<sub>2</sub>/Ni and Co(OH)<sub>2</sub>/Ni catalysts at a reaction time of 3 hours, a temperature of 25°C and applying a potential of 0,6V vs SCE.

To decrease more the contribution of side reactions, it is was decided to further reduce the reaction time at 1h (table 3.2). Indeed, reducing the reaction time from 3h to 1h had a beneficial effect on the Vanillin yield for all the catalysts. However, Ni bare still showed the best performances, with the highest Vanillin yield. Also, in this case, both the charge accumulated and the lignin conversion were greater for the Co(OH)<sub>2</sub>/Ni foam. Nevertheless, Lignin conversion for Ni bare and Ni(OH)<sub>2</sub>-Co(OH)<sub>2</sub>/Ni followed a strange trend that it was difficult to explain and that deserved further research in a future work.

Catalysts	Potential (V)	Time (h)	Temperature (°C)	Charge (C)	Vanillin Yield (% w/w)	Lignin Conversion (% w/w)
Ni bare	0,6	1	25	920	0,086	25
Ni(OH) <sub>2</sub> /Co(OH) <sub>2</sub>	0,6	1	25	691	0,040	49
Co(OH) <sub>2</sub>	0,6	1	25	1327	0,025	50

Table 3.2: Lignin conversion and Vanillin yield obtained from the electrolysis of Kraft lignin with Ni bare; Ni(OH)<sub>2</sub>-Co(OH)<sub>2</sub>/Ni and Co(OH)<sub>2</sub>/Ni catalysts at a reaction time of 3 hours, a temperature of 25°C and applying a potential of 0,6V

From the results obtained it could be stated that the vanillin yield at low times was greater than that at high reaction times. This confirmed that vanillin was an unstable compound and that it was likely to be involved in other reactions as a reagent at a later time [63]. In general, the catalyst that obtained the worst results was the Ni foam deposited with hydroxides of Co, the one that obtained the greatest yields was the Ni bare.

The results obtained were in line with the works reported by Raziye Ghahremani et al. [17]. They studied the electro-oxidation of Kraft lignin through the application of a constant potential over time, under conditions close to those used in this work. The reaction was conducted at room temperature with NaOH 1M as electrolyte, with a concentration of Kraft lignin of 10g/L in a three-compartment cell. Ni and/or Co anode electrodes were used at different molar ratios, with an applied potential of 0,354V vs SCE for 16 hours (Table 3.3).

Ghahremani et al.	Ni	Co	Ni <sub>8</sub> -Co <sub>2</sub>	Ni <sub>5</sub> -Co <sub>5</sub>	Ni <sub>2</sub> -Co <sub>8</sub>
Vanillin (w/w %)	0,0108	0,0288	0,0107	0,0250	0,0316
<b><u>This work (0,6V, 25°C)</u></b>	<b>Ni bare</b>	<b>Co/Ni</b>	<b>Ni(OH)<sub>2</sub>-Co(OH)<sub>2</sub>/Ni.</b>		
Vanillin (w/w%) 1 h	0,086	0,025	0,040		
Vanillin (w/w%) 3 h	0,065	0,015	0,005		

Table 3.3 Comparison between Vanillin yield obtained by Raziye Ghahremani et al. and those obtained in this work, from Kraft lignin 10 g/L electrolysis.

From the data summarized in table 3.3, it was clear that the vanillin yields reported in literature and in this work were in the same order of magnitude, therefore the results could be considered comparable.

In general, the yields in vanillin were relatively low, due to the intrinsic complexity of the lignin structure and the well-known difficulty in performing its depolymerization in a selective way [17]. In the following section the efforts made to characterize the side-products are summarized.

### 3.4.1 Characterization of side-products

The chromatograms obtained by GC-MS analyses for all the reaction conditions over the three types of catalysts confirmed that the electro-oxidation of lignin Kraft led to a complex products mixture. Unfortunately, it was not possible to characterize and quantify with certainty all the products present in the post-reaction mixture, therefore a trend in the by-products with changing of the reaction conditions could not be established. However, it was possible to confirm the formation of acetovanillone and vanillic acid (Table 3.4 and Figure 3.8 and 3.9), in agreement with results previously reported in the literature [17].

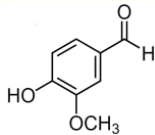
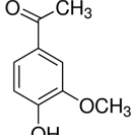
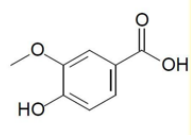
	Vanillin	Acetovanillone	Vanillic acid
<b>Retention time (min)</b>	23.3	25.5	27.5
<b>Chemical structure</b>			

Table 3.4: Retention times and chemical structure of the main products identified on the GC-MC.



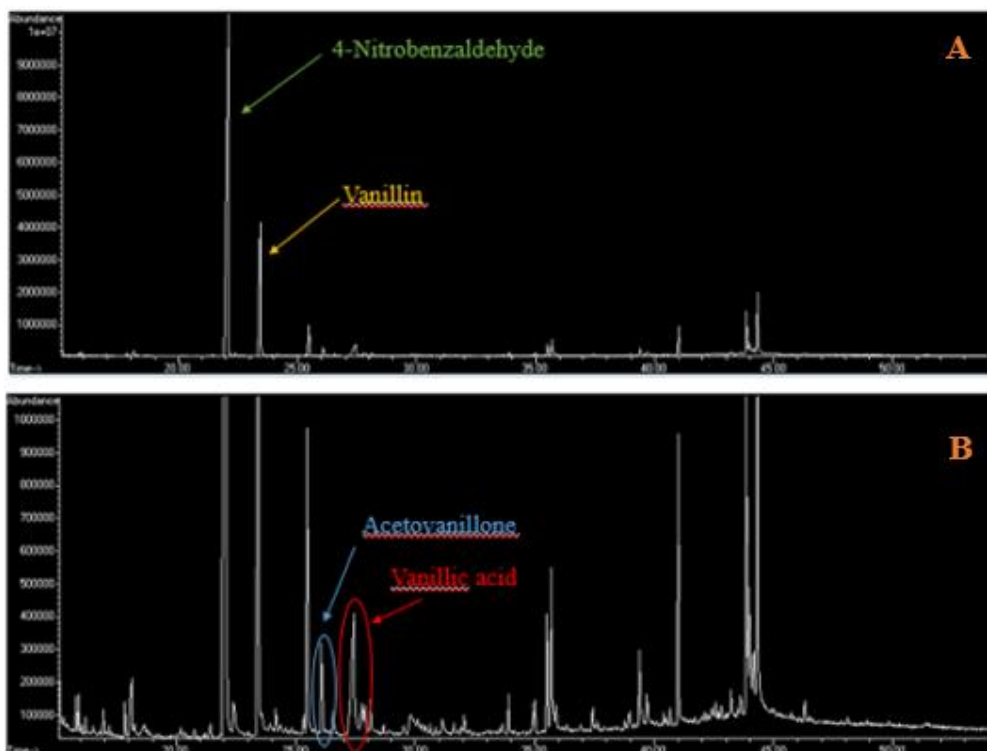


Figure 3.8: GC-MS Chromatogram for the electrolysis products of Kraft lignin 10g/L using as a catalyst  $\text{Ni(OH)}_2\text{-Co(OH)}_2/\text{Ni}$  . In the spectrum we see the characteristic peak of 4-Nitrobenzaldehyde, which was used as an internal standard (A).

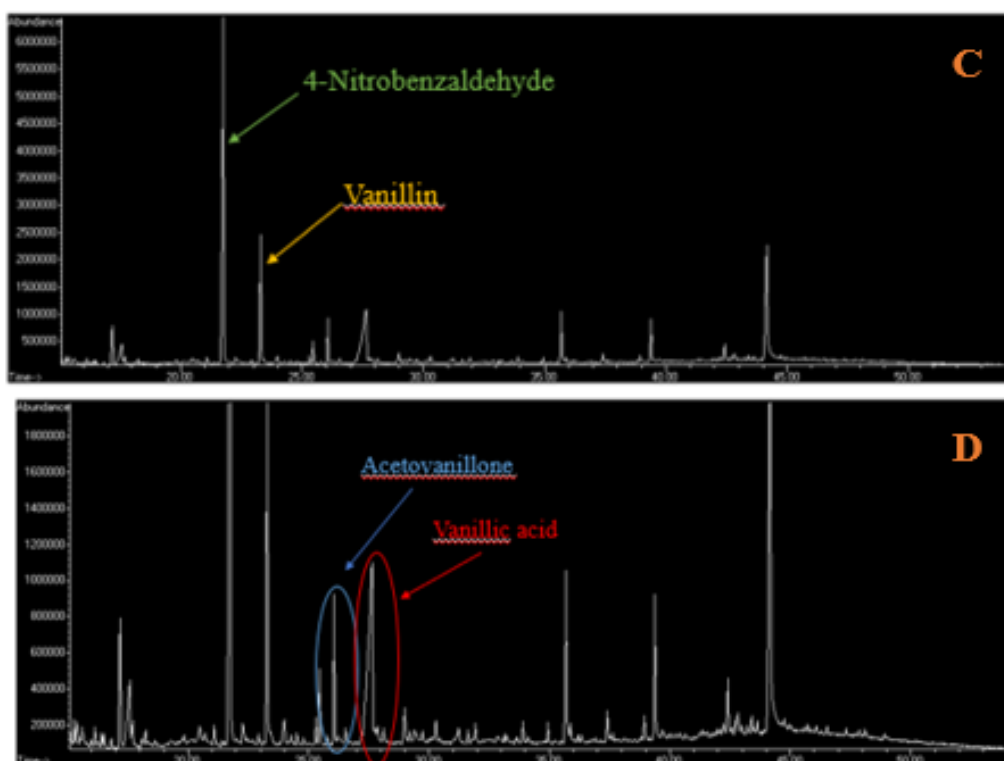


Figure 3.9: GC-MC Chromatogram for the electrolysis products of Kraft lignin 10g/L using as a catalyst  $\text{Co(OH)}_2/\text{Ni}$  . In the spectrum we see the characteristic peak of 4-Nitrobenzaldehyde, which was used as an internal standard (C).

In the  $^1\text{H-NMR}$  spectra some low intensity signals, in the range from 5 to 6 ppm, were recorded. In this area of the spectrum, the characteristic signals of protons bound to double bonds ( $\text{C} = \text{C-H}$ ) should be present. These signals indicated that oligomers may be present in the mix of reaction products. It should be noted that the structure of the oligomers was not elucidated in this work.

Lastly, both GC-MS and the  $^1\text{H-NMR}$  analyses suggested the presence in the reaction products mix of some carboxylic acids. The most frequent are: Cinnamic acid; Veratric acid, Benzoic acid, Maleic acid and Formic acid. However, a deeper characterization is required to confirm the presence of these compounds.

### 3.4.2 Characterization of the lignin after reaction

The post-reaction solid lignin residue was analyzed by ATR. This is commonly used as a qualitative technique to provide interesting information about the chemical bonds present in the lignin structure [95]. In figure 3.10, lignin pre-reaction and residual lignin post-reaction spectra, using Ni bare,  $\text{Ni(OH)}_2\text{-Co(OH)}_2/\text{Ni}$  and  $\text{Co(OH)}_2/\text{Ni}$  foams were displayed. Due to the complexity of the Kraft lignin structure, the spectra recorded were very complex, displaying many overlapped peaks. The assignment of the peaks shown in Table 3.5 was based on data reported in the literature [96].

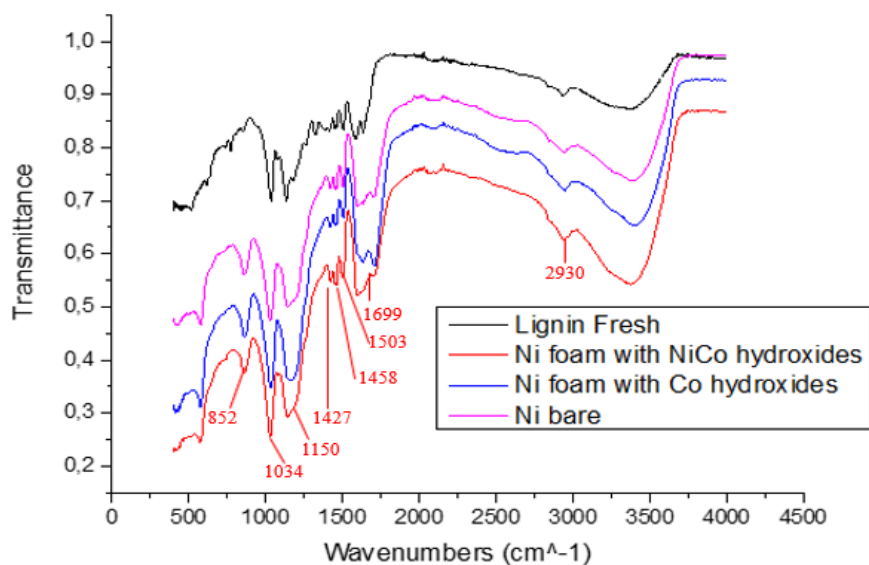


Figure 3.10: ATR spectra acquired for post-electrolysis residual lignin with Ni bare (pink line);  $\text{Ni(OH)}_2\text{-Co(OH)}_2/\text{Ni}$  (red line) and  $\text{Co(OH)}_2/\text{Ni}$  (blue line) catalysts and for fresh lignin pre-electrolysis. The spectrum was acquired between 380 and  $4000\text{ cm}^{-1}$

It was evident that between the fresh and the post-reaction lignin there were no remarkable differences. Evidently, the Kraft lignin during the electro-oxidation degraded only partially, leaving the main structure unaltered [95]. Therefore, the post-reaction structure did not present substantial differences compared to the fresh one.

The exceptions were the signal at  $852\text{ cm}^{-1}$ , which appeared only in the spectra of post-reaction lignin and the signal at  $1150\text{ cm}^{-1}$  related to the formation of the guaiacol and syringol residual, respectively, two of the constituent monomers of lignin. Finally, the signal at  $1699\text{ cm}^{-1}$  was related of the formation of C=O groups, indicating the degradation of the polymer (table 3.5).

<b>Bands</b>	<b>Absorption (<math>\text{cm}^{-1}</math>)</b>
Aromatic C-H out of plane deformation (G)	852
C-H and C-O deformations	1034
Aromatic C-H in plane deformation (S)	1150
Aromatic ring vibrations	1427
C-H deformations, asymmetric	1458
Aromatic ring vibrations	1503
C=O stretching (non-conjugated)	1699
OH stretching (in CH- and CH <sub>2</sub> -)	2930

Table 3.5: adsorption peaks distinguished in ATR spectra with their corresponding bonds.

### 3.5 Cyclic-voltammetry in NaOH 1M post- reaction

The application of the anodic potential during the experiments could modify the characteristics of the coating, in terms of structure and morphology as well as amount of deposited coating. Hence, firstly it was evaluated whether the activity in the OER and the oxidation/reduction phenomena, due to Ni and Co hydroxides/oxyhydroxides in the electrocatalysts, were modified. Comparing the CVs pre- and post-reaction in NaOH 1M for Ni bare, Ni(OH)<sub>2</sub>-Co(OH)<sub>2</sub>/Ni and Co(OH)<sub>2</sub>/Ni in Figure 3.11, some changes could be identified for all the three electrocatalysts.

The characteristic peaks of hydroxides species were slightly shifted towards less anodic potentials, compared to the potential values that they displayed in the pre-reaction CVs, for Ni bare (Figure 3.11C), and to more anodic potentials for Ni(OH)<sub>2</sub>-Co(OH)<sub>2</sub>/Ni and Co(OH)<sub>2</sub>/Ni catalysts (Figure 3.11A and 3.11B). This was a sign that the coating suffered from some modifications during experiments. The intensity of these peaks were almost the same for Ni

bare and  $\text{Ni(OH)}_2\text{-Co(OH)}_2/\text{Ni}$ , hence the concentrations of these species on surface did not largely changed. While the intensity of the peaks in the  $\text{Co(OH)}_2/\text{Ni}$  foam decreased significantly after reaction, probably due to the loss of the coating during the catalytic cycle.

The onset of the OER discharge post-reaction was shifted towards less anodic potential, compared the OER discharge pre-reaction, for Ni bare and also for  $\text{Ni(OH)}_2\text{-Co(OH)}_2/\text{Ni}$  catalysts, of ca 100 mV and 30 mV, respectively. This indicated an activation of these catalysts for the OER, in particular for Ni bare foam.

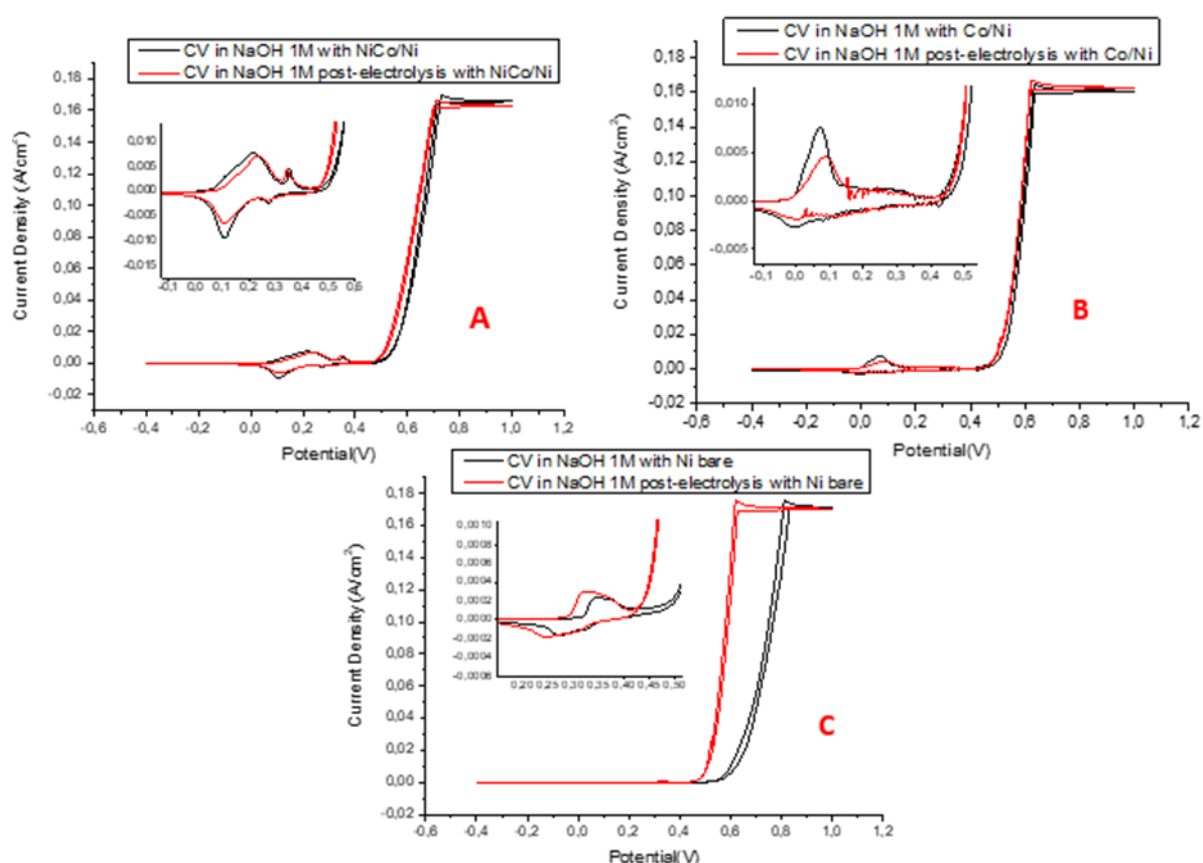


Figure 3.11: Cyclic-voltammetry in a 1M solution of NaOH pre-reaction (black line) and post-reaction (red line) for the electrode: A)  $\text{Ni(OH)}_2\text{-Co(OH)}_2/\text{Ni}$ ; B)  $\text{Co(OH)}_2/\text{Ni}$  and C) Ni bare.

### 3.6 Cyclic-voltammetry in Lignin 10g/L post- reaction

Comparing the CVs pre- and post-reaction in Kraft Lignin 10g/L, for the Ni bare,  $\text{Ni(OH)}_2\text{-Co(OH)}_2/\text{Ni}$  and  $\text{Co(OH)}_2/\text{Ni}$  catalysts (Figure 3.12), there were not observed any particular variation in the intensity and position of the hydroxides peaks, except for a small decrease in intensity for  $\text{Ni(OH)}_2\text{-Co(OH)}_2/\text{Ni}$  and  $\text{Co(OH)}_2/\text{Ni}$  foams. This difference was so small that

one cannot know whether it could be attributed to an effective deactivation of the foam or to the positioning of the electrodes slightly different from the pre-reaction CVs.

Also in this case, the peak of lignin oxidation, clearly visible only for Ni bare foam at 0,4V vs SCE, did not show significant differences and, in general, the CVs for all catalyst were not changed.

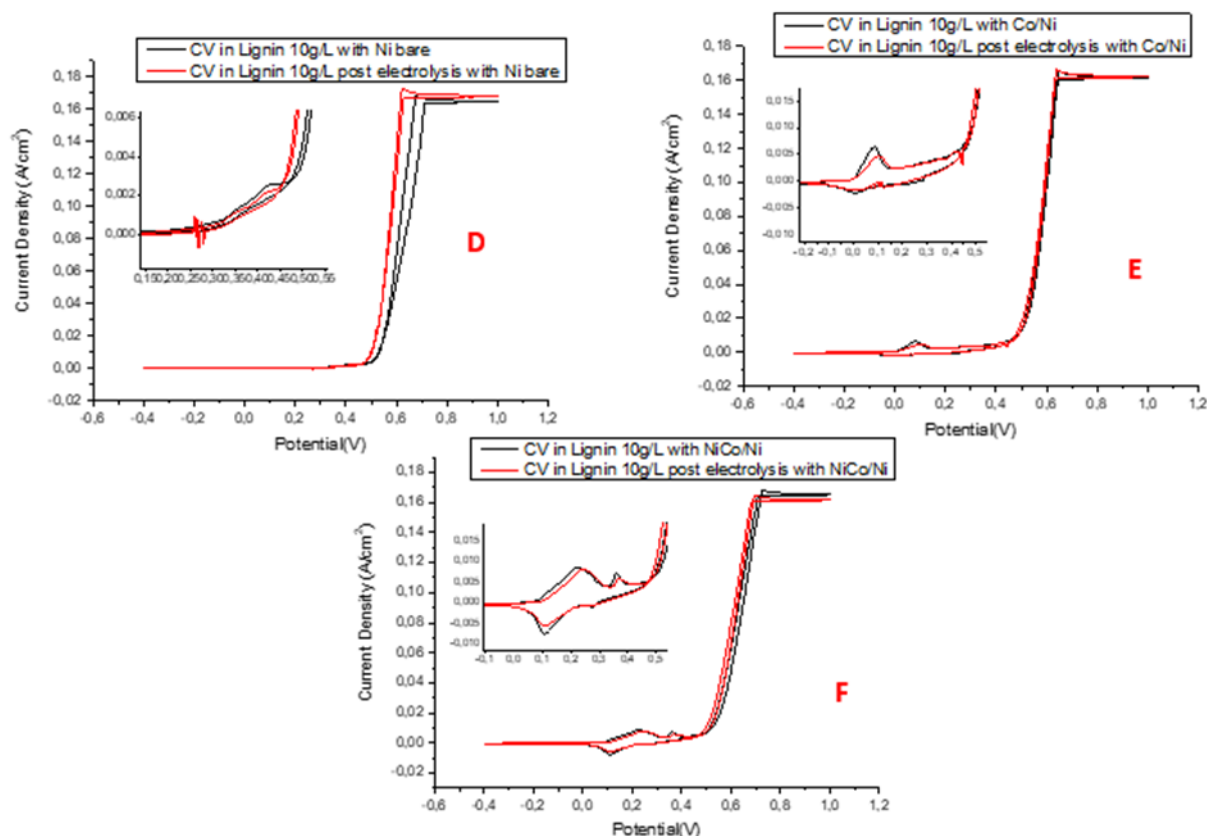


Figure 3.12: Cyclic-voltammetry in a 1M solution of NaOH pre-reaction (black line) and post-reaction (red line) for the electrode: D) Ni bare/Ni; E) Co(OH)<sub>2</sub>/Ni and F) Ni(OH)<sub>2</sub>-Co(OH)<sub>2</sub>/Ni

### 3.7 Characterization of the post-reaction catalysts

The characterization of the foams was carried out after the end of the catalytic cycle which included pre and post-reaction CVs and CA at 0,6V.

XRD and SEM analyses showed no differences in pre- and post-reaction foams for any of the three types of catalysts analysed. However, EDS analyses highlight the presence of oxygen in Ni bare, which before was absent, presumably due to the formation of Ni oxides.

Figure 3.13 showed the pre and post-reaction Raman spectra for the  $\text{Ni}(\text{OH})_2\text{-Co}(\text{OH})_2/\text{Ni}$  and  $\text{Co}/\text{Ni}$  foam. We can notice how the hydroxides peaks, described in paragraph 3.3, were still present in the post-reaction catalyst. Despite this, the peaks, for both catalysts, seemed to have a slightly lower definition and intensity, appearing broader than the pre-reaction ones. The explanation probably lies in the fact that part of the coating was detached during the catalytic cycle.

The peak at  $3600\text{ cm}^{-1}$  disappeared. Probably the intensity of the peak may be too low to allow detection or there may be no more water in the deposited layers on the surface of the foam; in addition, an inversion between the  $459$  and  $528\text{ cm}^{-1}$  signal intensity can be observed (figure 3.13A).

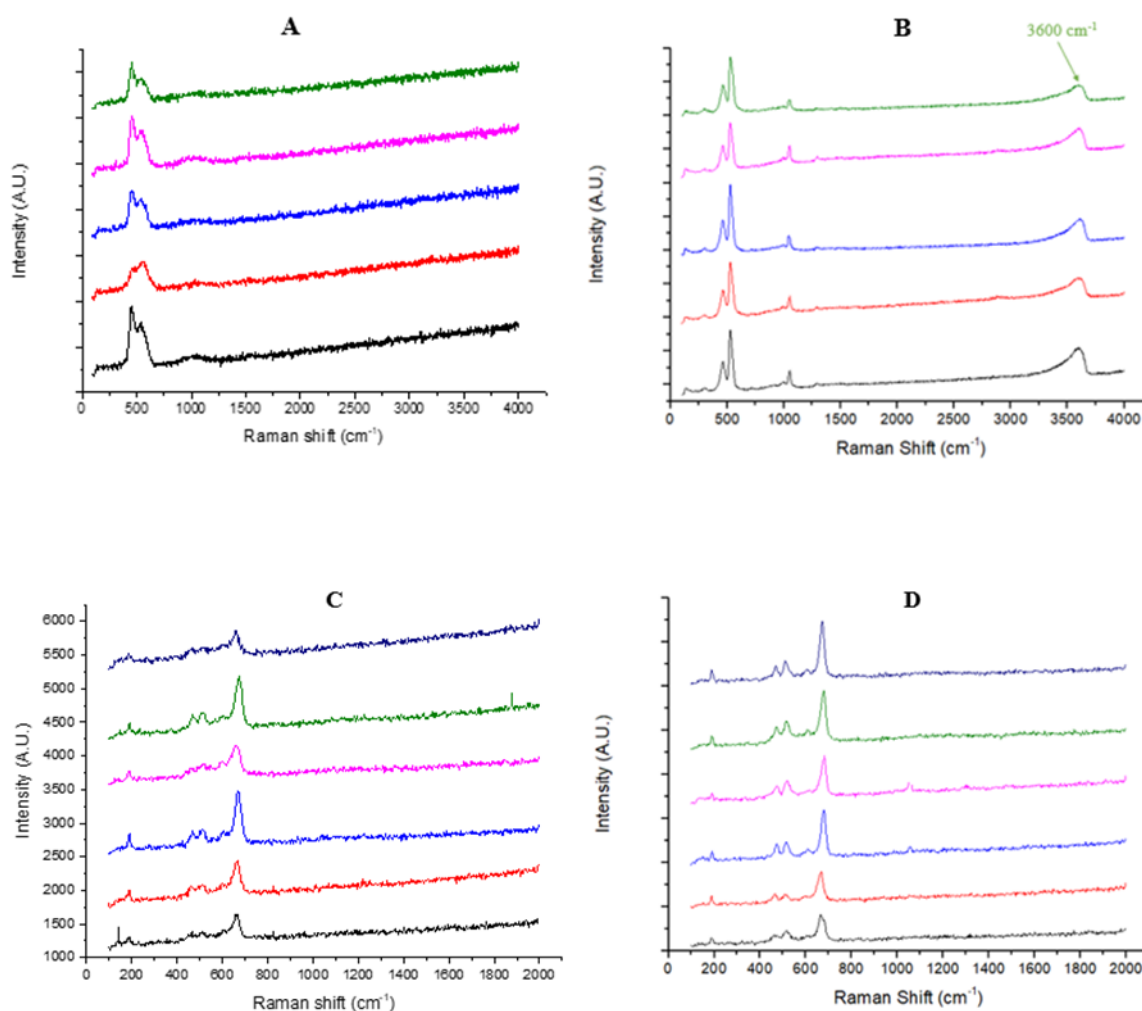


Figure 3.13 Raman spectra acquired in different sections of:  $\text{Ni}(\text{OH})_2\text{-Co}(\text{OH})_2/\text{Ni}$  electrode post-electrolysis (a) and pre-electrolysis (b) between  $100$  and  $4000\text{ cm}^{-1}$ ;  $\text{Co}(\text{OH})_2/\text{Ni}$  electrode post-electrolysis (c) and pre-electrolysis (d) between  $100$  and  $2000\text{ cm}^{-1}$ .

## 4. Conclusions

The electrocatalytic oxidation of Kraft lignin in basic media over 3D Ni bare, Co hydroxide/Ni foam and NiCo hydroxides/Ni foam catalysts is a challenging process that besides the target vanillin leads to the formation of several by-products such as acetovanillone, vanillin acid and oligomers. The yield in vanillin depends on both the reaction conditions, applied potential and time, and on the type of electrocatalyst, Ni bare foam, Co hydroxide/Ni foam and Ni-Co hydroxides/Ni foam.

The formation of oxohydroxides and the activation of water (through the  $\bullet$  OH in-situ generated) could contribute to the electrooxidation of Kraft lignin. Indeed, at potentials above 0.6 V vs SCE the absence of vanillin suggests that the unselective oxidation, characteristic of a radical mechanism, is occurring. On the other hand, at 0.6 V vs SCE vanillin could be produced, being the reaction time a fundamental parameter in lignin oxidation. Namely, regardless of the type of electrocatalyst, increasing the reaction time from 1 to 3 and 5 h, the vanillin repolymerization and further oxidation could be favoured. The presence of Ni-Co and Co hydroxides do not improve the catalytic activity of the Ni foam. The Co/Ni catalyst accumulates a higher charge and reaches a greater conversion, with a low vanillin yield, possibly due to the high activity of this electrode for both lignin degradation and OER, with a low tendency to selectively break the polymer bonds, hence leading to the production of a large range of by-products. For Ni-Co/Ni, the low vanillin yield and the low charge accumulated could be explained considering its low activity in the OER and a partial lignin degradation leading the production of oligomers and high molecular weight species.

Then, the catalytic performances of hydroxides-coated catalysts are worse than Ni bare foam; nevertheless, vanillin yield for Ni-Co hydroxides showed vanillin yield combined with low charge accumulated. These are promising halfway results, between those exhibited by Ni and Co/Ni electrocatalysts; therefore, it could be considered to modify the contribute of both elements, changing in Ni and Co molar ratios or by changing the thickness and morphology of the deposited layer, to enhance the catalytic activity.

## 5. References

- [1] L. Lorenzetti, ‘Studio di elettrocatalizzatori per l’ossidazione elettrochimica del glucosio’, Tesi di laurea, 2019.
- [2] F. Cherubini, ‘The biorefinery concept: Using biomass instead of oil for producing energy and chemicals’, *Energy Conversion and Management*, vol. 51, no. 7, pp. 1412–1421, Jul. 2010.
- [3] ‘Glossary of summaries - EUR-Lex’. <https://eur-lex.europa.eu/summary/glossary/energy.html>.
- [4] ‘2030 climate & energy framework’, *Climate Action - European Commission*, Nov. 23, 2016. [https://ec.europa.eu/clima/policies/strategies/2030\\_en](https://ec.europa.eu/clima/policies/strategies/2030_en).
- [5] ‘Market Report Series: Oil 2018 – Analysis’, *IEA*. <https://www.iea.org/reports/oil-2018>.
- [6] A. Mancini, ‘Idrolisi diretta di cellulosa e lignocellulosa in catalisi eterogenea’, magistrale, 2013.
- [7] ‘IEA-Bioenergy-Task42-Biorefining-Brochure-SEP2014\_LR.pdf’. [https://www.ieabioenergy.com/wp-content/uploads/2014/09/IEA-Bioenergy-Task42-Biorefining-Brochure-SEP2014\\_LR.pdf](https://www.ieabioenergy.com/wp-content/uploads/2014/09/IEA-Bioenergy-Task42-Biorefining-Brochure-SEP2014_LR.pdf).
- [8] B. Kamm, M. Kamm, P. R. Gruber, and S. Kromus, ‘Biorefinery Systems – An Overview’, in *Biorefineries-Industrial Processes and Products*, John Wiley & Sons, Ltd, 2008, pp. 1–40.
- [9] B. E. Dale and S. Kim, ‘Biomass Refining Global Impact–The Biobased Economy of the 21st Century’, in *Biorefineries-Industrial Processes and Products*, John Wiley & Sons, Ltd, 2008, pp. 41–66.
- [10] J.-P. Lange, ‘Lignocellulose conversion: an introduction to chemistry, process and economics’, *Biofuels, Bioproducts and Biorefining*, vol. 1, no. 1, pp. 39–48, 2007.
- [11] J. H. Clark, F. E. I. Deswarte, and T. J. Farmer, ‘The integration of green chemistry into future biorefineries’, *Biofuels, Bioproducts and Biorefining*, vol. 3, no. 1, pp. 72–90, 2009.
- [12] T. Werpy and G. Petersen, ‘Top Value Added Chemicals from Biomass: Volume I -- Results of Screening for Potential Candidates from Sugars and Synthesis Gas’, DOE/GO-102004-1992, 15008859, Aug. 2004.
- [13] Direttiva 2009/28/CE, F. Rosillo-Calle, “Manuale per un uso sostenibile”, Franco Muzzio editore, 2008



- [14] R. Jodice, E. Tomasinsig, “Energia dalle biomasse. Le tecnologie, i vantaggi per i processi produttivi, i valori economici e ambientali”, Trieste: Progetto Novimpresa, 2006.
- [15] Jaya Shankar Tumuluru, Christopher T Wright, Richard D Boardman, Neal A Yancey, and Shahab Sokhansanj, ‘A review on biomass classification and composition, co-firing issues and pretreatment methods’, presented at the 2011 Louisville, Kentucky, August 7 - August 10, 2011.
- [16] A. Khan, V. Nair, J. C. Colmenares, and R. Gläser, ‘Lignin-Based Composite Materials for Photocatalysis and Photovoltaics’, *Top Curr Chem (Z)*, vol. 376, no. 3, p. 20, Jun. 2018.
- [17] R. Ghahremani and J. A. Staser, ‘Electrochemical oxidation of lignin for the production of value-added chemicals on Ni-Co bimetallic electrocatalysts’, *Holzforschung*, vol. 72, no. 11, pp. 951–960, Nov. 2018.
- [18] A. Naseem, S. Tabasum, K. M. Zia, M. Zuber, M. Ali, and A. Noreen, ‘Lignin-derivatives based polymers, blends and composites: A review’, *International Journal of Biological Macromolecules*, vol. 93, pp. 296–313, Dec. 2016.
- [19] D. Kun and B. Pukánszky, ‘Polymer/lignin blends: Interactions, properties, applications’, *European Polymer Journal*, vol. 93, pp. 618–641, Aug. 2017.
- [20] B. M. Upton and A. M. Kasko, ‘Strategies for the Conversion of Lignin to High-Value Polymeric Materials: Review and Perspective’, *Chem. Rev.*, vol. 116, no. 4, pp. 2275–2306, Feb. 2016.
- [21] A. Agrawal and \*Nirmala Kaushik and Soumitra Biswas, ‘Derivatives and Applications of Lignin : An Insight’, *Derivatives and Applications of Lignin : An Insight*, vol. 01, no. 07, pp. 30–36, Jul. 2014.
- [22] M. Chávez-Sifontes and M. E. Domine, ‘LIGNINA, ESTRUCTURA Y APLICACIONES: MÉTODOS DE DESPOLIMERIZACIÓN PARA LA OBTENCIÓN DE DERIVADOS AROMÁTICOS DE INTERÉS INDUSTRIAL’, *Avances en Ciencias e Ingeniería*, p. 33, 2013.
- [23] G. Chauvette, M. Heitz, M. Rubio, J. Khorami, E. Chornet, and H. Ménard, ‘TG/DTG as a rapid method for the characterization of solid residues derived from liquefaction of lignocellulosics’, *Thermochimica Acta*, vol. 84, pp. 1–5, Mar. 1985.
- [24] J. Zakzeski, P. C. A. Bruijninx, A. L. Jongerius, and B. M. Weckhuysen, ‘The Catalytic Valorization of Lignin for the Production of Renewable Chemicals’, *Chem. Rev.*, vol. 110, no. 6, pp. 3552–3599, Jun. 2010.

- [25] V. K. Thakur, M. K. Thakur, P. Raghavan, and M. R. Kessler, 'Progress in Green Polymer Composites from Lignin for Multifunctional Applications: A Review', *ACS Sustainable Chem. Eng.*, vol. 2, no. 5, pp. 1072–1092, May 2014.
- [26] J.-W. Jeon, L. Zhang, Prof. J. Lutkenhaus, Fr. D. D. Laskar, Dr. J. P. Lemmon, Dr. D. Chai, Dr. M. I. Nandasiri, A. Hashmi, Prof. J. Xu, Dr. R. K. Motkuri, Dr. C. A. Fernandez, Dr. J. Liu, Dr. M. P. Tcker, P. B. McGrail, Prof. Bin Yang, Dr. S. K. Nude 'Controlling Porosity in Lignin-Derived Nanoporous Carbon for Supercapacitor Applications', *ChemSusChem*, vol. 8, no. 3, pp. 428–432, Feb. 2015.
- [27] H. Lu and X. S. Zhao, 'Biomass-derived carbon electrode materials for supercapacitors', *Sustainable Energy & Fuels*, vol. 1, no. 6, pp. 1265–1281, 2017.
- [28] S.-H. Li, S. Liu, J. C. Colmenares, and Y.-J. Xu, 'A sustainable approach for lignin valorization by heterogeneous photocatalysis', *Green Chem.*, vol. 18, no. 3, pp. 594–607, 2016.
- [29] M. Kleinert and T. Barth, 'Phenols from Lignin', *Chemical Engineering & Technology*, vol. 31, no. 5, pp. 736–745, 2008.
- [30] J. E. Holladay, J. F. White, J. J. Bozell, and D. Johnson, 'Top Value-Added Chemicals from Biomass - Volume II—Results of Screening for Potential Candidates from Biorefinery Lignin', Pacific Northwest National Lab. (PNNL), Richland, WA (United States), PNNL-16983, Oct. 2007.
- [31] C. Chio, M. Sain, and W. Qin, 'Lignin utilization: A review of lignin depolymerization from various aspects', *Renewable and Sustainable Energy Reviews*, vol. 107, pp. 232–249, Jun. 2019.
- [32] T. Kan, V. Strezov, and T. J. Evans, 'Lignocellulosic biomass pyrolysis: A review of product properties and effects of pyrolysis parameters', *Renewable and Sustainable Energy Reviews*, vol. 57, no. C, pp. 1126–1140, 2016.
- [33] O. Y. Abdelaziz, D. P. Brink, J. Prothmann, K. Ravi, M. Sum, J. G. Hidalgo, M. Sandahl, C. P. Hultberg, C. Turner, G. Liden, M. F. Gorwa-Granslund 'Biological valorization of low molecular weight lignin', *Biotechnology Advances*, vol. 34, no. 8, pp. 1318–1346, Dec. 2016.
- [34] X. Zhang, K. Rajagopalan, H. Lei, R. Ruan, and B. K. Sharma, 'An overview of a novel concept in biomass pyrolysis: microwave irradiation', *Sustainable Energy Fuels*, vol. 1, no. 8, pp. 1664–1699, Sep. 2017.

- [35] D. Duan, R. Ruan, Y. Wang, Y. Liu, L. Dai, Y. Zhao, Y. Zhou, Q. Wu ‘Microwave-assisted acid pretreatment of alkali lignin: Effect on characteristics and pyrolysis behavior’, *Bioresour. Technol.*, vol. 251, pp. 57–62, Mar. 2018.
- [36] T. N. Spirina, N. N. Saprykina, O.A. Andreeva, E. M. Kulikova, Yu. N. Sazanov, S. M. Krutov & V. E. Yudin, ‘Morphology of modified hydrolysis lignin’, *Russ J Appl Chem*, vol. 85, no. 5, pp. 794–798, May 2012.
- [37] Z. Yuan, S. Cheng, M. Leitch, and C. C. Xu, ‘Hydrolytic degradation of alkaline lignin in hot-compressed water and ethanol’, *Bioresour. Technol.*, vol. 101, no. 23, pp. 9308–9313, Dec. 2010.
- [38] N. Mahmood, Z. Yuan, J. Schmidt, and C. (Charles) Xu, ‘Production of polyols via direct hydrolysis of kraft lignin: Effect of process parameters’, *Bioresource Technology*, vol. 139, pp. 13–20, Jul. 2013.
- [39] K. B. H. Finch, R. M. Richards, A. Richel, A. V. Medvedovic, N. G. Gheorghe, M. Verziu, S. M. Coman, V. I. Parvulescu, ‘Catalytic hydroprocessing of lignin under thermal and ultrasound conditions’, *Catalysis today*, 2012.
- [40] S. Karagöz, T. Bhaskar, A. Muto, and Y. Sakata, ‘Effect of Rb and Cs carbonates for Production of Phenols from liquefaction of wood biomass’, *Fuel*, vol. 83, pp. 2293–2299, Dec. 2004.
- [41] N. Yan, C. Zhao, P. J. Dyson, C. Wang, L. Liu, and Y. Kou, ‘Selective degradation of wood lignin over noble-metal catalysts in a two-step process’, *ChemSusChem*, vol. 1, no. 7, pp. 626–629, 2008.
- [42] G. Fuchs, M. Boll, and J. Heider, ‘Microbial degradation of aromatic compounds - from one strategy to four’, *Nat. Rev. Microbiol.*, vol. 9, no. 11, pp. 803–816, Oct. 2011.
- [43] M. Ahmad, J. N. Roberts, E. M. Hardiman, R. Singh, L. D. Eltis, and T. D. H. Bugg, ‘Identification of DypB from *Rhodococcus jostii* RHA1 as a lignin peroxidase’, *Biochemistry*, vol. 50, no. 23, pp. 5096–5107, Jun. 2011.
- [44] Y.-H. P. Zhang, ‘Production of biofuels and biochemicals by in vitro synthetic biosystems: Opportunities and challenges’, *Biotechnol. Adv.*, vol. 33, no. 7, pp. 1467–1483, Nov. 2015.
- [45] T. Furuya, M. Miura, M. Kuroiwa, and K. Kino, ‘High-yield production of vanillin from ferulic acid by a coenzyme-independent decarboxylase/oxygenase two-stage process’, *N Biotechnol*, vol. 32, no. 3, pp. 335–339, May 2015.

- [46] J. P. Rosazza, Z. Huang, L. Dostal, T. Volm, and B. Rousseau, 'Review: biocatalytic transformations of ferulic acid: an abundant aromatic natural product', *J. Ind. Microbiol.*, vol. 15, no. 6, pp. 457–471, Dec. 1995.
- [47] J. Nielsen, C. Larsson, A. van Maris, and J. Pronk, 'Metabolic engineering of yeast for production of fuels and chemicals', *Current Opinion in Biotechnology*, vol. 24, no. 3, pp. 398–404, Jun. 2013.
- [48] B. Nyamunda, F. Chigondo, M. Moyo, U. Guyo, M. Shumba, and T. Nharingo, 'HYDROGEN PEROXIDE AS AN OXIDANT FOR ORGANIC REACTIONS', *Journal of Atoms and Molecules*, vol. 3, pp. 23–44, Feb. 2013.
- [49] B. Wang and Z. Long, 'Preparation of Aromatic Aldehydes from Lignin Oxidation with a Perovskite-Type Catalyst', *Applied Mechanics and Materials*, 2011.
- [50] H. Deng *et al.*, 'Activity and Stability of Perovskite-Type Oxide LaCoO<sub>3</sub> Catalyst in Lignin Catalytic Wet Oxidation to Aromatic Aldehydes Process', *Energy Fuels*, vol. 23, no. 1, pp. 19–24, Jan. 2009.
- [51] K. Ruuttunen and T. Vuorinen, 'Developing Catalytic Oxygen Delignification for Kraft Pulp: Kinetic Study of Lignin Oxidation with Polyoxometalate Anions', *Industrial & Engineering Chemistry Research*, vol. 44, pp. 4284–4291, Apr. 2005.
- [52] W. G. Forsythe, M. D. Garrett, C. Hardacre, M. Nieuwenhuyzen, and G. N. Sheldrake, 'An efficient and flexible synthesis of model lignin oligomers', *Green Chem.*, vol. 15, no. 11, pp. 3031–3038, Oct. 2013.
- [53] J. Miller, L. EVANS, A. LITTLEWOLF, and D. TRUDELL, *Batch Microreactor Studies of Lignin Depolymerization by Bases. 1. Alcohol Solvents*. 2002.
- [54] Q. Song, F. Wang, and J. Xu, 'Hydrogenolysis of lignosulfonate into phenols over heterogeneous nickel catalysts', *Chem. Commun.*, vol. 48, no. 56, pp. 7019–7021, Jun. 2012.
- [55] J. G. Huddleston, A. E. Visser, W. M. Reichert, H. D. Willauer, G. A. Broker, and R. D. Rogers, 'Characterization and comparison of hydrophilic and hydrophobic room temperature ionic liquids incorporating the imidazolium cation', *Green Chem.*, vol. 3, no. 4, pp. 156–164, Jan. 2001.
- [56] M. Cocero, A. Cabeza, N. Abad, T. Adamovic, L. Vaquerizo, C. M. Martinez, M. V. Pazo-Cepeda 'Understanding biomass fractionation in subcritical & supercritical water', *The Journal of Supercritical Fluids*, vol. 133, Aug. 2017.
- [57] V. S. Bagotsky, *Fundamentals of Electrochemistry*. John Wiley & Sons, 2005.

- [58] B. Konkena, J. Masa, W. Xia, M. Muhler, and W. Schuhmann, ‘MoSSe@reduced graphene oxide nanocomposite heterostructures as efficient and stable electrocatalysts for the hydrogen evolution reaction’, *Nano Energy*, vol. 29, pp. 46–53, Nov. 2016.
- [59] N.-T. Suen, S.-F. Hung, Q. Quan, N. Zhang, Y.-J. Xu, and H. M. Chen, ‘Electrocatalysis for the oxygen evolution reaction: recent development and future perspectives’, *Chem. Soc. Rev.*, vol. 46, no. 2, pp. 337–365, Jan. 2017.
- [60] C. F. Zinola, *Electrocatalysis: Computational, Experimental, and Industrial Aspects*. CRC Press, 2010.
- [61] E. Santos and W. Schmickler, *Catalysis in Electrochemistry: From Fundamental Aspects to Strategies for Fuel Cell Development*. John Wiley & Sons, 2011.
- [62] C. A. Martínez-Huitle and S. Ferro, ‘Electrochemical oxidation of organic pollutants for the wastewater treatment: direct and indirect processes’, *Chem. Soc. Rev.*, vol. 35, no. 12, pp. 1324–1340, Nov. 2006.
- [63] P. Mandal, B. K. Dubey, and A. K. Gupta, ‘Review on landfill leachate treatment by electrochemical oxidation: Drawbacks, challenges and future scope’, *Waste Management*, vol. 69, pp. 250–273, Nov. 2017.
- [64] C. A. Martínez-Huitle and L. S. Andrade, ‘Electrocatalysis in wastewater treatment: recent mechanism advances’, *Química Nova*, vol. 34, no. 5, pp. 850–858, 2011.
- [65] G. Hilt, ‘Basic Strategies and Types of Applications in Organic Electrochemistry’, *ChemElectroChem*, vol. 7, no. 2, pp. 395–405, Jan. 2020.
- [66] R. L. Doyle and M. E. G. Lyons, ‘The Oxygen Evolution Reaction: Mechanistic Concepts and Catalyst Design’, in *Photoelectrochemical Solar Fuel Production: From Basic Principles to Advanced Devices*, S. Giménez and J. Bisquert, Eds. Cham: Springer International Publishing, 2016, pp. 41–104.
- [67] S. Liu, L. Bai, A. P. van Muyder, Z. Huang, X. Cui, Z. Fei, X. Li, X. Hu, and P. Dyson. ‘Oxidative cleavage of  $\beta$ -O-4 bonds in lignin model compounds with a single-atom Co catalyst’, *Green Chem.*, vol. 21, no. 8, pp. 1974–1981, Apr. 2019.
- [68] O. Movil-Cabrera, A. Rodriguez-Silva, C. Arroyo-Torres, and J. A. Staser, ‘Electrochemical conversion of lignin to useful chemicals’, *Biomass and Bioenergy*, vol. 88, pp. 89–96, May 2016.
- [69] Y. J. Shih, Y. H. Huang, and C. P. Huang, ‘In-situ electrochemical formation of nickel oxyhydroxide (NiOOH) on metallic nickel foam electrode for the direct oxidation of ammonia in aqueous solution’, *ELECTROCHIM ACTA*, vol. 281, pp. 410–419, Aug. 2018.

- [70] D. Di Marino, T. Jestel, C. Marks, Dr. J. Viell, M. Blindert, Dr. S. M. A. Kriescher, Prof. A. C. Spess, Prof. M. Wessling ‘Carboxylic Acids Production via Electrochemical Depolymerization of Lignin’, *ChemElectroChem*, vol. 6, no. 5, pp. 1434–1442, Mar. 2019.
- [71] P. H. Ho, E. Scavetta, D. Tonelli, G. Fornasari, A. Vaccari, and P. Benito, ‘Hydrotalcite-Type Materials Electrodeposited on Open-Cell Metallic Foams as Structured Catalysts’, *Inorganics*, vol. 6, no. 3, Art. no. 3, Sep. 2018.
- [72] G. Cuono, ‘Elettrodeposizione di idrossidi doppi a strato contenenti cobalto su supporti di diversa natura’, Tesi di laurea, 2017.
- [73] D. Schmitt, C. Regenbrecht, M. Hartmer, F. Stecker, and S. R. Waldvogel, ‘Highly selective generation of vanillin by anodic degradation of lignin: a combined approach of electrochemistry and product isolation by adsorption’, *Beilstein J. Org. Chem.*, vol. 11, no. 1, pp. 473–480, Apr. 2015.
- [74] M. Zirbes, D. Schmitt, N. Beiser, D. Pitton, T. Hoffmann, and S. R. Waldvogel, ‘Anodic Degradation of Lignin at Active Transition Metal-based Alloys and Performance-enhanced Anodes’, *ChemElectroChem*, vol. 6, no. 1, pp. 155–161, Jan. 2019.
- [75] J. Xing, S. Wu, and K. Y. Simon Ng, ‘Electrodeposition of ultrathin nickel–cobalt double hydroxide nanosheets on nickel foam as high-performance supercapacitor electrodes’, *RSC Advances*, vol. 5, no. 108, pp. 88780–88786, 2015.
- [76] C. A. Martínez-Huitle, M. A. Rodrigo, I. Sirés, and O. Scialdone, ‘Single and Coupled Electrochemical Processes and Reactors for the Abatement of Organic Water Pollutants: A Critical Review’, *Chem. Rev.*, vol. 115, no. 24, pp. 13362–13407, Dec. 2015.
- [77] M. Zirbes, L. L. Quadri, M. Breiner, A. Stenglein, A. Bomm, W. Schade, and S. R. Waldvogel, ‘High-Temperature Electrolysis of Kraft Lignin for Selective Vanillin Formation’, *ACS Sustainable Chem. Eng.*, vol. 8, no. 19, pp. 7300–7307, May 2020.
- [78] C. Z. Smith, J. H. P. Utley, and J. K. Hammond, ‘Electro-organic reactions. Part 60[1]. The electro-oxidative conversion at laboratory scale of a lignosulfonate into vanillin in an FM01 filter press flow reactor: preparative and mechanistic aspects’, *J Appl Electrochem*, vol. 41, no. 4, pp. 363–375, Apr. 2011.
- [79] P. Ho Hoang, ‘Open-cell metallic foams coated by electrodeposition as structured catalysts for energy and environmental applications’, PhD Thesis, alma, 2018.
- [80] K. Qvortrup, ‘Biological Field Emission Scanning Electron Microscopy Roland A. Fleck and Bruno M. Humbel (Eds.), Wiley, Hoboken, NJ, 2019. 752 pp. ISBN: 1118654064’, *Microscopy and Microanalysis*, vol. 26, no. 2, pp. 363–363, 2020.
- [81] J. R. Ferraro, *Introductory raman spectroscopy*. Elsevier, 2003.

- [82] Granite, 'What is Raman Spectroscopy? | Raman Spectroscopy Principle', *Edinburgh Instruments*. <https://www.edinst.com/blog/what-is-raman-spectroscopy/>.
- [83] K. R. Hebbar, *Basics of X-Ray Diffraction and its Applications*. New Delhi: IK International Publishing House, 2013.
- [84] M. R. de Rooij, 'Electrochemical methods: Fundamentals and applications', *Anti-Corrosion Methods and Materials*, 2003.
- [85] J. G. Smith, *Chimica organica*. Milano: McGraw-Hill Education, 2007.
- [86] D. A. Skoog, J. F. Holler, S. R. Crouch, and L. Sabbatini, *Chimica analitica strumentale*. Napoli: Edises, 2009.
- [87] A. Gorassini, 'Spettrofotometria infrarossa in riflettanza totale attenuata', p. 22.
- [88] 'BRUKER, «Attenuated Total Reflection (ATR) – a versatile tool for FT-IR spectroscopy,»
- [89] L. Aguilera, P.C.M. Aguilar, Y. Leyet Ruiz, A. Almeida, J. Agostinho Mereira, R.R. Passos, & L.A. Pocrifka 'Electrochemical synthesis of  $\gamma$ -CoOOH films from  $\alpha$ -Co(OH)<sub>2</sub> with a high electrochemical performance for energy storage device applications', *J Mater Sci: Mater Electron*, vol. 31, no. 4, pp. 3084–3091, Feb. 2020.
- [90] S. A. Asher, 'UV resonance Raman spectroscopy for analytical, physical, and biophysical chemistry. Part 2', *Analytical chemistry*, vol. 65, no. 4, pp. 201A–210A, 1993.
- [91] D. S. Hall, D. J. Lockwood, C. Bock, and B. R. MacDougall, 'Nickel hydroxides and related materials: a review of their structures, synthesis and properties', *Proc. R. Soc. A.*, vol. 471, no. 2174, p. 20140792, Feb. 2015.
- [92] J. Yang, H. Liu, W. N. Martens, and R. L. Frost, 'Synthesis and Characterization of Cobalt Hydroxide, Cobalt Oxyhydroxide, and Cobalt Oxide Nanodiscs', *J. Phys. Chem. C*, vol. 114, no. 1, pp. 111–119, Jan. 2010.
- [93] S. G. Bratsch, 'Standard Electrode Potentials and Temperature Coefficients in Water at 298.15 K', *Journal of Physical and Chemical Reference Data*, vol. 18, no. 1, pp. 1–21, Jan. 1989.
- [94] N. Tokmak and M. Urgan, 'Production and Characterization of Electroactive Nickel Oxides Grown on Nickel Foam by Anodic Oxidation in KOH Melts for Supercapacitor Applications', *MRS Advances*, vol. 2, no. 54, pp. 3237–3247, Nov. 2017.
- [95] C. A. Cateto, M. F. Barreiro, and A. E. Rodrigues, 'Monitoring of lignin-based polyurethane synthesis by FTIR-ATR', *Industrial Crops and Products*, vol. 27, no. 2, pp. 168–174, Mar. 2008.

- [96] S. Lupeng, X. Zhang, F. Chen, and F. Xu, 'Fast pyrolysis of Kraft lignins fractionated by ultrafiltration', *Journal of Analytical and Applied Pyrolysis*, vol. 128, Nov. 2017.